SUPER RESOLUTION ALGORITHMS FOR INDOOR POSITIONING SYSTEMS

G M ROSHAN INDIKA GODALIYADDA

NATIONAL UNIVERSITY OF SINGAPORE

2010

SUPER RESOLUTION ALGORITHMS FOR INDOOR POSITIONING SYSTEMS

G M ROSHAN INDIKA GODALIYADDA

(*B. Sc. in Electrical and Electronic Engineering, University of Peradeniya)*

A THESIS SUBMITTED

FOR THE DEGREE OF DOCTOR OF PHILOSOPHY

DEPARTMENT OF ELECTRICAL & COMPUTER ENGINEERING

NATIONAL UNIVERSITY OF SINGAPORE

2010

Dedication

To my parents, my wife and brother,

Acknowledgements

Though there is only one name on thesis title, writing a dissertation is a collaborative effort. This work would have been impossible without the guidance and assistance of a huge network of people. Hence, I would forthwith like to thank everyone who has made this thesis possible.

I would like to express my sincere gratitude and appreciation to my supervisor Associate Professor Hari K. Garg, for the invaluable guidance and constant encouragement he provided. His vast experience and innovative insight was a made this all possible. You were the force behind every success in my PhD.

My thanks also go out to the immensely talented and ever resourceful Dr. Himal Suraweera who was a pillar of support, with his gracious advice and constant support. Many other colleagues helped me with their friendship and advice throughout my research work. Special thanks go to my friends and colleagues Kumudu Gamage and Duminda Ariyasinghe at NTU.

Finally I would like to thank my family for their love, understanding and support when it was most needed. I thank my wife Renu, for being there with me in good times and bad, with her endless love. I would also like to thank my mother, for her constant belief in me, and her timely words of wisdom; my father for being the perfect role model for me with his passion, dedication and conviction; my brother for his invaluable assistance, and for being my best friend through the years.

Thanks all!

National University of Singapore G M R I Godaliyadda

07 July 2010

Table of Contents

Summary

The hostile nature of indoor radio environments and the rapid growth of commercial indoor positioning systems have placed a significant emphasis on developing robust localization techniques. The challenging problem of accurate positioning in hostile indoor environments with severe multipath and noise conditions is tackled through the introduction of the MUSIC super resolution algorithm. Due to its higher resolution capability and superior noise immunity, compared to other standard correlation techniques, it can be utilized to provide accurate time delay estimates under LoS conditions. The resultant pseudo-spectrums obtained by using this method, can also be used as location information rich fingerprints for NLoS conditions as well.

The research work presented in this thesis focuses on the introduction of new variants in addition to the standard FD-MUSIC algorithm, such as the TD-MUSIC algorithm for more versatile and accurate performance. In-depth behavioural analysis is presented on the FD-MUSIC, FD-EV and TD-MUSIC algorithms to properly understand the strengths and limitations of each of the methods. The ESPRIT algorithm is introduced as an alternative, for systems that wish to forego a peak detection process at the expense of diminished accuracy. The variation of the steering vector pulse spread enabled us to identify the *spectral leakage phenomenon* of the TD-MUSIC algorithm, thereby enabling us to use it for our own advantage under certain conditions. The Eigen value de-weighting of the FD-EV method, is identified for having the capability to *resurface underestimated signal peaks submerged beneath the noise floor,* under friendly SNR and bandwidth conditions. The superior resolution capability, bandwidth versatility and noise immunity of the

TD-MUSIC algorithm is then demonstrated. Finally, we introduce the TD-EV method, which effectively combines the positive attributes of the TD-MUSIC algorithm and the FD-EV algorithm. This is done in order to utilize the superior resolution capability, noise immunity and bandwidth versatility of the TD-MUSIC algorithm and the resurfacing capability of the FD-EV method. Thus it is demonstrated how the TD-EV method emerges as the ultimate performer, under band limited conditions with low SNR, while the signal subspace dimension is underestimated.

List of Figures

List of Tables

List of Abbreviations

2-D	2 Dimensional
3-D	3 Dimensional
ACM	Auto Correlation Matrix
AOA	Angle of Arrival
AP	Access Points
AWGN	Additive White Gaussian Noise
CN-TOAG	Closest Neighbour with TOA grid
DDP	Dominant Direct Path
DGPS	Differential Global Positioning System
DOA	Direction of Arrival
DOLPHIN	Distributed Object Location System for Physical-Space Internetworking
DOP	Dilution of Precision
DP	Direct Path
DP-TOA	Direct Path Time of Arrival
EMD	Earth Mover Distance
ESPRIT	Estimation of Signal Parameters via Rotational Invariance Techniques

EV	Eigen Value
EU	European Union
FBCM	Forward Backward Correlation Matrix
FCM	Forwards Correlation Matrix
FD-MUSIC	Frequency Domain Multiple Signal Classification
FD-EV	Frequency Domain Eigen Value
LoS	Line-of-Sight
LS	Least Squared
GLONASS	Global Navigation Satellite System
GPS	Global Positioning System
GNSS	Global Navigation Satellite Systems
IFFT	Inverse Fast Fourier Transform
ISM	Industrial Scientific Medical
MLP	Multi-Layer Perceptron
MP	Matrix Pencil
MUSIC	Multiple Signal Classification
N-D	N Dimensional
NC	No Coverage
NDDP	Non-Dominant Direct Path
NLoS	Non Line-of-sight
NUDP	Natural Undetected Direct Path

RF	Radio Frequency
RFID	Radio Frequency Identification
RSS	Received Signal Strength
RTOF	Roundtrip Time of Flight
SMP	Shortest M-Vertex Perimeter
SNR	Signal to Noise Ratio
SUDP	Shadowed Undetected Direct Path
SVM	Support Vector Machine
TD-MUSIC	Time Domain Multiple Signal Classification
TD-EV	Time Domain Eigen Value
TOA	Time of Arrival
TDOA	Time Difference of Arrival
UDP	Undetected Direct Path
UE	User Equipment
US	United States
UWB	Ultra Wide Band
WLAN	Wireless Local Area Network
WLS	Weighted Least Squares

Chapter 1

Introduction

The very essence of human nature can be characterized by the never-ending thirst to explore the unknown. The first humans who ventured out of familiar surroundings in search of better sources of food sparked the beginning of an age of exploration that hasn't ceased to this very day and no doubt will continue for times to come. As we speak, the never-ending voyages to the depths of the ocean floors, uncharted lands and the final frontier space itself, continue with the man's undying desire to discover what is beyond the horizon.

As exploration went beyond the known, to the unknown, to what was beyond where one had ever been before, the necessity to attain ones position with respect to a known reference system arose (for example while hunting your current position with respect to your home or nearby water hole). This was the birth of the very first primitive navigation and positioning system. Distance and direction were measured from prominent landmarks to describe location, giving birth to the concept of coordinate systems and reference points. Measuring distance and direction accurately was now of the utmost importance.

Without an exception, as all of man's creations which are flawed upon conception, positioning systems also require continual upgrades. Increasing accuracy is the primordial necessity in positioning, and the increase of which would lead man beyond the borders of what was possible; what was known; what was once beyond

our grasp; and what was merely science fiction only perhaps a year back. It is the potential that accurate positioning has upon our day to day needs in this millennium that has lead to such a rapid growth in a sector, which only half a century before was still in infancy. So much of our needs are tied to where we are at a given time and the significance of identifying where someone else is of equal importance. The launch of such behemoth projects as the GPS system and the Galileo system, serves evidence to the importance of positioning in this day and age.

1.1 Limitations of GPS Systems

The dawn of the new millennia has witnessed a significant surge in wireless systems. Lately the ever growing, wide ranging, wireless technological applications have shown for a need of integrating location aware functionality in wireless systems to cater to some of our diverse requirements. As it may be evident accurate location estimation is the key research task for any location aware system. The most popular and widely used positioning system, the GPS was originally developed by the US Department of Defence and is presently managed by the US Air Force. It is currently the only fully functional satellite navigation system in the world. Other systems, such as the Russian GLONASS system, the EU Galileo system and the Chinese Beidou system have limited operation, and are in the process of being developed as alternatives to GPS.

GPS, despite its success and global acceptance has a number of limitations. Satellite navigation systems do not work well in heavily urbanized metropolitan areas with high-rise buildings (e.g. New York, Singapore, Tokyo) aptly named urban canyons. The existence of multiple structures, of varied geometry, in the surrounding

environment presents multiple reflective surfaces, thereby causing the presence of multi-paths as depicted in Figure 1.1. LoS signals transmitted from the geostationary satellites tend to diminish in strength as a result of free space loss. Further, high-rise buildings in urban environments at times block the LoS between the GPS receiver and the transmitter, hence completely blocking the direct path signal as shown in Figure 1.1. This renders GPS receivers unable to function properly due to the absence of the direct path [1]. The effects of multi-path and Non-LoS conditions are evident in data collected by Trimble™ manual [2] when measuring a vehicle's heading error while driving on a straight street in a dense urban environment, as shown in Figure 1.2.

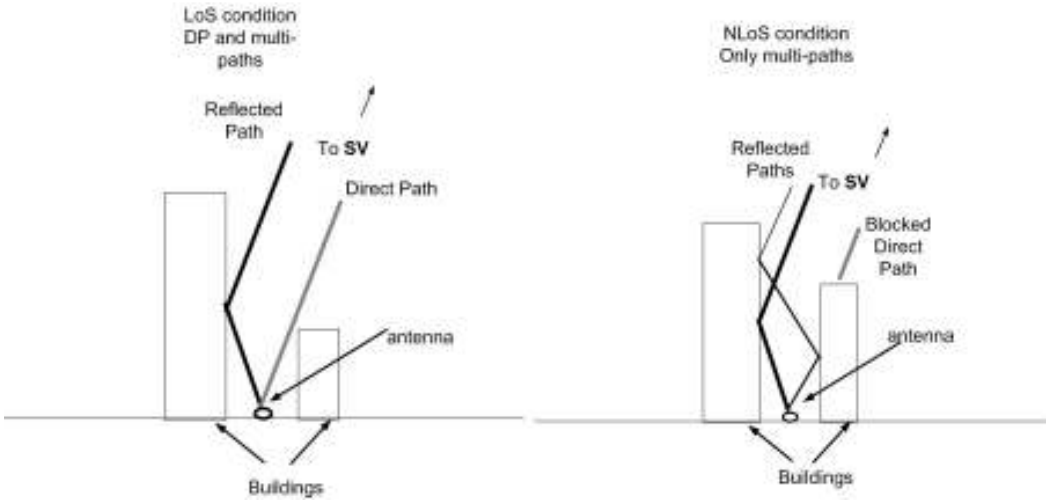

Figure 1.1 Direct and reflected multi-path GPS signals

Figure 1.2 Raw GPS heading errors while driving along a straight street in a dense urban environment (*image taken from [2]*)

GNSS are subjected to even more hostile channel conditions when operating indoors and underground. The severe multi-path conditions render these systems practically inept to handle localization under such conditions. Unlike outdoor positioning systems, an indoor positioning system would experience severe multi-path effects and near-far effects [3]. It should be noted that the positioning algorithms in GPS systems were not designed to withstand the severe multi-path and noise conditions present in indoor environments. Further the level of precision required in small regions for certain indoor applications is beyond the range of most GPS receivers. Even if the signal does penetrate the barriers, GPS receiver sensitivity may not be sufficient in indoor environments to accurately capture the weak satellite signals transmitted [4]. Depending on the indoor building geometry and their material distribution pattern, large attenuations and non-homogeneities may occur causing the signals measured by the receivers to only be NLoS signals that may cause large position errors in standard GPS systems, as illustrated in Figure 1.3.

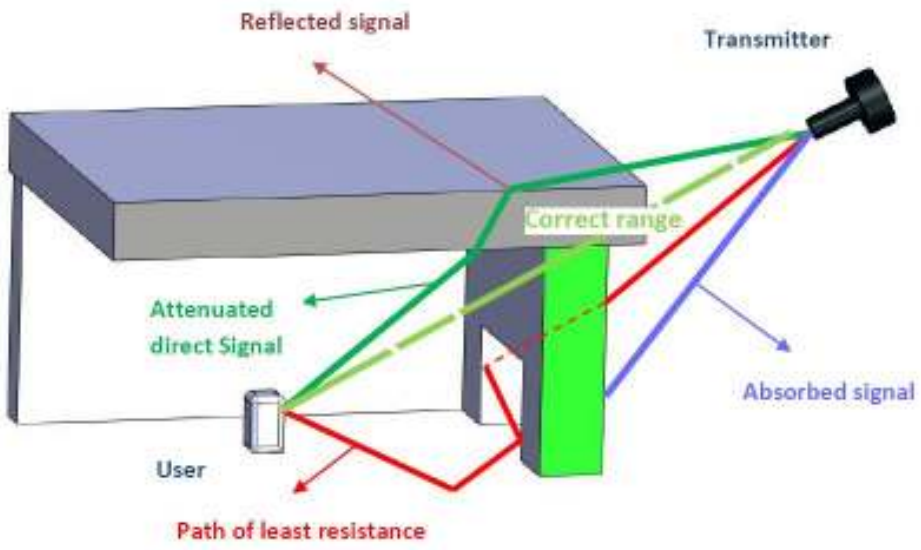

Figure 1.3 Possible GPS signal propagation paths into a building

1.2 Motivation

The primary progress in indoor positioning system technology has been made during the past decade or so. The rapid growth in research interest for Non-GPS positioning systems especially for indoor environments was due to the previously mentioned limitations of GPS when operating under these hostile channel conditions. Therefore, both the research and commercial products in this area are relatively new, and many people in academia and within the industry are currently involved in the research and development of these systems. An astonishing growth of wireless systems has been witnessed in recent years, as location awareness has become a prime necessity for any wireless system. Wireless localization technologies have entered the realm of consumer applications, as well as security, defence and public safety logistics, and medical, manufacturing industrial, entertainment, exploration and

transport systems as well as many other applications. Since wireless information access is now widely available, there is a high demand for accurate positioning in wireless networks, especially for indoor and underground environments [5, 6].

Research interest for Non-GPS based positioning systems has surged in the last decade. Therefore our research work focused on two main aspects:

I. Introducing versatile parameter estimation based positioning algorithms with enhanced performance, operating under LoS conditions in hostile indoor environments with severe multi-path and low SNR conditions.

II. Development of a robust *location information rich* fingerprint, as the unique identifier for location based fingerprinting systems, operating under NLoS conditions, commonly present in indoor environments.

It is commonly accepted among research circles that TOA based UWB wireless sensor networks are the most accurate for indoor geolocation [7] among all currently researched variants, for LoS conditions The synchronization requirement of TOA systems can be limited just either to transmitter side or receiver side as shown in [8] by utilizing a TDOA scheme. Other parameter estimation techniques such as the RSS based positioning systems for instance, suffer severe deviations from mean signal strengths due to fading, its accuracy suffers greatly with distance, and finally it is very sensitive to the estimated path-loss model parameters [9]. AOA estimation techniques require antenna arrays at each node to determine the angular power spectrum which is required for Direction of Arrival estimation [10].

Conventional TOA estimation techniques which utilize either inverse fast Fourier transforms or correlation based methods, though simplistic, (used in GPS systems) are highly error prone, under severe multi-path conditions and have very low

noise immunity. It is known that the indoor channel consists of a large number of closely spaced multi-paths that arrive at the receiver side in clusters under DDP conditions [11]. When the time intervals between two adjacent multi-paths within a cluster are too close together, as customary in indoor environments, both these methods fail to resolve the direct path properly. The peak of the direct path lobe which symbolizes the time delay of the LoS signal is shifted, as a result of the overlaps between unresolved multi-path lobes and the actual direct path lobe, as illustrated in Figure 1.4. The resolution of these standard methods is limited by the inverse of the signal bandwidth. For example in inverse fast Fourier transform based techniques, the bandwidth required is the inverse of the minimum time delay in the channel. This means for one meter distance resolution, we need 300 MHz bandwidth, which is a significant amount for common systems such as 802.11 a, b and g. Thus it becomes impossible to resolve more closely spaced multipath signals, an essential criterion for many indoor applications [12]. Therefore multi-path is the primary source of error under DDP conditions [11].

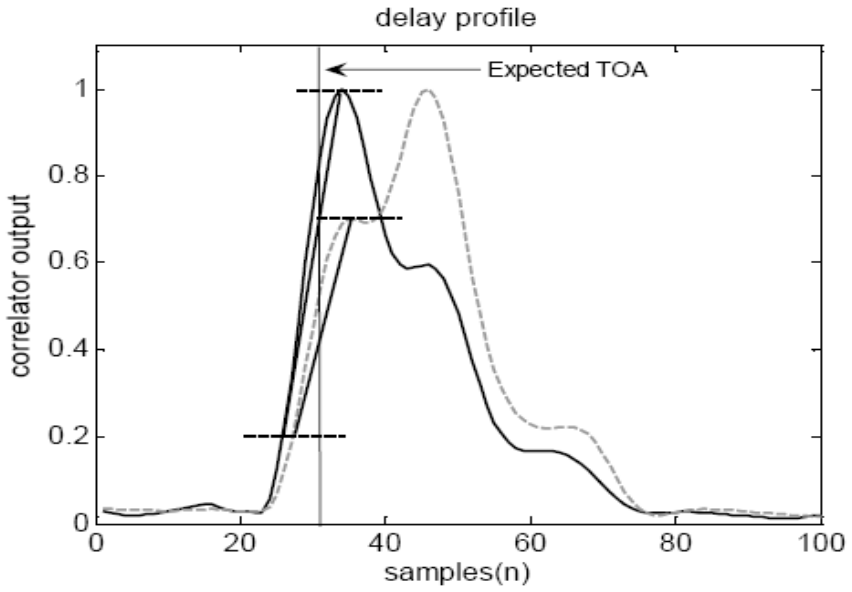

Figure 1.4 Correlator output of a delay profile depicting the side lobe shift effect on the direct path (the attenuated direct path case depicted by the dashed line)

Therefore use of super-resolution methods tends to be more attractive as a means of improving the spectral efficiency and measurement accuracy of a positioning system. Generally, a good super-resolution method must be robust, have high noise immunity, high resolution capability, high accuracy and low bandwidth requirements. Due to the higher bandwidth in UWB signals, the fine time resolution can be accurate to within one inch [13]. However under dense multi-path conditions as mentioned above the accuracy of the direct path TOA estimate is affected by the processing algorithm's resolvability. In addition, our agenda is to develop versatile algorithms capable of producing, robust location information rich signatures for NLoS conditions, and accurate location estimates even for commercial low-budget systems having poor noise performance. Thus our interest is primarily focused on utilizing the principles of subspace separation for the development and improvement of super resolution algorithms, first introduced in [14, 15] for spectral estimation applications. This improves the resolution capability of the TOA estimation process. Super

Resolution techniques are a bandwidth efficient method of extracting the time delay parameters in a multi-path system bathed in noise. Its high resolution, as will be shown later, even enables the separation of closely spaced signal components from one another in band limited environments with severe multi-path effects. Super resolution techniques are mainly of two types; parametric techniques such like the Prony algorithm and Eigen analysis based frequency estimation techniques such as the MUSIC algorithm.

The Prony algorithm is used in variety of methods for localization. In the basic method it equates the frequency sample points in a received signal spectra of a multipath channel used for indoor position estimation, to time sample points in a standard Prony application used for complex frequency estimation. Thus estimating complex frequencies via the Prony method is equivalent to obtaining the parameters of complex sinusoids generated in the frequency domain due to time delayed signals in the time domain of the indoor positioning channel [10]. This fundamental mapping logic is used in most localization systems. In another method, a Multi Carrier system was proposed for TDOA estimation as detailed in [8]. The Prony algorithm was used to obtain the time delay values of a multi-carrier signal received under noise. Estimation of frequencies of multiple anharmonically spaced sinusoidal signals from a noisy linear combination is summarized in [15]. The state space approach [16] which permits exact solution of P component frequencies and amplitudes, for $M > 2P$ samples can be considered, and the model order selections can be based on [17]. Thus given a transmitted signal with M components in its multi carrier comb, we may extract the measurement parameter:

$t_0 - \tau_{kn}$,

where t_0 is the source clock offset and τ_{kn} is the time of arrival of the kth path between the transmitter and nth receiver sites). The number of multi-paths is assumed to be:

$$N \leq \left[\frac{M-1}{2}\right] - 1,$$

where N is the number of multi-paths. From which TDOAs can be calculated through the cancellation of offset times since the source is common. TDOAs of the multipaths will yield large errors when applied to the location algorithm thus enabling the system to isolate the TDOAs of the DP.

As opposed to the prior method the Eigen analysis based frequency estimation techniques have superior noise immunity. These techniques have been proposed for use in TOA estimation quite recently due to the added advantages they offer in resolution and noise immunity. The additional benefits the Eigen based methods offer over parametric methods in terms of noise immunity have being comparatively analyzed in [14]. The MUSIC algorithm in the frequency domain was suggested for localization in [18], as an alternative for the previously mentioned correlation based and inverse fast Fourier transform based techniques. Here possible diversity scenarios were also explored. The primary focus was on mapping the basic MUSIC algorithm fundamentals to a TOA estimation framework in the frequency domain, and comparing the resolution enhancement to the aforementioned traditional time delay estimation techniques. In addition to these the MP algorithm was utilized in [19] for indoor positioning applications. These techniques have mainly focused on mapping the professed super resolution techniques used for spectral estimation and direction of arrival estimation, in array systems, to a TOA estimation framework, while operating completely in the frequency domain, in an indoor positioning environment. Eigen

value de-weighting was done in these works to primarily reduce the spurious nature of the pseudo-spectrum as suggested in [20]. This analysis was primarily focused on appreciating the resolution enhancement achievable compared to the correlation based and inverse fast Fourier transform based methods. All solutions in this analysis focused on providing reliable time delay estimates merely for indoor positioning systems operating only under LoS conditions. Further, there wasn't any emphasis given to development of variants to the standard MUSIC algorithm. Also no in-depth behavioural analysis was conducted to identify strengths and weaknesses or limitations of these methods so that they can be improved upon according to the prevailing environmental conditions. The multi-path effect was considered only as a 'noisy element' as opposed to actual information that can be used for the benefit of positioning. Thus our research work focused on the next-step which was to explore these super resolution techniques in detail and depth, so that it can provide the means to develop more robust and versatile algorithms that can provide solutions for positioning problems in both LoS and Non-LoS indoor environments.

1.3 Contributions

As the need of providing positioning solutions for indoor environments in both LoS and Non-LoS is an essential practical requisite, our research focused on developing algorithms and solutions that would benefit for both scenarios. Thus in our two fold approach the pseudo-spectrum generated as output of the suggested algorithms were examined as reliable sources of information for both LoS and Non-LoS scenarios.

I. The peaks of the pseudo-spectrum were considered as possible inputs for time delay estimation based systems, operating under LoS conditions.

II. The overall multi-path spread obtained by the pseudo-spectrum was explored as a possible candidate for a location based fingerprint under Non-LoS conditions.

Previous research work on super resolution techniques has primarily focused on mapping methods such as MUSIC and Prony algorithms, to a TOA estimation framework suited for indoor positioning. Emphasis was on simply mapping these methods to provide a resolution improvement compared to simpler time delay estimation techniques, such as correlation based and inverse Fast Fourier Transform based techniques. Their domain of operation was frequency domain and Eigen value de-weighting was only done to reduce the spurious nature of the peaks. In addition these methods focused only on providing positioning solutions to TOA estimation systems operating under LoS conditions. Therefore our work focused on the next step in terms of super resolution algorithms for indoor environments.

First in this research, we introduced the TD-MUSIC algorithm in addition to the FD-MUSIC algorithm, by making modifications in the objective function and steering vector to accommodate for the domain change. Then an in-depth behavioural analysis of both these techniques and the FD-EV method was conducted. The algorithm's behaviour was comprehensively analyzed under normal as well as hostile radio conditions. This enabled us to properly understand the limitations, and to test the versatility of these methods, so that positive attributes and suitable application scenarios can be identified for each variant, hence allowing us to provide possible improvements. Algorithms were developed as viable candidates for localization in

indoor environments where low resolution techniques such as correlation based methods have proven to be ineffective. In our work, emphasis was on constructing versatile super resolution algorithms capable of handling the most adverse conditions prevailing in indoor environments (for example Low SNR; limited bandwidth; erroneous estimation of signal subspace dimensions).

A mathematical model of the ESPRIT algorithm was developed for time delay estimation in indoor positioning. The ESPRIT algorithm is an alternative method to the MUSIC super resolution algorithm, in the direction of arrival estimation problems for array-based systems. It has the virtue of not relying on a peak detection process for parameter estimation. The downside of this is that it can only be used in an impulsive response case or if the signal spectrum is flat in the frequency sampling region. In addition, it is not as accurate an estimation tool as the MUSIC algorithms, and cannot generate the visual output that is required for a delay profile based fingerprint in Non-LoS environments. However, it is presented here as a viable alternative for systems which desire less computations at the expense of accuracy.

The extensive behavioural analysis conducted on the TD-MUSIC, FD-MUSIC and FD-EV algorithms under varying conditions enabled us to comparatively scrutinize the resolution capability, noise immunity, bandwidth versatility and impact of erroneous estimation of the signal subspace dimension of these techniques. Under the severe multi-path conditions prevailing in indoor environments, path resolvability becomes a key performance indicator. Considering that one of the fundamental reasons for utilizing super resolution based techniques compared to other approaches is its path resolvability, it is only fitting that the algorithms we developed provided the best possible resolution under hostile channel conditions. Path resolvability of these algorithms were comparatively analysed by identifying which methods continued to

accurately resolve all multi-paths present, while path separation between adjacent multi-paths were gradually decreased. It is important to keep in mind that an effective multi-path resolution comprises of two key steps. First, the algorithm should be able to identify the existence of two separate signal paths which is ensured when there is evidence of two separately identifiable peaks present in the resultant pseudo-spectrum. Second, for the process to be deemed complete, the peaks must be placed at the correct locations corresponding to the relevant time delays. This is a fundamental criterion in resolution because as stated earlier the 'peak shift' that takes place due to adjacent paths causes an estimation error which is one of the underlying reasons for opting to use a super resolution technique in the first place. It was observed that the TD-MUSIC algorithm introduced in this work provided the best path resolvability in terms of path separation capability, when compared with its frequency domain counterparts.

We further analyzed the effects of relative gain variations of multi-path components to understand which techniques have better ability to resolve significantly weaker multi-paths. The analysis provided us with evidence of the TD-MUSIC algorithm's superior resolution capability, for detection and resolution of low gain multipaths. As the ability to provide location rich information is an essential criterion for fingerprint generation, the TD-MUSIC algorithm's ability to resolve significantly weaker multi-paths, is of great significance for location based fingerprinting systems.

The impact SNR conditions have on the pseudo-spectrum 'shape' and ability of the algorithm to resolve the multipaths under low SNR conditions is a measurement of the method's 'noise immunity'. Noise immunity becomes the underlying criterion for selection if we were to select a less expensive signalling technique such as ultra sound or audible sound for the positioning application. On the

other hand even for UWB based systems, the signal processing tool's noise separation capability is essential for generating an accurate multi path profile of the transmitter to receiver channel. Part of the noise present maybe the resultant of interfering dynamic scatterers present at the real-time application stage, which were absent during the calibration stage of a location based fingerprinting positioning system used under NLoS conditions. It was verified in this research work that the introduced TD-MUSIC algorithm had a superior noise performance, thus making TD-MUSIC the prime candidate for high noise – low cost and Non-LOS location based finger printing applications.

The *spectral leakage phenomena* of the TD-MUSIC algorithm was identified for the first time by the research work presented in this thesis. It was discovered that the TD-MUSIC algorithm yields an *optimum deviant* for a given channel bandwidth, based on the signal template selected, and environmental conditions present. These *deviants* of the TD-MUSIC algorithm were produced by varying the pulse spread of the steering vector. When the algorithm behaviour was analyzed under varying band-width conditions, the TD-MUSIC algorithm emerged the most robust under band-limited environments, as it provided the least amount of shape deformation in the pseudo-spectrum under bandwidth fluctuations. Further, under certain bandwidth conditions it was discovered that the optimum deviant of the TD-MUSIC algorithm not only outperformed its frequency domain counterparts, but the original TD-MUSIC algorithm as well, to produce an extremely reliable pseudo-spectrum. Thus under low bandwidth conditions *the spectral leakage phenomena* can actually be used to our advantage if the *optimum deviant* is known in advance. This can therefore be done by using the *ultimate performer* for the given channel conditions to generate the pseudo-spectrum for time delay estimation or location based fingerprint construction.

A critical parameter for TOA estimation and location based fingerprint generation under subspace separation techniques is the value of the signal subspace dimension or the assumed number of signal paths in the channel. The inaccurate estimation of signal subspace dimension causes erroneous TOA estimates and generates deceiving multi-path profiles for standard MUSIC algorithms. Thus most previous research was focused on developing techniques to accurately determine the number of signal paths prior to subspace separation. The Eigen Value method was only suggested in spectral estimation, to reduce the spurious nature of the pseudo-spectrum. In this work we were able to identify for the first time, that the Eigen value de-weighting done in FD-EV method resulted in *resurfacing of the under estimated signal peaks, which were otherwise submerged beneath the noise floor* for the MUSIC algorithms. But it was also noticed that this performance was achievable only under friendly bandwidth and SNR conditions. This result is of great importance, since, for the first time we have means of *resurfacing submerged peaks when the signal subspace dimensions were underestimated,* thereby relieving the computational burden at the pre-subspace separation stage.

These discoveries lead us to develop the TD-EV method, which encompassed the "*best of both worlds"*, that is it strives to combine the positive attributes of both the TD-MUSIC algorithm and FD-EV methods'. As expected it was observed in this work, that the TD-EV method inherited the superior resolution capability, bandwidth versatility and the noise immunity of the TD-MUSIC algorithm, and the FD-EV method's ability to resurface the underestimated signal peaks submerged beneath the noise floor even under the most hostile radio channel conditions. The TD-EV method only suffers a slight but affordable decrease in resolution, while inheriting all the positive attributes of the TD-MUSIC and FD-EV algorithms. The TD-EV method

produces the only informative pseudo-spectrum output, under band limited channel conditions with low SNR, where the signal subspace dimension is underestimated, while all other methods failed, thereby further establishing its superior versatility.

1.4 Overview of Thesis Content

The contents of this thesis are organised as follows:

Chapter 1 Provides a general overview and introduction of the thesis. Describes the motivation behind the work and contributions achieved.

Chapter 2 Contains a detailed assessment of indoor positioning systems literature in relation to the proposed research work. Presents application possibilities for indoor localization.

Chapter 3 Contains a theoretical analysis of the super resolution techniques developed in our research. Details on practical constraints are presented.

Chapter 4 The results of the behavioural analysis for the FD-MUSIC, FD-EV and TD-MUSIC are presented. The effects due to the variations of the steering vector pulse spread are studied and the spectral leakage phenomenon is introduced. The impact of erroneous estimation of the signal subspace dimension is analyzed and the resurfacing capability of the FD-EV method is presented.

Chapter 5 The versatility of the time domain techniques is verified. The superior resolution capability, noise immunity and bandwidth versatility of the TD-MUSIC algorithm is demonstrated. The TD-EV algorithm is

introduced to combine the versatility of the TD-MUSIC algorithm and resurfacing capability of the FD-EV method.

Chapter 6 Concludes the dissertation by summarizing the findings and outlining possible future work.

Chapter 2

Indoor Positioning Systems, Solutions and Applications Scenarios

This chapter first reviews appropriate topics from both scientific and other referenced sources of literature pertinent to this research in order to put the work presented in the next few chapters in perspective. It provides a detailed overview of various indoor positioning techniques as well as the evolution of research work in indoor positioning through the recent past. This aims to provide the reader with an understanding about the general direction as well as the extent of research work in this area. As there is a wide array of positioning solutions suggested in the literature, we aim to provide an effectively informative overview of all the major types of positioning solutions. The final section of the chapter presents the wide range of applications that have risen out of indoor positioning systems. So the reader may fully appreciate the reasons behind the sudden surge in research interest towards development of indoor localization solutions in the last decade or so.

Different applications may require different types of location information. For example many applications may require a physical location which is expressed as coordinates on a 2-D/3-D map. Some may require a symbolic location expressed in a statement such as “user is in room 2A” or “object has reached gate B1 in terminal 2”etc. Obtaining symbolic location is becoming increasingly important with the growth of context aware applications in wireless technology. The context aware

applications strive to combine both content and location to create an *ambient intelligent internet of things*. In addition, relative location refers to location with respect to a known baseline or reference frame. Finally, the absolute location can be given using the parameters longitude, latitude, and altitude. Whatever the desired output may be the positioning system needs to rely on accurate parameters or fingerprints at the navigation solution stage to generate a reliable position estimate. Our work focuses on the signal processing stage of a positioning system where the algorithms researched extracts raw noisy inputs from the sensor network and converts them into reliable parameter estimates or location information rich fingerprints, so that the final stage of the system can provide accurate positioning information to the end user in accordance to the desired application scenario.

It needs be pointed out that the actual positioning takes place either on the receiver or the transmitter depending on the network topology utilized. There are four main topologies used in positioning systems [21]. In the first topology, the remote positioning system has a mobile transmitter whose signal is received by several fixed measurement units and the positioning is determined in a master station. The reverse of this, the second topology, is the self-positioning system where the mobile receiver determines its own location based on signals received by fixed transmitters at known locations. In both these cases if the positioning is done using fingerprinting, it is not necessary to have prior knowledge of the locations of the fixed units. As for the final two topologies, if a wireless data link is provided to send the positioning result, from a remote positioning system to the mobile user, it is called an indirect self-positioning system and conversely when the data link provides the remote system with the result derived from a mobile transceiver it is called an indirect remote positioning system. Here it should be pointed out that our work focuses on determining the time delay

estimate or generating the location based fingerprint, irrespective of the network topology at a single link level. This information is then processed by the navigation system at the mobile user, or the remote system, to provide the actual location.

It is not easy to theoretically model the radio propagation in indoor environments because of severe multi-path conditions, Non-LoS conditions, and site-specific parameters such as floor layout, moving objects, and numerous reflecting surfaces. There is no good model for indoor radio multi-path characteristic so far [6]. Therefore various parameter based positioning systems, as well as fingerprinting schemes, have been suggested to provide feasible solutions to the wide variety of scenarios.

2.1 Various Parameter Estimation techniques used for Positioning

We will first examine the various parameter estimation techniques available for indoor positioning in LoS environments. These techniques use triangulation as means of identifying the location of a given user. Triangulation is using properties of triangles to determine target location. It has two derivatives namely lateration and angulation.

2.1.1 Lateration Techniques

In the lateration technique location of the target is determined based on distance to the target from multiple reference points whose location is previously known through surveying techniques. It is also called *range measurement techniques*. Most initial positioning systems including GPS use multi-lateration to determine user

location. Tri-lateration refers to determining location based on three reference points as it is the theoretical minimum requirement for determination of a 3-D coordinate based on range measurements. But as range measurements contain range errors due to various factors such as synchronization errors, multi-path and noise etc. The range estimated using the measured parameter is called a pseudo-range, and rather than a point the tri-lateration results yields an area. Thus multi-lateration, which makes use of more than three range measurements, is used in practice and LS or WLS based techniques are used to determine the navigation solution from the noisy measurements.

All these techniques are referred to as parameter estimation based techniques due to the fact that they resort to measuring a parameter from which the distance can be calculated, rather than direct distance measurement. In localization research, parameters such as TOA, TDOA, RTOF and RSS are used to determine range.

We need to utilize the most accurate and cost-effective parameter estimation technique from the aforementioned lateration techniques. The next phase of the system is of significant importance as well, because what is ultimately desired is a 3-D position estimate. Here we provide a summary of a standard navigation solution based on a linearization scheme utilizing a Taylor series approximation for a TOA based GPS system. This will enable us to better understand the importance of minimizing range errors for parameter based systems. This system can utilize any of the four topologies mentioned previously as its architecture (the basic calculation remains the same while the receiver transmitter notations gets altered). If we are to use a pure TOA scheme, the clock offset of the user will be the fourth variable to be determined, in addition to the 3-D coordinates. This in turn will result in a minimum requirement of four time delay estimates for accurate positioning. If a TDOA based

technique is to be used, as mentioned in [22], the need to synchronize the user clock with the source clocks becomes irrelevant.

Let us consider a case detailed in [23] where the noisy time delay measurements are available from at least four sources, the user position $\boldsymbol{U} = (x_u \quad y_u \quad z_u)$ and receiver clock offset t_u, are to be determined. Here we take the case where the user acting as a receiver does its own calculation. The reverse case where the user is the transmitter is identical in its approach to determine the navigation solution. If $\boldsymbol{S_j} = (x_j \quad y_j \quad z_j)$ is the position of the j^{th} transmitter and ρ_j is the time delay measurement pertaining to the j^{th} transmitter:

$$\rho_j = \| \boldsymbol{S_j} - \boldsymbol{u} \| + ct_u \tag{2.1}$$

$$\rho_j = f\,(x_u, y_u, z_u, t_u) \tag{2.2}$$

Now there are four non-linear equations and four unknowns. Therefore it is possible to either use a tedious closed form solution or linearize the equation set using the Taylor series approximation. In the Taylor series approximation method, LS or WLS approach will be used to obtain the position from the noisy measurements. In the latter case, increase in the number of sources will yield a better position estimate. In both cases an approximate initial solution is used and iterated till a certain convergence bound is met. The matrix formulation of the problem can be summarized as $(for\ n = 4\ case)$:

$$\boldsymbol{\Delta\rho = H\Delta X} \tag{2.3}$$

where,

$\boldsymbol{\Delta\rho} = \begin{pmatrix} \Delta\rho_1 \\ \Delta\rho_2 \\ \Delta\rho_3 \\ \Delta\rho_4 \end{pmatrix}$, H = $\begin{bmatrix} a_{x1} & a_{y1} & a_{z1} & 1 \\ a_{x2} & a_{y2} & a_{z2} & 1 \\ a_{x3} & a_{y3} & a_{z3} & 1 \\ a_{x4} & a_{y4} & a_{z4} & 1 \end{bmatrix}$, $\Delta\boldsymbol{X} = \begin{pmatrix} \Delta x_u \\ \Delta y_u \\ \Delta z_u \\ -\mathrm{c}\Delta t_u \end{pmatrix}$ and Δ denotes the deviation from the linearization point. Note $\begin{pmatrix} a_{xi} \\ a_{yi} \\ a_{zi} \end{pmatrix}$ is the unit vector from the linearization point to the i^{th} transmitter. If the linearization point is close enough to the user from (2.3) we get,

$$\boldsymbol{\Delta X = H^{-1}\Delta\rho} \tag{2.4}$$

Formulating solution in LS fashion yields:

$$\boldsymbol{\Delta X = (H^T H)^{-1}H^T\Delta\rho} \tag{2.5}$$

or WLS:

$$\boldsymbol{\Delta X = (H^T R_n^{-1} H)^{-1}H^T R_n^{-1}\Delta\rho} \tag{2.6}$$

where $\boldsymbol{R_n^{-1}}$ is the covariance matrix associated with the measurement errors. If $\boldsymbol{\rho_T}$ is the vector of error free time delay values, $\boldsymbol{\rho_L}$ is the vector of time delay values computed at the linearization point and $\boldsymbol{d\rho}$ represents the net error in time delay values,

$$\boldsymbol{\Delta\rho = \rho_T - \rho_L + d\rho} \tag{2.7}$$

and similarly,

$$\boldsymbol{\Delta X = X_T - X_L + dX} \tag{2.8}$$

where $\boldsymbol{X_T}$ is the error free position and offset time, $\boldsymbol{X_L}$ the position and time defined as the linearization point, and $\boldsymbol{dX}$ the error in the position and time estimate. Thus:

$$\mathbf{d}\boldsymbol{X} = [\boldsymbol{(H^T H)^{-1}H^T}]\mathbf{d}\boldsymbol{\rho} = \boldsymbol{K d\rho} \tag{2.9}$$

since $(\boldsymbol{\rho_T} - \boldsymbol{\rho_L}) = \boldsymbol{H}(\boldsymbol{x_T} - \boldsymbol{x_L})$**.** Matrix $\boldsymbol{K}$ maps error in time delay measurements to error in computed position and time (neglecting linearization errors). Equation (2.9) is analogous with the relationship:

$$e_{\text{pos}} = e_{geo} \times e_{\text{TOA}} \tag{2.10}$$

where e_{pos} is the overall error in the positioning solution, e_{geo} is the error due to the geometric factor and e_{TOA} is the time of arrival estimation error. This relationship shows the importance of obtaining accurate time delay estimates, as well as minimizing the geometric factor, termed as DOP in popular terminology. The DOP parameters depend on the relative positioning of the sources with respect to the user in 3-Dimentional space. Therefore the reliable TOA estimates obtained utilizing our super resolution techniques, coupled with careful planning at installation of system, will improve DOP results in accurate positioning solutions. It should be noted that the DOP in the vertical and the horizontal planes can be improved by having better spatial diversity among APs and the UE.

2.1.1.1 TOA Techniques

It is widely accepted in the research community that TOA based UWB systems are the most accurate [7] parametric based system in LoS environments. Thus TOA estimation has become the most popular choice for parameter estimation in localization in UWB based, as well as Non-UWB based systems. In TOA based systems the one-way propagation time from AP to UE is used. The distance from AP to UE is directly proportional to the measured DP-TOA parameter as depicted in Figure 2.1. As mentioned in the earlier section a theoretical minimum of three TOA estimates is required for a 3-D position estimate. The actual navigation solution can

use the geometric method of intersection of circles to obtain the position. Practically due to noise in the range measurements the intersection will demarcate a probable area rather than a point. In addition as there is a time offset due to the synchronization error between the clocks in the AP network (an assumption can be made that the clocks in the AP network are synchronized) and the UE, another unknown is added to the navigation solution, thus a minimum of four TOA estimates are needed to obtain a position in the 3-D space. Thus multi-lateration techniques that utilize LS or WLS formulations enable accurate positioning in the presence of noisy measurements.

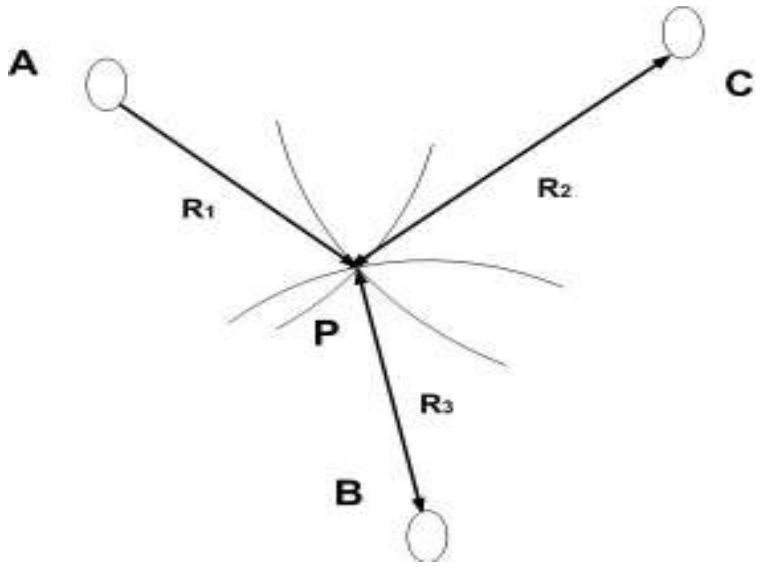

Figure 2.1 Tri-lateration based on TOA measurements

For most systems the speed of light ($c = 3 \times 10^6 ms^{-1}$) is the propagation speed that acts as the proportionality constant binding the TOA estimate with distance. This implies that a slight error in the TOA estimation process even in the order of a few microseconds could result in an error in the order of meters in the position estimate. This makes the accurate estimation of the TOA estimation

parameter paramount. It has been discovered that multi-path is the main source of ranging error for TOA based systems under DDP conditions due to resolution limitations of the time delay estimation techniques [11]. In traditional TOA based indoor geolocation systems we use the inverse fast Fourier transform of the received signal or a matched filter output in a correlation based scheme received above a certain detection threshold to estimate the DP-TOA, and thereby calculate the distance between AP and UE. The direct sequence spread spectrum based techniques in [25, 26] for example utilize such schemes. In a single path ideal environment, the actual expected and estimated DP is the same. However, in multi-path environments where adjacent multi-paths are closely spaced to the DP, the peak of the channel profile is shifted from the expected TOA resulting in a TOA estimation error. This can be solved by utilizing the super resolution techniques newly found in this research work, which can resolve the closely spaced multi-paths effectively, thereby yielding accurate TOA estimates for LoS conditions.

Some economical wireless sensor networks utilize ultra sound and audible sound for localization, while using RF signals for synchronization. The simple wireless sensor network Beep [27] uses audible sound for positioning and wireless LAN for synchronization. DOLPHIN an ultra sound based distributed positioning system with signalling and synchronization done by a RF pulse has been proposed in [28]. Both these systems use simple correlation or counter based peak detection algorithms for the TOA estimation process. Even with such simple methods; for example Beep yields accuracy to within 2 feet in 97% of cases for the 2-D case and a corresponding accuracy to within 3 feet in 95% of cases for the 3-D case. The fact that the speed of sound is significantly less than the speed of light reduces the errors in distances caused by incorrect time delay estimation. This has made such systems

attractive for commercial indoor positioning systems [29]. Ultrasonic and audible sound systems display poor performance under noisy conditions and such occurrences are frequent in indoor environments [30]. Use of noise immune super resolution techniques introduced in our work may significantly improve the performance of such cost-effective systems. Though our work utilizes impulsive type UWB signals in the GHz range for analytical purposes, one need not limit the possibility of application to just UWB based systems. Our emphasis is on constructing robust signal processing techniques that can produce desirable outputs independent of the underlying communication platform.

2.1.1.2 TDOA Techniques

The idea of TDOA estimation is to determine position of the UE by considering the difference in signal arrival times from multiple APs, rather than absolute time of arrival from each AP as done in previous section. For each TDOA estimate, the UE lies on a hyperboloid with a constant range difference between the two APs. The equation of the hyperboloid is given by:

$$R_{i,j} = \sqrt{(x_i - x)^2 + (y_i - y)^2 + (z_i - z)^2} - \sqrt{(x_j - x)^2 + (y_j - y)^2 + (z_j - z)^2} \quad (2.11)$$

where $(x_i \quad y_i \quad z_i)$ and $(x_j \quad y_j \quad z_j)$ represent the locations of the fixed APs i, j and $(x \quad y \quad z)$ represent the UE location. A closed form Non-linear solution to the hyperboloid equation set generated by multiple measurements of (2.11) for various (i, j) AP sets was suggested in [31]. The easier solution is to linearize the equations through a Taylor series expansion and obtain location through an iterative algorithm [32, 33].

A 2-D location can be obtained as depicted in Figure 2.2 by the intersection of two or more hyperbolas. Similarly through intersection of three or more hyperboloids the 3-D location can be obtained. Notice to generate two hyperbolas for a 2-D coordinate 3 APs is required.

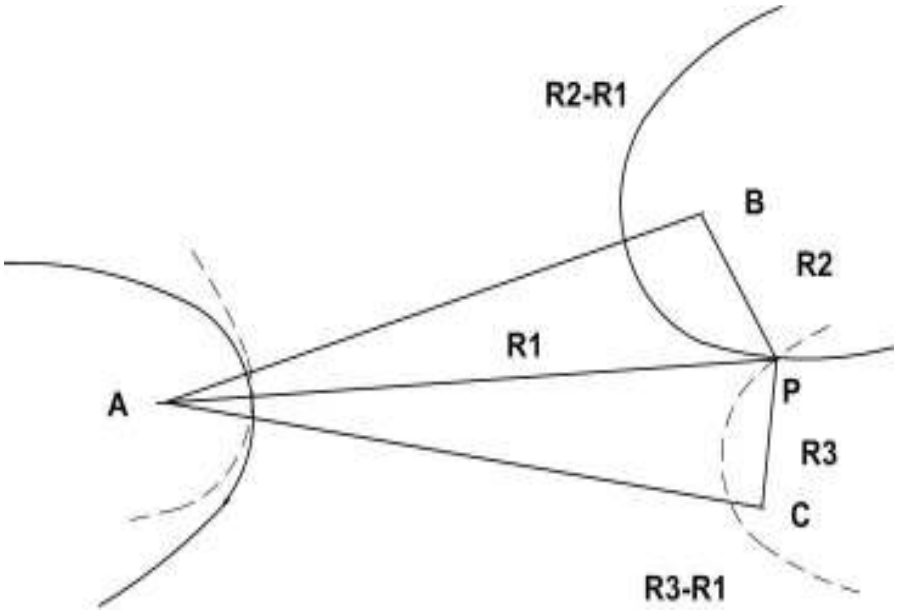

Figure 2.2 Positioning based on TDOA measurements

The TDOA parameters are normally obtained via cross correlation of received signals. If the transmitted signals from the APs are identical and all the AP clocks are properly synchronized the TDOA is obtained from the cross correlation function:

$$\hat{R}_{x_i,x_j}(\tau) = {}^{1}/_{T} \int_0^T x_i\,(t).\,x_j\,(t-\tau).\,dt \tag{2.12}$$

where $x_i\,(t)$ and $x_j\,(t)$ are signal received by UE from AP_i and AP_j. The TDOA is the τ value that maximizes $\hat{R}_{x_i,x_j}(\tau)$. The main advantage of TDOA scheme is that it cancels out the correlated errors between the differenced signal paths. This is very similar to the double differencing concept used in GPS [23]. What this signifies in a practical sense is that there is no need to synchronize the UE or the mobile unit clock

with the fixed AP network clock, as the offset error is cancelled out due to the differencing. As mentioned earlier obtaining the range measurements through super resolution techniques directly and differencing them is more accurate in indoor environments with severe multi-path conditions compared to correlation based methods. As examples of practical TDOA systems, in [8] a multi-carrier UWB system utilizing Prony method and in [22] frequency translator based system utilizing a TDOA scheme is presented.

2.1.1.3 RTOF Techniques

This method measures the roundtrip time traversed by the signal from the UE to the fixed AP and back. The range measurement mechanism and the positioning algorithm can be the same as of a TOA based system. As opposed to the TOA method in this method a more relaxed time synchronization method can be utilized. Even as the mechanism is similar to the operation of radar, the AP is not a passive reflector, hence the existence of a processing delay. The system can be considered as a simple probe request and response system where the AP sends back an acknowledgment to the incoming probe request (see Figure 2.3). The processing delay at the AP is not deterministic, and may result in a large positioning error especially for small range systems. However for long and medium range systems, as the delay is negligible, compared to the transmission time, it can be ignored. In [1] the WLAN standard protocol is utilized to negate the effect of the processing delay. The AP measures the time difference between it receiving the request and it sending the acknowledgment, and transmits that value. The UE can use this transmitted value, and the time difference it measures on its own to cancel out the effect of the processing delay. Another scheme to obtain the roundtrip times of WLANs is presented in [34]. Finally

the concept of modulated reflection can be utilized to obtain RTOF for short range systems [35].

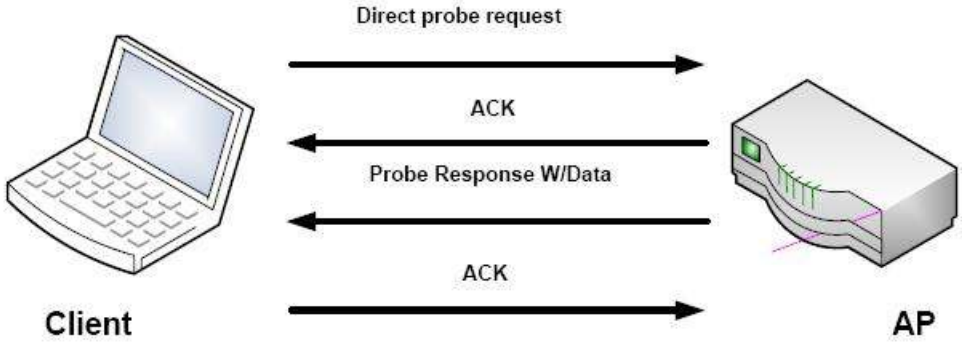

Figure 2.3 Mechanism of a RTOF based system

It should be realized that for all these time delay estimation techniques the measured time delay estimates have to be for the DP. The need for a LoS path between UE and all APs is essential for the success of these methods. If the first dominant path above the defined threshold is not the DP, that would result in a large range error.

2.1.1.4 Received Signal Phase Techniques

The received signal phase methods use carrier signal phase to determine location of target. Signals are transmitted from APs as pure sinusoids with zero phase offset simultaneously. Signal transmitted from AP to UE has a finite transmission delay, which is measured as the phase delay at the UE. The delay translated to distance is measured as a fraction of the wavelength.

$$D_i = \frac{c\phi_i}{2\pi f} \tag{2.13}$$

where $i = 1{:}n$ (n is the number of APs) and $S_i(t) = \sin(2\pi f t + \phi_i)$ are the received signal from i^{th} AP. As long as $(0 < \phi_i < 2\pi)$ i.e. as long as the maximum range measurement is less than the signal wavelength the ambiguity problem can be avoided. Otherwise similar to GPS, the carrier phase ambiguity needs to be resolved through an ambiguity resolution process [23]. Once the phase is known the navigation solution is similar to that of TOA schemes.

2.1.1.5 RSS Techniques

RSS or signal attenuation based techniques attempt to calculate the distance based on the signal attenuation or path loss from AP to UE. Theoretical and empirical models are used to map degradation in signal strength along the propagation path into distance. In [9], the mean received power of the signal is measured for a specific duration:

$$P_R = \frac{1}{t_b - t_a}\int_{t_a}^{t_b} |p(t) * h(t) + n(t)|^2 dt \tag{2.14}$$

The received power P_R is modelled using the transmitted pulse shape $p(t)$ convolved with the channel impulse response $h(t)$. Additionally a white Gaussian noise component $n(t)$ is taken into account. Then the mean decay of the signal strength is modelled using a path loss model such as:

$$P_R = P_0 - 10n log\left({}^{d}/_{d_0}\right) + S \tag{2.15}$$

where P_0 is the power at reference point, d_0 is the distance away from the source, and S is a log normal random variable with zero mean accounting for the large scale fading. As can be noted, the greatest virtue of the RSS technique is its simplicity in theory and its implementation. But the RSS technique suffers severe deviations from

its mean signal strength due to multi-path fading and shadowing. Second, its accuracy suffers greatly with distance, and third, it is very sensitive to the estimated path-loss model parameters. Therefore even with a careful calibration scheme, the RSS technique produces much worse results in terms of accuracy as compared to its counter parts. The accuracy of this method can be improved by utilizing pre-measured RSS contours centred on the AP [36]. In [37] the first path power as well as strongest path power statics have been utilized to obtain reliable position estimates. For LoS environments, it was shown that the first path signal power static provides sub-meter level accuracy for a low complexity positioning system using UWB signalling. Similarly the strongest path static provided a reliable metric for Non-LoS environments, as more location rich information is contained there. This result again highlights the importance of utilizing information provided by the full multi-path profile for localization as suggested in this research work.

A better way of utilizing the RSS technique for positioning is to employ it as a signature for a closest neighbour determination algorithm as employed in [38]. Similar to most signature-based systems, this method produces better results compared to the direct approach, and it uses RSS measurements obtained from multiple APs to improve accuracy. For a system with m APs the pre-calibrated k^{th} reference point entry on the radio map and observed vector are respectively:

$$\boldsymbol{z}\,(x_k, y_k) = [z_{k1} \quad z_{k2} \quad \dots \quad z_{km}]$$

and

$$\boldsymbol{o} = [p_1 \quad p_2 \quad \dots \quad p_m]$$

Then the Euclidean distance vector, which is to be minimized in the closest neighbour algorithm, will be:

$$D_k = \sqrt{\sum_{i=1}^{m}(p_i - z_{ki})^2} \quad (2.16)$$

But the resolution of such an algorithm will be limited by the resolution of the grid defined for the location based fingerprinting system. And its calibration process, as a resultant will be tedious. However location-based fingerprinting schemes are becoming more popular in indoor positioning research and will be covered in more detail in Section 2.2 of this chapter.

As various information obtained from signal strength measurement contain *location rich information* that can be utilized to form linguistic variables. For the fuzzy logic system introduced in [39], a two stage fuzzy logic approach is used for positioning in a WLAN based system. The signal strength parameter used in their application is the SNR. The fuzzy logic system uses, matching between calibration and observation data, of parameters such as mean value of SNR, max value of SNR and standard deviation of SNR for positioning. Parameters which contain *location rich information* can be used as reliable inputs to a fuzzy logic system. This places an added importance on the resultant pseudo-spectrums generated in this work, as they contain location specific details about the surrounding environment through its detailed high resolution multi-path profile.

2.1.2 Angulation Techniques

AOA based methods use the intersection point of several pairs of angular directional lines, each formed by the circular radius from a fixed AP, to obtain the position of the target mobile UE. As illustrated in Figure 2.4 a minimum of two AOA values, from two reference APs, are required to obtain the 2-D location of the mobile UE, according to basic triangulation. Estimation of AOA, known as direction finding,

is accomplished by the use of an antennae array or directional antennae. Although no synchronization is required, these schemes have the disadvantage of requiring relatively large and complex hardware [10]. In addition the location estimate accuracy degrades, as mobile UE moves further away from the reference APs. Finally the accuracy of the AOA estimates of a wireless positioning system will be further limited by the directivity of the measuring aperture, shadowing and multi-path reflections arriving from misleading directions due to the hostile channel conditions prevailing in indoor environments. It should be noted that in certain literature AOA estimation is referred to as DOA estimation. More detailed accounts of these techniques can be found in [40, 41].

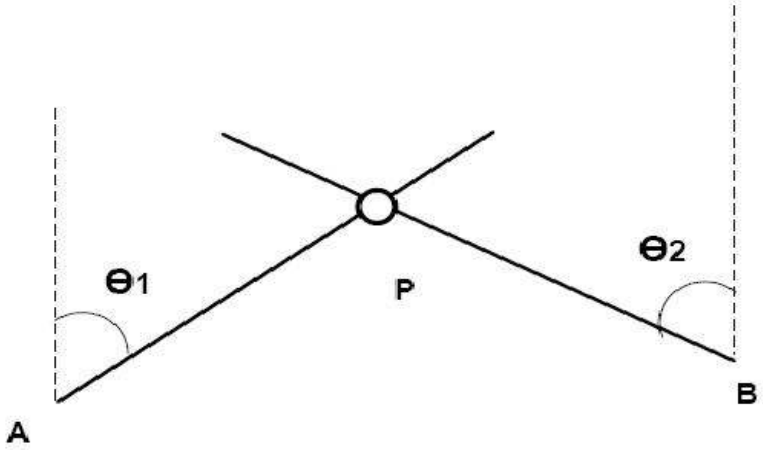

Figure 2.4 Positioning based on Angulation

2.2 Location based Fingerprinting Techniques

Location based fingerprinting refers to positioning methods which first collect features of the surroundings (a fingerprints of the scene) at a pre-defined resolution (see Figure 2.5), stores them in a database, and then matches the information (fingerprint) obtained at a real-time application stage to the closest a priori fingerprint(s) to estimate location. RSS based fingerprints were the first and most popularly used fingerprinting technique due to its simplicity in theory and application. The fingerprint should contain some information from the received signal(s) that are location dependant. There are two main stages in location based fingerprinting:

I. Offline stage (or the calibration stage): A site survey is performed and grid points are decided according to the resolution requirement. After which the coordinates and fingerprints of the respective grid points are collected and stored.

II. Online stage (or the real-time application stage): The UE measures a fingerprint from an unknown location, and uses a matching technique to determine the location, by utilizing the correlations between measured and stored fingerprints.

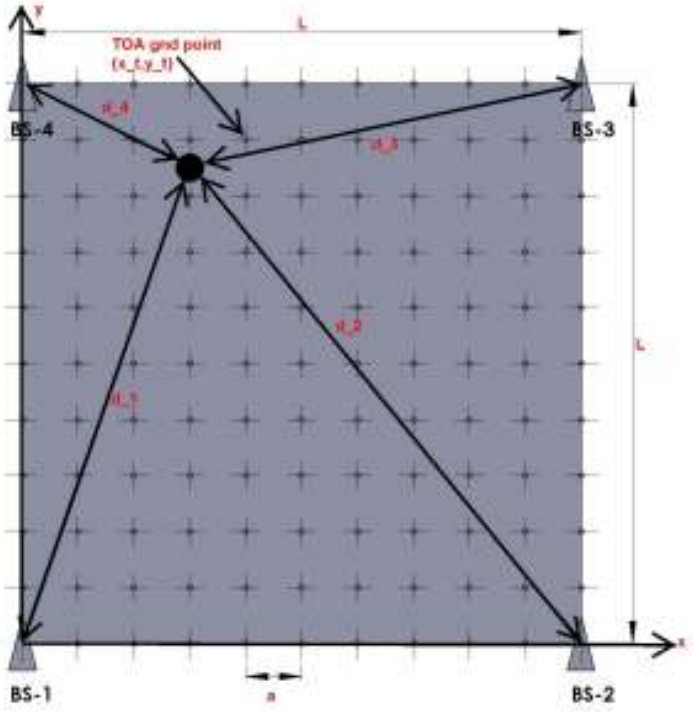

Figure 2.5 Grid point distribution for a location based fingerprinting technique

As classified and analyzed in detail in [7, 11] the indoor channel can be broadly categorized into DDP, NDDP, UDP and NC cases. For the first two cases in this classification, the DP is detectable. Thus standard time delay estimation based localization techniques can be applied with reasonable accuracy, while the super resolution based techniques introduced in this thesis may be used to further minimize the ranging error. As the NC case simply implies that there is no coverage, since no detectable signal is received by the user (the total power is below threshold), therefore it is not analyzed or addressed further in our discussions.

Location based fingerprinting techniques were first introduced due to the existence of the UDP cases. UDP condition occurs when the average received power of the DP falls below an established threshold. The UDP case was first observed in [43]. In detectable DP environments, the TOA of the first detected path is close to the

TOA of the DP, resulting in smaller range errors. Whereas for UDP conditions where the DP is below the detectable threshold, time delay estimation techniques can result in large errors, because AP to UE distance is estimated by using time delay parameters obtained from a Non-LoS path as illustrated in Figure 2.6.

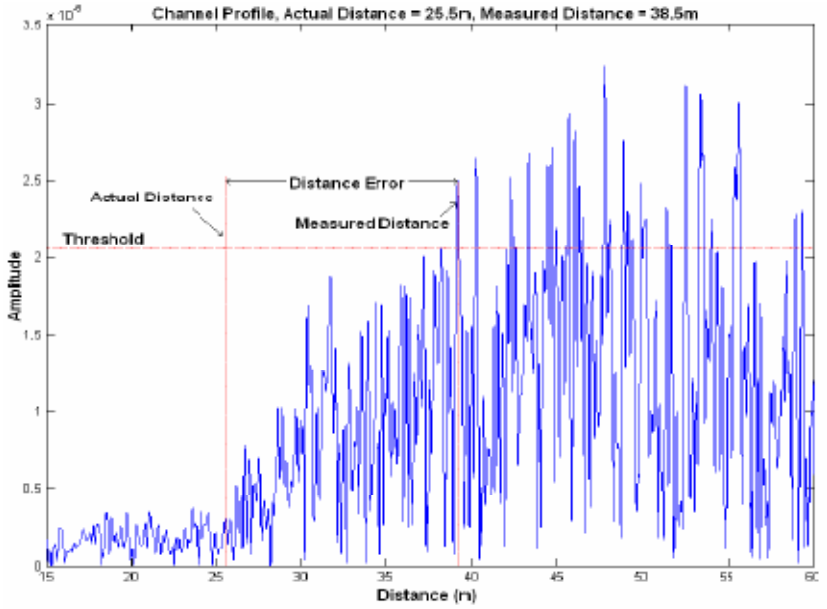

Figure 2.6 UWB channel measurement for UDP case resulting in a large range error for time delay estimation techniques (*image taken from [7]*)

It is identified that the UDP case can be subdivided as NUDP (Natural UDP) and SUDP (Shadowed UDP). NUDP conditions occur when the direct path fades below the threshold. In this case the DP is not detectable anymore, but the next detectable path is within the same cluster as the DP. As this path is relatively closer to the DP this condition results in smaller range errors. For the SUDP case unlike the NC scenario, the total power received is sufficient to establish a communication link between transmitter and receiver. Nevertheless, the entire first cluster which contains the DP is blocked. This results in a much larger range error from time delay

estimation techniques, which now rely on a Non-LoS path from the next cluster to conduct the range estimation. Normally for these SUDP scenarios the first cluster of paths containing DP is totally blocked by metallic obstacles, such as elevator shafts, metal chambers, metal doors etc. The distribution of these scenarios on an indoor environment with walls as well as a metallic object is illustrated in Figure 2.7. This was obtained from research work conducted in [11]. This visualizes the severity and impact of UDP cases in indoor environments. The SUDP case was generated by placing a metallic object parallel to the vertical axis.

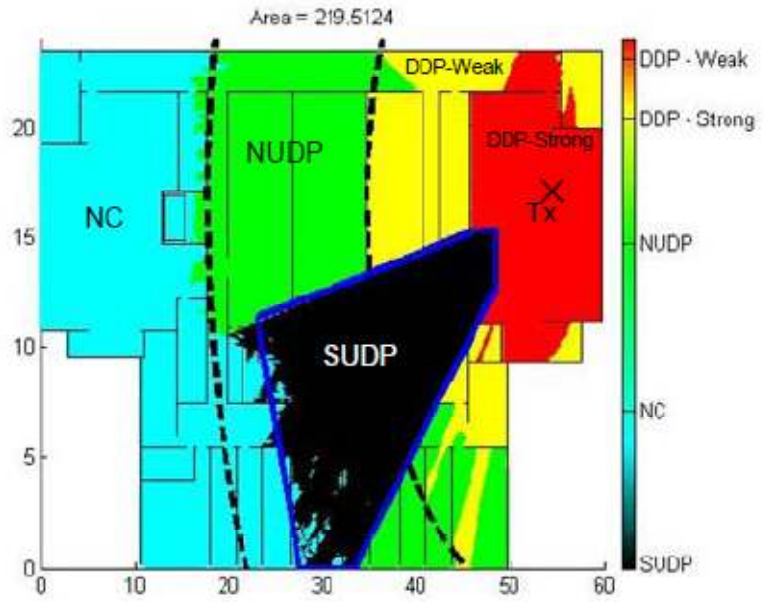

Figure 2.7 Distribution of various channel conditions on an indoor environment (*image taken from [11]*)

Therefore our work which attempts to present a viable solution for both LoS and Non-LoS conditions, through the same signal processing algorithm, is of great practical importance, as it enables the same underlying technology to be used in a different manner, when transferring from a DDP to UDP environment. In the

proceeding sections of this chapter, elaborations of various location-based fingerprinting techniques will be presented, so that the importance of selecting proper *location-based fingerprints with location rich information* can be fully appreciated.

RSS based fingerprints have been the most popular approach in initial fingerprinting related work, as comprehended in the earlier Section 2.1.1.5. There it was presented, how an m-dimensional RSS based vector was constructed for each of the grid points, based on RSS values obtained from $'m'$ APs. These vectors were stored in a database, and then matched with the m-dimensional observation vector, using a Euclidean distance minimization scheme to obtain the current location of the UE [38]. In [44], RSS values obtained from APs in an existing wireless LAN were used to construct a radio map to obtain positioning estimates. Similarly a TOA based vector can be utilized as a location-based fingerprint, as done so in the CN-TOAG algorithm implemented in [45]. Here the range values calculated from TOA estimates of four APs are used to construct a basic fingerprint. Similar to the RSS based vector scheme mentioned before, a Euclidean distance minimization is used for fingerprint matching. The accuracy of the location estimate will be highly dependent in the granularity of the TOA grid. The granularity of the grid can be increased for better accuracy at the expense of database size, thus increasing the computational time of the estimation algorithm.

It should be noted that the fundamental reason for opting for a fingerprinting based positioning scheme, was to achieve better positioning accuracy in NLoS conditions. It is not simply another option to be used instead of TOA estimation for LoS conditions, as was the case with most of these approaches mentioned above. This implies that making an assumption that the received fingerprint may contain information about the DP is not prudent. Therefore the location based fingerprint

utilized should be selected, such that it contains location specific information even for NLoS cases where the DP is absent. In addition, similar to the parameter based estimation techniques, the RSS or TOA vector based schemes rely on multiple APs, for generation of a fingerprint. Also it is known that the DP-TOA and RSS values are not reliable parameters in their raw form for localization in indoor environments with severe multi-path conditions.

In [46] a novel approach utilizing the spatial power spectrum of the received signal was used to form the fingerprint. The receiver was equipped with a circular antenna with beam forming capability, so that the direction of its main beam can be steered towards any desired angle. The antenna beam was rotated 360 degrees around the field of view to construct the spatial power spectrum. The spatial power spectrum obtained, even with a single transmitter, had a unique shape for each grid point, thus making it a more location information rich fingerprint as compared to previous methods. Thus comparable positioning accuracy can be obtained even with the use of one or two APs. Other methods mentioned before in this section, were shown to yield large positioning errors, when the number of APs are reduced. This is due to the lack of *location rich information* contained in a fingerprint generated using just RSS or TOA values for a single AP measurement. The added benefit offered by this work was that, for the first time, an actual image was used as the location signature. Thus image matching techniques such as EMD can be utilized for the fingerprint matching phase. EMD was introduced in [47] as a distance metric with applications in content-based image retrieval. The ability of this metric to match perceptual similarity better than others, makes it an attractive method for localization applications. EMD measures the minimum cost that must be incurred, to transform one signature to another, as the basis of its matching technique. This work allowed us for the first time

to entertain the possibility of using the pseudo-spectrums generated in our work, as possible inputs for location-based fingerprinting schemes. The detailed noiseless multi-path profiles generated using super resolution techniques (discovered in this research work) provide the best means of identifying a given grid point uniquely, based even on a single AP measurement. Hence the resultant pseudo-spectrums generated in this thesis, can be reasonably assumed to contain the *location rich information* much needed for a robust location-based fingerprinting technique for indoor localization.

Various other systems have been proposed by researchers, which utilize the location dependant information of fingerprints for localization in a variety of ways. Linguistic *location dependant variables* are formed based on signal strength measurements; to implement a two-stage fuzzy logic based fingerprinting system in [39]. In [48] a MLP network with one hidden layer is used for a neural network based positioning system.

The MLP network mentioned above is trained to produce 2D/3D co-ordinates based on signal strength dependant inputs. There it was observed the *k*-nearest neighbour based methods achieve results similar to the results of the neural network based method. We feel that the absence of *location rich information,* which takes into account the complex dependencies between signals and position in the input signature, is the reason for this observation. Only RSS values from a few APs were used as the inputs in this method. Therefore our pseudo-spectrum output, which contains detailed multi-path profile information of the environment, as seen from the receiver, is an ideal input candidate for this neural network-based system. The *location rich information* present in this signature may allow the neural to capture the complex dependencies between signals and position more effectively. Even for the

fuzzy logic-based systems, the more *location rich information* input variables capture, the more accurate the system will be. The reasoning behind this is similar to the principle used in robotics for environment recognition [49]. The more information the signature contains, the more unique and location dependant it becomes. Thus, what is presented here as the resultant pseudo-spectrum output of our super resolution algorithm, can actually be thought of as the *ultimate location information rich fingerprint* for radio map construction, under non-LOS conditions. Now we shall present the basic types of location-based fingerprinting algorithms that use pattern reorganization for localization.

2.2.1 Probabilistic Method

This method considers the presence of $'n'$ possible location candidates. Its decision rule is defined by:

$$Choose\ L_i\ if\ P\ (\boldsymbol{C_i} \mid \boldsymbol{o})\ >\ P\ \left(\boldsymbol{C_j} \mid \boldsymbol{o}\right) \tag{2.17}$$

for $\forall\, j$ where $i\ \neq j$;

and,

n is the size of fingerprints stored in database during off-line phase;

$\boldsymbol{C_i} \forall\ [\,1\,, n\,]$ are the possible location candidates;

$\boldsymbol{o}$ is the observed signal strength vector;

$P\ (\boldsymbol{C_i} \mid \boldsymbol{o})$ is the probability US is in location $\boldsymbol{C_i}$ given observation vector was $\boldsymbol{o}$;

$P\ (\boldsymbol{C}_i)$ is the probability of UE being in location $\boldsymbol{C_i}$.

Now using Baye's rule, the decision rule can be restructured as below, if the probability of the UE on each grid point is identical.

$$\text{Choose } L_i \text{ if, } P(\boldsymbol{o} \mid \boldsymbol{C_i}) > P(\boldsymbol{o} \mid \boldsymbol{C_j}) \tag{2.18}$$

where,

$P(\boldsymbol{o} \mid \boldsymbol{C_i})$ is the probability signal vector $\boldsymbol{o}$ is received given that UE is at $\boldsymbol{C_i}$.

Assuming each location candidate to be Gaussian, the mean and standard deviation of each candidate can be calculated. If each of the AP measurements is independent, the overall likelihood of each candidate can be obtained by multiplying the likelihoods for each AP measurement value for that particular candidate. Localization based on probabilistic methods for wireless networks have been discussed in detail in [50].

Further, the accuracy of grid based fingerprinting schemes are limited by the granularity of the grid. Therefore a weighting approach can be utilized for position estimation, which in turn enables us to obtain a location result between grid points. This can be done by weighting the likelihood of each candidate with its coordinate.

$$(\hat{x}, \hat{y}) = \sum_{i=1}^{n} P(\boldsymbol{s} \mid \boldsymbol{L_i}).(x_{\boldsymbol{L_i}}, y_{\boldsymbol{L_i}}) \tag{2.19}$$

2.2.2 kNN Weighted Averaging Methods

In this approach the N-D Euclidean distance from the observation vector to the fingerprints on the database are first calculated. Then the k closest neighbours are chosen, and the final position is obtained by averaging them in signal space directly, or by weighting them based on Euclidean distance and averaging them. Even for a method that uses something other than N-D Euclidean distance as the matching parameter, still the parameter defined can be used to determine the k-closest

neighbours and the weighting can be done in a similar manner. The parameter 'k' should be decided based on the situation, as it is a key tuning parameter for the system. This method has its advantages based on the assumption that 'k' neighbours cannot be all deviated from the general vicinity of the actual UE position. In addition it also removes the grid granularity constraint on performance to some extent, but introduces 'k' as an additional parameter that determines system performance. In our case as actual details of the environment are included in the location based fingerprint this increases the chances of the fingerprint to match perceptual similarity. This ability implies that the resultant pseudo-spectrum outputs of our super resolution algorithms can utilize interpolative techniques such as kNN weighted averaging method more effectively to enhance performance.

2.2.3 Neural Network based Methods

As mentioned previously, neural network based methods have being proposed for localization based on fingerprints [48]. The location-based fingerprint, and the coordinates of the grid points, is the inputs and targets during the off-line training phase of the neural network. MLP network with one hidden layer is used, and the weights are obtained at the training phase. Input signature is first multiplied by the input layer weight matrix and bias is added if chosen. After passing through the hidden layer transfer function, the output is multiplied by the trained hidden layer weight matrix and a bias is added. The output of the MLP network as specified will be the estimated coordinates of the UE. The neural network strives to capture the complex dependencies between the coordinate and the signature, during the training phase, so that all the location information of the signature can be effectively used for

positioning. This underlines the importance of choosing a location information rich signature that can feed much location dependant information to the neural network for accurate positioning.

2.2.4 SVM Methods

Support Vector Machine is a new technique for data classification and regression with a lot of promise. It is a great tool for machine learning, as well as statistical analysis, hence it suits for classification and regression applications, making it ideal for localization based on fingerprints. SVM has already been used in wide variety of applications in science, engineering and medicine [51, 52]. The theoretical background on SVM can be found on [53, 54]. These techniques have also been used in location based fingerprinting [55, 56].

2.2.5 SMP Methods

This method is used for location-based fingerprinting systems that utilize multiple APs. In the online phase it creates a candidate pool for each of the APs independently. Considering a case where there exists M APs, an M-vertex polygon is created by one candidate from each of the AP pools. The M-vertex polygon with the minimum perimeter is assumed to contain the UE, thus the coordinate of the shortest M-vertex perimeter is then averaged to obtain the location of the UE. This method has been used for localization [57].

2.3 Proximity Algorithms

These algorithms provide symbolic positioning information using a dense grid of APs with known locations. In this method when an AP detects the UE, we assume that the UE is now in the general vicinity of that particular AP. If more than one AP detects the UE it is assumed that the UE is attached to the AP with the strongest signal. This method is extremely simple to implement and can only be used to provide a general idea about the UE location. Systems which use Cell-ID or RFID for localization are examples of this method. They can only provide information such as which room or cell a user is in.

2.4 Technologies used for Indoor Localization

Now we discuss some of the popular technologies used for indoor localization systems in research as well as commercial sector.

2.4.1 GPS based methods

GPS and its differential modification, DGPS [58] are some of the most successful and popular outdoor positioning systems. However, limitation of satellite vehicle signal reception in heavily urbanize areas, due to high rise buildings and poor coverage of GPS satellite signal for indoor environments, decreases its accuracy and limits its performance. In addition, the GPS system which was designed mainly for outdoor environments, with clear LoS between satellite and receiver, does not operate

well under the severe multi-path conditions and Non-LoS conditions prevailing in indoor and underground environments.

In both research and commercial sectors, for indoor location estimation, a wide array of solutions based on GPS technology has been explored in the last decade or so. One of the solutions proposed is the weak signal GPS receiver. The integration time of the GPS receiver is increased so that the weak GPS signal with a low SNR can be acquired [59]. This comes at the cost of very slow acquisition times (due to the extensive search) or the need of aiding data such as rough position, which have to be provided by other networks. For instance, a wireless handset is used to collect location information from both the GPS constellation and a wireless mobile network in certain assisted GPS applications. These measurements are then combined at the location server to provide a positioning solution.

Pseudolites (Pseudo-satellites) work like real GPS satellites using a distinct Gold code to make them appear unique within the environment in which it is used. For the GPS receiver the pseudolite appears as yet another GPS satellite. However, the hardware associated with such a system is expensive. In addition, exact time synchronization of the different pseudolites is paramount. Such systems have been popular for aircraft landing systems, as they provide the added increase in Horizontal-DOP required for a rapidly converging solution, which is essential for such applications. However for indoor applications, as pointed out previously, the added complexity in design and the higher costs, limits its commercial viability.

Further, the use of a GPS repeater that transmits a repeated GPS signal in its own disjointed time slot [60, 61] after acquiring the original signal from a roof antenna has been proposed (see Figure 2.8). The GPS position obtained from each repeater is the same as long as they are all connected to the same roof antenna.

Therefore, the clock bias with respect to each repeater is calculated, and, as the repeater positions are pre-determined, the position of the UE relative to the roof antenna can be obtained. This combined with the initially obtained roof antenna location yield the position of the UE. In [22] an alternate repeater based system that uses a translated carrier frequency on the 2.4 GHz ISM band was suggested.

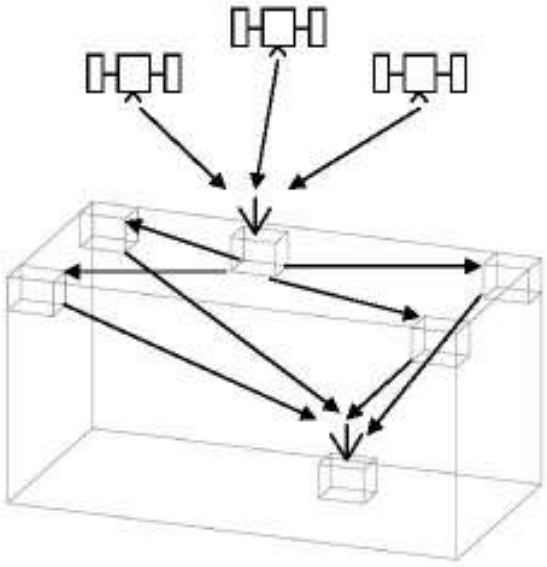

Figure 2.8 Indoor Positioning using GPS Repeaters

Even for these techniques the underlying position determination technology is GPS, a technology that relies on conventional time of arrival (TOA) estimation techniques, designed with channel conditions prevailing in outdoor environments in mind. Thus, they may also be error prone in the presence of severe multi-path conditions prevailing in indoor environments. Therefore research interest for Non-GPS based positioning systems has grown significantly.

2.4.2 RFID Methods

RFID methods store and retrieve data through electromagnetic transmission to an RF compatible unit [62]. RFID system has several basic components, which include a number of RFID readers, RFID tags, and the communication facility between them. The RFID reader is able to read the data emitted from RFID tags. RFID readers and tags use a defined RF and protocol, to transmit and receive data. RFID tags can be either passive or active.

Passive RFID tags acts as a passive element that reflects the signal transmitted to them from a reader, and adds information by modulating the reflected signal. They are much lighter, smaller in size, less expensive than the active tags and operate without a battery. They make use of LF, HF, UHF and microwave frequencies. The active tags are effectively transceivers that can transmit their own ID and other additional data to an interrogation unit from the RFID network. They use both UHF and microwave frequencies. The active RFID has much longer range, hence being suitable for tracking high unit value products moving in a harsh assembly processes. The SpotON [63] RFID technology, a well known technology, uses radio signal strength for 3-D location sensing. SpotON tags use signal strength to estimate inter-tag distances: exploit density of tags and correlation of multiple signals to improve accuracy. Location sensing is done by homogenous sensor nodes, in an Ad Hoc manner, without a central control. Another RFID location sensing system, LANDMARC [64], uses extra fixed location reference tags to help location tuning, thereby increasing accuracy without additional readers.

2.4.3 Cellular based Methods

Many systems have used cellular mobile networks to obtain location of outdoor clients. Accuracy of methods using Cell-ID or enhanced observed time difference are generally low ranging, in the range of 50-200m depending on the cell size. The accuracy of this method in general is much higher in dense urban areas as opposed to rural areas [65].

Indoor positioning using a cellular mobile is possible if several base stations cover the building in question, or a signal from a single base station with strong RSS is received by mobile users. In [66], a GSM based indoor localization system is presented with the use of wide signal strength fingerprints. The method uses readings from multiple GSM cells, and readings of additional GSM channels, which are strong enough to be detected, yet too weak for communication. The system uses signal strength fingerprints, and the kNN technique to achieve media accuracy within a floor of about 2.5 m. These same techniques can be applicable to IS-95 CDMA and 3-G mobile networks.

2.4.4 UWB Solutions

UWB systems send ultra-short pulses less than 1ns in duration with a low duty cycle (typically 1:1000), thus translating in to an UWB in the frequency domain. UWB signals are transmitted for a much shorter duration than those in other conventional systems. The UWB tags consume less power, and can operate in a broader spectrum. UWB can be used in close proximity to other systems with low interference, due to differences in signal types and the spectrum used. The UWB signal passes easily through walls and, clothing, however, liquid and metallic material

cause interference. As mentioned before it is widely accepted in the research community that TOA based UWB systems are the most accurate [7] parametric based system for use in LoS environments. Thus, UWB is a popular choice especially for time delay estimation techniques in indoor environments.

2.4.5 WLAN (IEEE 802.11) Systems

With a typical gross bit rate of up to 108 Mbps, and range of 50-100 m, IEEE 802.11 is currently the dominant wireless protocol standard. The midrange WLAN operating in 2.4 GHz ISM band, has become very popular in hotspots and enterprise locations in recent years. Therefore, it has become appealing for indoor localization researchers to use the existing WLAN infrastructure with the addition of an additional location server.

The properties of the standard WLAN protocol were utilized to negate the effect of the processing delay in a RTOF based systems in [1]. The fact that the AP transmits its own delay in acknowledging a probe request enables the client to remove the processing time from the measured RTOF value.

The fact that the RSS parameter is included in the WLAN protocol, makes RSS based localization a convenient choice for localization in WLANs. For example in [44], the in-building WLAN based user system adopts a closest neighbour in signal space technique, similar to the kNN approach. The RSS values obtained in the off-line phase were used to construct a radio map to acquire position estimates. In addition they also introduced a propagation modelling approach that utilizes a *wall and floor attenuation factor* based model, rather than an outdoor fading model to improve accuracy to about 2-3 m.

Systems proposed in [67, 68] use probabilistic methods, proposed previously, for localization. The location candidate with the highest likelihood is chosen. Increasing the number of samples at each grid point is shown to improve accuracy. This is because an increase in the number of samples used, results in an increases in the reliability of the mean and standard deviation estimates of the Gaussian distributions estimated at each grid point. Further, a grid based Bayesian localization method for a small region, and a probabilistic approach, was used to estimate device location for WLAN networks proposed in [69, 70] respectively.

In [71], a neural network based approach was proposed for localization in WLAN networks. They had adopted an MLP architecture, with a one-step secant training method. With only five samples of RSS values in each grid point, they were able to achieve an average distance error of 3m. Authors of [72] compared the neural network based approaches, with probabilistic, and nearest neighbor approaches, to determine that the neural networks give 1 m error 72% of the time.

2.5 Application Scenarios

Indoor positioning applications are wide ranging; spanning from security and defence, to commercial, entertainment, exploration, underground mining, search and rescue operations, all the way to location based file sharing. The development of context-aware networks has increased the importance of localization technology; such networks utilize user location information and the content information surrounding the user, for numerous applications.

In the field of security, indoor positioning systems can provide vital information by tracking personal and/or important cargo/devices in airports, where

GPS is incapable of meeting such requirements. Assistance can be offered to the visually impaired, through location and context-aware networks, for object identification, indoor navigation (obstacle detection) and for carrying out other certain tasks while indoors.

The underground mining industry stands to gain a great deal from Non-GPS positioning applications as well; the underground positioning problem is analogous to the indoor problem in many ways. Mines may run for many kilometres underground, making access to various locations both time consuming, and complicated (see Figure 2.9). The importance of localization within a mine is of significant importance, and relates to both people and as well as machines. Out of many potential uses of positioning tracking mobile vehicle movements of haul trucks, determining precise location of individuals (e.g., during surveying) and machinery such as drill bits, shovel buckets, and bulldozer blades are a few that are essential to this industry [73]. In addition, for search and rescue operations carried out in mines in case of emergencies, accurate and efficient tracking of rescue personal, estimation of the possible locations of victims, and the suggestion of possible pathways through the tunnels for rescuers to expedite the search and rescue operation, are of paramount importance.

Figure 2.9 Underground Mine (*image taken from [73]*)

Another application would be, coupling an individual's file access on a wireless network with his/her current location on the premises, thus restricting access to sensitive material, by providing access only while the person is within a high security area. For example, if an individual enters a certain institute, upon entry, the user is classified as a standard visitor and given access only to general introductory documentation relating to the institute. Now, if he/she enters a specific division or laboratory area, he/she is given access to documents relating to that specific section or lab technology. Further, the institute may only allow access to certain confidential files, if the user is located in specific areas within the institute. These areas may only be accessible to high clearance persons.

Asset management is another area that will benefit from location aware technology. It will enable tracking of digital devices within a cooperate structure. For example, it enables the system to ascertain whether certain devices have been moved within the premises. This technology will also be useful for locating medical devices in a hospital. RFID technology is used for detection of products stored in a

warehouse, for inventory management. All of these can be done successfully through careful integration of asset databases with positioning systems.

Fire fighters and police personnel can be aided by indoor positioning applications in search and rescue missions. More importantly, in cases where one needs to keep track of his/her own piers or subordinates, for effective execution of safe recovery manoeuvres similar to the requirements in underground mining rescue operations.

Indoor positioning has a significant place in the digital home as well. For example, a location aware laptop can determine the existence of communicable digital devices in the home. A location aware tag can be used to track a child's location at all times in a populated indoor arena.

Underwater mining and exploration can also benefit from SONAR-ID systems based on a principle similar to an effective indoor positioning application.

Location-based advertisements can ensure buyers to selectively receive promotional advertisements and information, by strategically placing messaging near where buyer behavior can be most effectively influenced. For instance, a user will receive coupons only when he/she enters a shopping mall or receive promotional tour offers only when close to a travel agency.

On the other hand, location based social networking will further enhance, internet based social networking such as Facebook, Friendster, Hi5, MySpace, Orkut, etc. by allowing users additional information about user location to enhance the networking experience. Location-based security systems essentially allow additional protection through both user/password and location information. For example, a malicious user who had successfully hacked the system's password will not be granted access to the system through location information acquired about the position

of the legitimate users of the premises or the system. If the legitimate users of the premises or system are detected to be out of the range of a pre-defined area for entry allowance the hacker will be denied access. Also, indoor tracking of people and assets are particularly useful for lost-and-found applications e.g., finding cars in a large parking lot. Location based hand-offs for wireless indoor networks and location based routing for ad hoc networks are some other possible application scenarios.

Aforementioned example applications, offered by location awareness, will enable ubiquitous and context aware network services, which necessitates the location of the wireless device, to be accurately estimated under any environment. One of the key challenges in order to realize these applications in GPS denied environments, with high location accuracy, is the efficiency and preciseness of localization under both LoS and NLoS scenarios.

Chapter 3

Theoretical Background

The analysis of the theoretical foundations of the four super resolution algorithms introduced in this research work, namely the TD-MUSIC, the FD-MUSIC, the FD-EV and the TD-EV algorithms are stated below. The MUSIC super resolution algorithm as described earlier in this thesis has two main variants, TD-MUSIC and FD-MUSIC, for TOA estimation applications, with the fundamental difference between them being the domain of operation. In addition, the FD-EV method in which the denominator of the objective function is de-weighted by the corresponding Eigen values is also introduced. The de-weighing, though primarily suggested to eliminate the spurious nature of the pseudo-spectrum, was found to have other positive implication for an indoor positioning framework. While FD-MUSIC is analogous in its basic structure to the MUSIC algorithm in spectral estimation, the TD-MUSIC is in fact a new innovation with its own unique characteristics and added versatility. Finally the TD-EV method is introduced, which has *inherited the best of both worlds*. It has the versatility of the TD-MUSIC algorithm and the special attributes of the FD-EV method. This chapter details the theoretical foundations of all four of these techniques, whose behaviours and attributes will be analyzed further in later chapters. Then a mathematical model for the use of the ESPRIT algorithm for time delay estimation is introduced. Finally, a procedural analysis on the practical limitations, possible remedies for these limitations, and a summary of diversity techniques available for practical indoor positioning systems is presented.

3.1 Indoor Channel Model

The multi-path indoor channel model for the presence of $'M'$ dominant multi-paths:

$$h(n) = \sum_{m=1}^{M} \alpha_m \delta(n - \tau_m), \quad (3.1)$$

$for\ n = 1 \rightarrow N,$

where

α_m is the path gain for the m^{th} signal path,

τ_m is the path gain for the m^{th} signal path.

Consider the q^{th} realization for the received signal under multi-path and AWGN conditions:

$$y^q(n) = \sum_{m=1}^{M} \alpha_m^q s(n - \tau_m) + w^q(n), \quad (3.2)$$

$for\ n = 1, .., N.$

It is assumed that path delays in adjacent snapshots (realizations) or diversity branches remain unchanged.

$w^q(n)$ is the n^{th} white Gaussian noise sample of the q^{th} realization.

3.2 TD-MUSIC Algorithm

Equation (3.2) can be represented in matrix form for a time domain sample window of length *N* as:

$$\boldsymbol{y^q} = \boldsymbol{S\alpha^q} + \boldsymbol{w^q}, \tag{3.3}$$

where

$\boldsymbol{y^q} = [y^q(1) \quad \dots \quad y^q(N)]^T_{N\times 1}$,

$\boldsymbol{\alpha^q} = \left[\alpha_1^q \quad \dots \quad \alpha_M^q\right]^T_{M\times 1}$,

$\boldsymbol{w^q} = [w^q(1) \quad \dots \quad w^q(N)]^T_{N\times 1}$,

and

$\boldsymbol{S} = [\underline{s}(n-\tau_1) \quad \dots \quad \underline{s}(n-\tau_M)]_{N\times M}$,

where the time domain generalized signal vector is defined as:

$$\boldsymbol{\underline{s}(n-\tau_i)_{N\times 1}} = [s(1-\tau_i) \quad \dots \quad s(N-\tau_i)]^T. \tag{3.4}$$

As can be noticed the signal vector $\boldsymbol{\underline{s}(n-\tau_i)_{N\times 1}}$ is a time shifted version of the original transmitted signal with the time shift corresponding to the time delay variable.

Then the auto correlation matrix $\boldsymbol{R_{yy}}$ in the time domain is formulated for the received signal $y(n)$.

Let, $\boldsymbol{s_i = \underline{s}(n-\tau_i)}$,

and if the auto correlation matrix is defined as below from (3.3):

$$\boldsymbol{R}_{yy} = E\left[\boldsymbol{y}^q \boldsymbol{y}^{q^T}\right] = \boldsymbol{S}\, E\left[\boldsymbol{\alpha}^q \boldsymbol{\alpha}^{q^T}\right] \boldsymbol{S}^T + E\left[\boldsymbol{w}^q \boldsymbol{w}^{q^T}\right],$$

as $E\left[\boldsymbol{\alpha}^q \boldsymbol{w}^{q^T}\right] = E\left[\boldsymbol{w}^q \boldsymbol{\alpha}^{q^T}\right] = 0.$

this can be rewritten as:

$$\boldsymbol{R}_{yy} = \boldsymbol{SPS}^{\boldsymbol{T}} + \sigma_w^2 \boldsymbol{I}_{\boldsymbol{N}\times\boldsymbol{N}}, \tag{3.5}$$

where $E\left[\boldsymbol{w}^q \boldsymbol{w}^{q^T}\right] = \sigma_w^2 \boldsymbol{I}$ and $E\left[\boldsymbol{\alpha}^q \boldsymbol{\alpha}^{q^T}\right] = \boldsymbol{P}$,

where E[.] is the expectation operator.

Matrix $\boldsymbol{P}$ is of rank M and positive definite and symmetric and theoretically of Toeplitz form. The surface plot of such an ACM is depicted below in Figure 3.1. Thus for $N \geq M$:

$$\boldsymbol{P} = \sum_{i=1}^{N} \mu_i \boldsymbol{v}_i \boldsymbol{v}_i^T = \sum_{i=1}^{M} \mu_i \boldsymbol{v}_i \boldsymbol{v}_i^T \tag{3.6}$$

$$\boldsymbol{R}_{yy} = \sum_{i=1}^{M} \mu_i \boldsymbol{v}_i \boldsymbol{v}_i^T + \sum_{i=1}^{N} \sigma_w^2 \boldsymbol{v}_i \boldsymbol{v}_i^T \tag{3.7}$$

$$\boldsymbol{R}_{yy} = \sum_{i=1}^{M} (\mu_i + \sigma_w^2)\, \boldsymbol{v}_i \boldsymbol{v}_i^T + \sum_{i=M+1}^{N} \sigma_w^2\, \boldsymbol{v}_i \boldsymbol{v}_i^T = \sum_{i=1}^{N} \lambda_i \boldsymbol{v}_i \boldsymbol{v}_i^T, \tag{3.8}$$

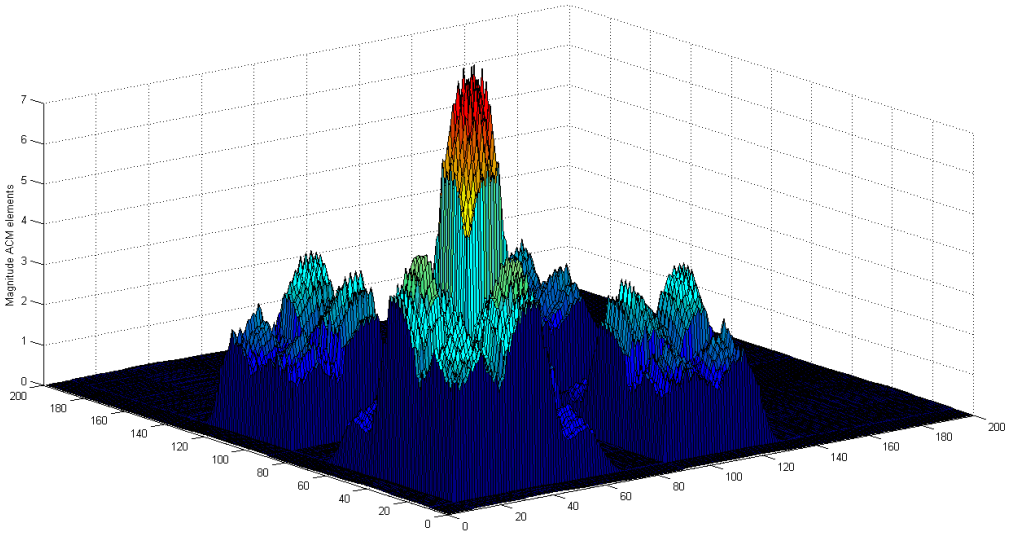

Figure 3.1 Surface Plot of $\boldsymbol{R}_{yy}$

where $\lambda_i \; for \; i = 1{:}N$ are the principle Eigen values of the auto correlation matrix. Therefore from (3.8) the Eigen values of $\boldsymbol{R}_{yy}$ will be such that, theoretically $\lambda_1 > \lambda_2 \ldots \lambda_M > \lambda_{M=1} = \cdots = \lambda_N = \sigma_w^2$. A simulated Eigen value spread of $\boldsymbol{R}_{yy}$ for 10 dominant signal paths is plotted below in Figure 3.2.

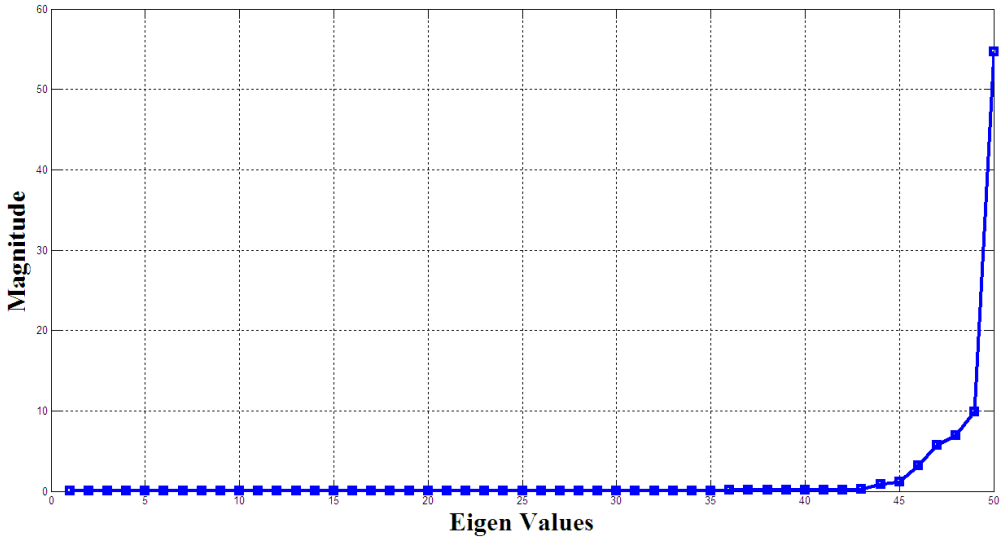

Figure 3.2 Eigen value spread for 10 significant signal paths

Next, Eigen decomposition is performed on the auto correlation matrix. Now the M Principle Eigen vectors will correspond to the signal subspace, where as the Eigen vectors corresponding to the smallest $N - M$ Eigen values span the noise subspace. Hence,

signal subspace : $\boldsymbol{U}_s = [\boldsymbol{v}_1 \quad \ldots \quad \boldsymbol{v}_M]$;

noise subspace : $\boldsymbol{U}_N = [\boldsymbol{v}_{M+1} \quad \ldots \quad \boldsymbol{v}_N]$.

$$\left(\boldsymbol{R}_{yy} - \sigma_w^2 \boldsymbol{I}\right)\boldsymbol{v}_i = \boldsymbol{0} = \boldsymbol{SPS}^{\boldsymbol{T}}\boldsymbol{v}_{\boldsymbol{i}}\,, \tag{3.9}$$

for $i = M + 1 : N$. Therefore as $\boldsymbol{P}$ is positive definite, noise subspace spanned by $\boldsymbol{U}_N$ is orthogonal to signal subspace spanned by $\boldsymbol{S}$,

$$\boldsymbol{S^T v_i = 0} \tag{3.10}$$

for $i = M + 1 : N$. The estimated dimension of the signal subspace (estimated by analysing the magnitude spread of the Eigen values of the ACM matrix) is used for subspace separation based on the magnitudes of the Eigen value spread. The orthogonality between the generalized signal vector, or the *'steering vector'* $\underline{\boldsymbol{s}}(\boldsymbol{n-\tau})$, and the noise subspace $\boldsymbol{U_N}$, is used to evaluate the objective function:

$$F_{\text{TD-MUSIC}}(\tau) = \frac{1}{\underline{\boldsymbol{s}}(\boldsymbol{n-\tau})^T \boldsymbol{U_N U_N^T} \underline{\boldsymbol{s}}(\boldsymbol{n-\tau})}. \tag{3.11}$$

The peaks of the *'Pseudo-Spectrum'* generated by evaluation of (3.11) correspond to the time delays of each multi-path. Correct estimation of signal subspace dimension is paramount for the MUSIC algorithms, as will be shown later in the behavioural analysis of Chapter 4. However in most practical systems, as there is a certain degree of colour in the noise, signal subspace dimension identification by Eigen value magnitudes is not always as reliable.

It should also be noted that the steering vector running through arbitrary path delay values is assumed to be a replica of the transmitted signal that was originally sent, hence implying that the algorithm assumes no distortions in the signal shape took place. This however does not hold due to the fact that shape deformations in the signal take place due to the band limited nature of the channel and spectral leakages in the subspace separation phase.

For the proper implementation of the TD-MUSIC algorithm, for impulse radio UWB system or any other pulse delay estimation based system, the time domain window or the data matrix length should be selected such that:

$$l_d \leq l_w - l_p \tag{3.12}$$

where,

l_d is the delay spread,

l_w is the window length,

and

l_p is the pulse width.

When the steering vector is shifted above the upper bound specified by (3.12) the delayed pulse of the steering vector gets clipped, as shown in Figure 3.3 As it is clipped further, the numerator of objective function defined in (3.11) tends to approach zero. In turn this produces a pseudo-spectrum that exponentially rises to infinity, as depicted in Figure 3.4. Even though, the peaks that correspond to the multi-paths are produced in the correct locations by the TD-MUSIC algorithm, for the delay values above the upper bound specified by (3.12), the magnitude of the pseudo-spectrum rapidly raises to infinity, thereby making the local peaks generated below the upper bound negligible. Therefore, the window length should be selected according to the condition specified in (3.12). Cyclic wraparound for the steering vector is not possible as it creates a false sense of periodicity, while giving rise to initial ambiguity problems, similar to the ones present in GPS systems. In addition to the ambiguity it creates, this causes the pseudo-spectrum shape to be deformed.

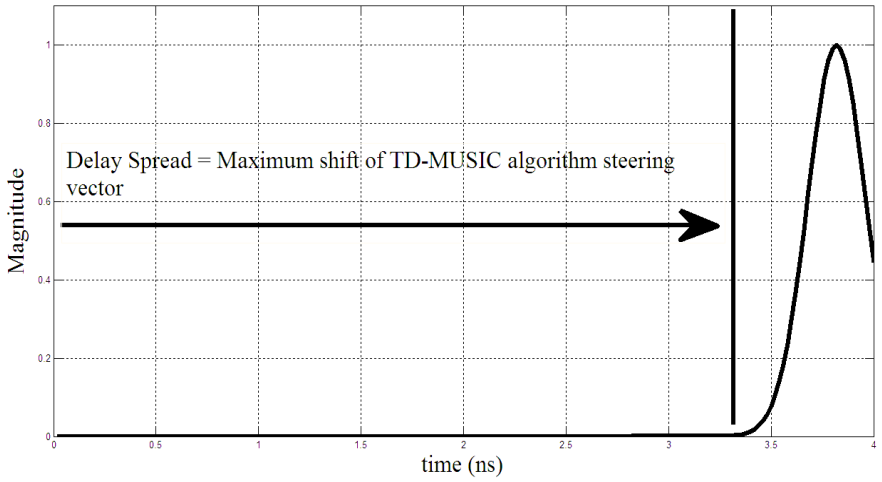

Figure 3.3 Over-shifting of the TD-MUSIC steering vector

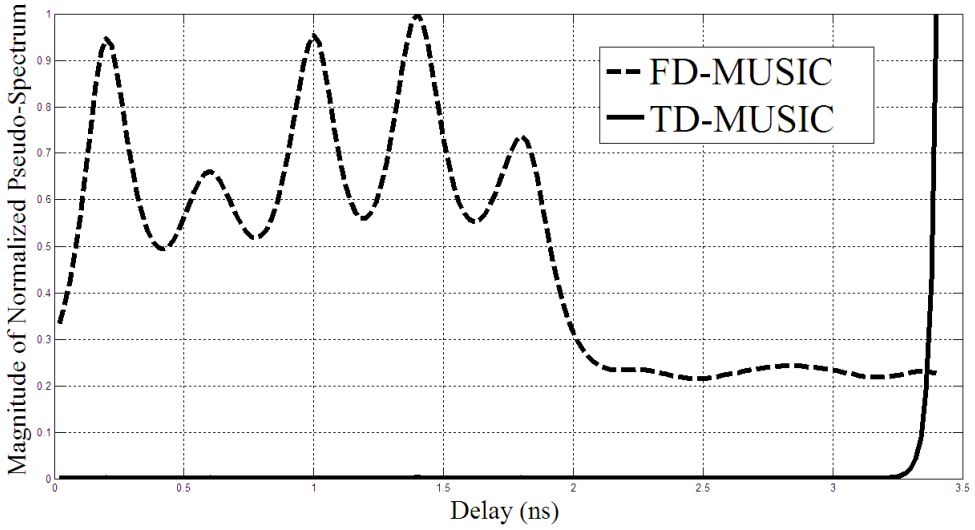

Figure 3.4 Pseudo-Spectrums of TD-MUSIC and FD-MUSIC algorithms when steering vector for TD-MUSIC algorithm is shifted over the upper bound

3.3 FD-MUSIC Algorithm

By considering the Fourier transform of (3.2) as the data vector, we can write:

$$Y^q(f) = \sum_{m=1}^{M} \alpha_m^q S(f) e^{-j2\pi f \tau_m} + w(f), \tag{3.13}$$

$for\ f = \ f_1\ to\ f_k.$

Which when presented in matrix form is:

$$\boldsymbol{Y^q} = \acute{\boldsymbol{S}}\ \boldsymbol{\alpha}^q + \ \boldsymbol{W}^q, \tag{3.14}$$

where,

$\boldsymbol{Y}^q = \ [Y^q(f_1) \quad \ldots \quad Y^q(f_k)]_{k\times 1}^T,$

$\boldsymbol{\alpha}^q = \ \left[\alpha_1^q \quad \ldots \quad \alpha_M^q\right]_{M\times 1}^T,$

$\boldsymbol{W}^q = \ [W^q(f_1) \quad \ldots \quad W^q(f_k)]_{k\times 1}^T,$

and

$\acute{\boldsymbol{S}} = \ [\underline{s}(\tau_1) \quad \ldots \quad \underline{s}(\tau_M)]_{k\times M},$

where the frequency domain generalized signal vector or steering vector is defined as:

$\underline{\boldsymbol{s}}(\boldsymbol{\tau_i})_{\boldsymbol{k\times 1}} = [S(f_1)e^{-j2\pi f_1 \tau_i} \quad \ldots \quad S(f_k)e^{-j2\pi f_k \tau_i}]^T.$

Now similar to the TD-MUSIC algorithm case, constructing the autocorrelation matrix and then separating the noise and signal subspaces, an objective function can be defined so that a pseudo-spectrum can be evaluated as,

$$\boldsymbol{R}_{YY} = E\left[\boldsymbol{Y}^q \boldsymbol{Y}^{q^T}\right] = \acute{\boldsymbol{S}}\ \boldsymbol{P}\ \acute{\boldsymbol{S}}^T + \ k\sigma_W^2 \boldsymbol{I}, \tag{3.15}$$

and

$$F_{\text{FD}-\text{MUSIC}}(\tau) = \frac{1}{\underline{\boldsymbol{S}}(\boldsymbol{\tau_i})^H \boldsymbol{U}_{\hat{N}} \boldsymbol{U}_{\hat{N}}^H \underline{\boldsymbol{S}}(\boldsymbol{\tau_i})}\ . \tag{3.16}$$

respectively. Thus the steering vector is a frequency weighted version of the steering vector (or frequency based Eigen vector) used in earlier spectral estimation techniques. The major differences are, the time delay variable replacing the frequency variable, and the frequency sample points replacing the time samples used in spectral estimation. The frequency weighting parameters depend on the Fourier transform of the original signal sent.

The general flow diagram of the MUSIC algorithms is summarized in Figure 3.5 to highlight the basic steps followed. First the data vectors are extracted in time or frequency domain, and the auto correlation matrix formulated. The number of signal subspace dimension is estimated via magnitudes of Eigen values or other alternate methods. The subspace separation is then performed and the defined objective functions are evaluated according to (3.11) or (3.16). The generated pseudo-spectrum output is then utilized to determine time delay estimates, and/or construct a location based fingerprint, according to the positioning system used.

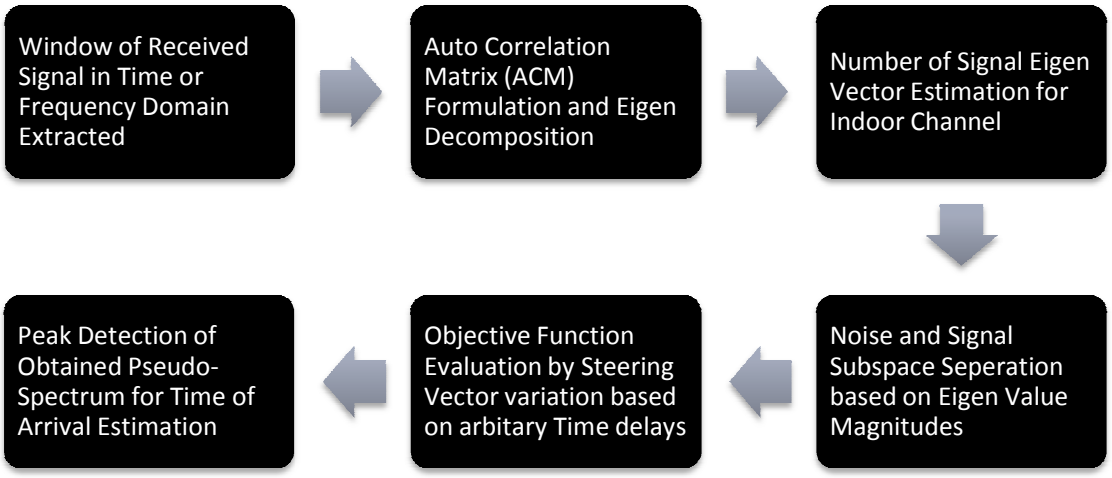

Figure 3.5 Flow Chart of Basic Super Resolution TOA Estimation Algorithm

3.4 FD-EV Algorithm

In view of reducing the spurious nature of the pseudo-spectrum, Eigen value de-weighting was suggested in [74] for the standard MUSIC algorithm. Thus by de-weighting the objective function of the FD-MUSIC algorithm, we obtain the FD-EV method, whose objective function is defined below:

$$F_{\mathrm{FD-EV}}(\tau) = \frac{1}{\underline{\boldsymbol{S}}(\boldsymbol{\tau_i})^{\boldsymbol{H}}\left(\sum_{k=M+1}^{N} {}^{1}/_{\lambda_{\mathrm{FD-k}}} \boldsymbol{v}_{\mathbf{FD-k}} \boldsymbol{v}_{\mathbf{FD-k}}^{\boldsymbol{H}}\right)\underline{\boldsymbol{S}}(\boldsymbol{\tau_i})} . \tag{3.17}$$

Here $\boldsymbol{v}_{\mathbf{FD-k}}$ and $\lambda_{\mathrm{FD-k}}$ are the noise Eigen vectors and corresponding Eigen values of the auto correlation matrix evaluated in the frequency domain. As can clearly be seen, the steering vector of the FD-EV method is $\underline{\boldsymbol{S}}(\boldsymbol{\tau_i})$, same as the steering vector for the FD-MUSIC algorithm. When this method was introduced for time delay estimation in indoor positioning system we were able to identify an additional benefit of the Eigen value de-weighting. For the first time it was observed that for certain bandwidth and SNR conditions, the Eigen value de-weighting of the FD-EV method enabled *signal peaks submerged beneath the noise floor for the MUSIC algorithms to resurface.* This discovery will be presented more comprehensively in Section 4.3 of this thesis. This feature, adds a new dimension to the importance of frequency domain Eigen value de-weighting, when generating the pseudo-spectrum for the FD-EV method in indoor positioning applications.

3.5 TD-EV Algorithm

The capability of the Eigen-value de-weighting process in the FD-EV method to resurface submerged signal peaks below the noise floor for a constrained

environment, and the versatile nature of the TD-MUSIC algorithm to operate under low SNR conditions and bandwidth limited environments, resulted in the creation of this new algorithm. It strives to combine the positive attributes of both algorithms mentioned above, to present itself as the ultimate super resolution technique. The objective function for this method is evaluated as below in the time domain:

$$F_{\mathrm{TD-EV}}(\tau) = \frac{1}{\underline{\boldsymbol{s}}(\boldsymbol{n}-\boldsymbol{\tau})^{\boldsymbol{T}}\left(\sum_{k=M+1}^{N} {}^{1}/_{\lambda_{\mathrm{TD-k}}} \boldsymbol{v}_{\mathbf{TD-k}} \boldsymbol{v}_{\mathbf{TD-k}}^{\boldsymbol{T}}\right)\underline{\boldsymbol{s}}(\boldsymbol{n}-\boldsymbol{\tau})} . \tag{3.18}$$

Here $\boldsymbol{v}_{\mathbf{TD-k}}$ and $\lambda_{\mathrm{TD-k}}$ are the noise Eigen vectors and corresponding Eigen values of the auto correlation matrix evaluated in the time domain. The steering vector is of the same form as the TD-MUSIC algorithm. The detailed analysis and results of the TD-EV method's ability to combine *the best of both worlds* is presented later in Section 5.5.

3.6 ESPRIT as a Tool for Time Delay Estimation

In [75, 76], the ESPRIT algorithm was introduced as an alternative method to the MUSIC super resolution algorithm, in the direction of arrival estimation problems for array-based systems. The primary virtue of this algorithm is that it does not rely on a peak detection process for parameter estimation. The downside is, that it can only be used in an impulsive response case or if the signal spectrum is flat in the frequency sampling region. In addition, it isn't as accurate an estimation tool as the MUSIC algorithms, and cannot generate the visual output that is required for a delay profile based fingerprint.

In this work, a mathematical model of a versatile form of the ESPRIT algorithm was suggested as a possible alternative for TOA estimation. This was done by making sure that the data vectors, $\overline{X}$ and $\overline{Y}$, were constructed by using odd and

even frequency samples from the impulse response spectra, thus making sure none of the data samples used for $\overline{X}$ were reused for $\overline{Y}$. By defining the data vectors as such, we were able to replicate the array displacement shift effect of the standard ESPRIT algorithm in a TOA estimation framework for indoor positioning systems when constructing the $\overline{X}$ and $\overline{Y}$, data vectors. This is proven below by showing that the equations thus are of the same form as the standard ESPRIT formulation. This confirms that the method suggested below is in the same spirit as the original ESPRIT algorithm, with the displacement between the two identical sub-array systems equated to a frequency shift in our method. Consider the channel impulse response as:

$$h(t) = \sum_{k=0}^{L_p-1} a_k \delta(t - \tau_k) \tag{3.19}$$

where $a_k = |\alpha_k| e^{j\theta_k}$. The Fourier transform of $h(t)$ is,

$$H(f) = \sum_{k=0}^{L_p-1} a_k e^{-j2\pi f \tau_k}. \tag{3.20}$$

Let the received signal spectrum be denoted as,

$X\,(\,f_o + \,n\,\Delta f\,) = x\,(n)$,

and let us consider the total number of sample points L in the received signal spectrum to be even. Let us now define the data vectors:

$$\overline{\boldsymbol{X}} = \,[x(1) \quad x(3) \quad \ldots \quad x(L-1)]^T_{\frac{L}{2}\times 1}, \tag{3.21}$$

and

$$\overline{\boldsymbol{Y}} = \,[x(2) \quad x(4) \quad \ldots \quad x(L)]^T_{\frac{L}{2}\times 1}. \tag{3.22}$$

Thus, the q^{th} realization of the data vector $\overline{\boldsymbol{X}}$ can be written as,

$$\overline{\boldsymbol{X}}^{\boldsymbol{q}} = \overline{\boldsymbol{V}}.\boldsymbol{a}^{\boldsymbol{q}} + \boldsymbol{W}^{\boldsymbol{q}}{}_{\mathbf{odd}} \tag{3.23}$$

where

$$\overline{\boldsymbol{V}} = \begin{bmatrix} e^{-j2\pi(f_0+\Delta f)\tau_o} & \cdots & e^{-j2\pi(f_0+\Delta f)\tau_{L_P-1}} \\ e^{-j2\pi(f_0+3\Delta f)\tau_o} & \cdots & e^{-j2\pi(f_0+3\Delta f)\tau_{L_P-1}} \\ \vdots & \ddots & \vdots \\ e^{-j2\pi\left(f_0+\overline{\mathrm{L}-1}\Delta f\right)\tau_0} & \cdots & e^{-j2\pi\left(f_0+\overline{\mathrm{L}-1}\Delta f\right)\tau_{L_P-1}} \end{bmatrix}_{\frac{L}{2}\times L_p},$$

$$\boldsymbol{a} = [a_0 \quad a_1 \quad \cdots \quad a_{L_{p-1}}]^T_{L_P\times 1},$$

and

$$\boldsymbol{W_{odd}} = [w(1) \quad w(3) \quad \ldots \quad w(L-1)]^T_{\frac{L}{2}\times 1}.$$

Similarly as above data vector $\overline{\boldsymbol{Y}}$ can be expressed as,

$$\overline{\boldsymbol{Y}}^{\boldsymbol{q}} = \overline{\boldsymbol{V}}.\boldsymbol{\Phi}.\boldsymbol{a}^{\boldsymbol{q}} + \boldsymbol{W}^{\boldsymbol{q}}_{\mathbf{even}} \tag{3.24}$$

where

$$\boldsymbol{\Phi} = \begin{bmatrix} e^{-j2\pi\Delta f\tau_0} & \cdots & 0 \\ \vdots & \ddots & \vdots \\ 0 & \cdots & e^{-j2\pi\Delta f\tau_{L_p-1}} \end{bmatrix}_{L_P\times L_P},$$

and

$$\boldsymbol{W_{even}} = [w(1) \quad w(3) \quad \ldots \quad w(L-1)]^T_{\frac{L}{2}\times 1}.$$

Thus, the two correlation matrices are of the form:

$$\boldsymbol{R}_{\overline{XY}} = E\left[\overline{\boldsymbol{X}}^q\overline{\boldsymbol{Y}}^{q^H}\right] = \overline{\boldsymbol{V}}\,\boldsymbol{A}\boldsymbol{\Phi}^H\,\overline{\boldsymbol{V}}^H,$$

and

$$\boldsymbol{R}_{\overline{XX}} = E\left[\overline{\boldsymbol{X}}^q\overline{\boldsymbol{X}}^{q^H}\right] = \overline{\boldsymbol{V}}\,\boldsymbol{A}\,\overline{\boldsymbol{V}}^H + \sigma_w^2\boldsymbol{I}$$

where $\boldsymbol{A} = E[\boldsymbol{a}^{\boldsymbol{q}}\boldsymbol{a}^{\boldsymbol{qH}}]$.

As the matrices $\boldsymbol{R}_{XX}$ and $\boldsymbol{R}_{XY}$ as well as the equations (3.23) and (3.24) are of the same form as the formulations in [75, 76] for the standard ESPRIT algorithm, thus the time delay parameters can be obtained using any of the techniques used for DOA estimation in the standard ESPRIT algorithm. To meet this end a total least squares (TLS) approach can be used as suggested in [75]. TLS-ESPRIT approach for obtaining DOA parameters can be used by constructing $\overline{\boldsymbol{Z}} = \left[\overline{\boldsymbol{X}} \quad \overline{Y}\right]^T$. This can be considered as an alternate solution, to the MUSIC algorithm, when peak detection is deemed too complex for a parameter estimation based positioning system for a LoS environment.

3.7 Procedural Analysis

This section aims to provide a detailed analysis of the practical issues that may arise, when utilizing these super resolution techniques introduced in this thesis, for indoor positioning systems. In the practical implementation of the MUSIC super resolution algorithm there are several issues worth consideration. The construction of the auto correlation matrix with a limited data sample is one of them. Due to the difficulties in the acquisition of multiple snapshots in practise, researchers have suggested segmentation of the data sequence to achieve a similar effect. However, if we are to utilize multiple realizations, the diversity techniques that can utilized to meet the requisite are of interest.

3.7.1 Auto Correlation Matrix

Earlier in the theoretical analysis we obtained the auto-correlation matrix under the assumption that multiple realizations of the data vectors are available. Thus the auto correlation will be obtained as:

$$\boldsymbol{R}_{yy} = E\left[\boldsymbol{y}^q \boldsymbol{y}^{q^H}\right] = \frac{1}{P} \sum_{q=1}^{P} \boldsymbol{y}^q \boldsymbol{y}^{q^H} \tag{3.27}$$

where P is the number of snapshots available. Although if only one snapshot of data of length N was available, then the sequence is divided into W consecutive data segments of length L. Then the auto correlation matrix is obtained as:

$$\boldsymbol{R}_{yy} = \frac{1}{W} \sum_{q=1}^{W} \boldsymbol{y}(q)\, \boldsymbol{y}^{\boldsymbol{H}}(q) \tag{3.28}$$

where $W = N - L + 1$ and $\boldsymbol{y}(q) = [y(k) \quad y(k+1) \quad \ldots \quad y(k+L-1)]^T$. An ACM obtained via (3.28) is called FCM in popular terminology.

For the super-resolution TOA estimation techniques, the data vector is obtained by sampling the received channel frequency response uniformly over a given frequency band. In order to avoid aliasing in the time domain, similar to the time-domain Nyquist sampling theorem, the frequency-domain sampling interval Δf, should satisfy this condition:

$$1/\Delta f \geq \tau_{\max}, \tag{3.29}$$

where $(\tau_{\max} = \max_i(\tau_i))$ is the maximum delay of the measured multipath radio propagation channel.

The measurement data is assumed to be stationary. Thus, the correlation matrix of the data is Hermitian (conjugate symmetric) and Toeplitz (equal elements along all diagonals). However, the estimate of the correlation matrix, based on the actual measurement data of small finite length, is may not be Toeplitz depending on

the estimator used. The estimate of the correlation matrix can be further improved by constructing the FBCM:

$$\boldsymbol{R}_{yy}^{FB} = \frac{1}{2}(\boldsymbol{R}_{yy} + \boldsymbol{J}\boldsymbol{R}_{yy}^{*}\boldsymbol{J}) \tag{3.30}$$

Where superscript * denotes conjugate and $\boldsymbol{J}$ is the $(L \times L)$exchange matrix. It is easily seen that $\boldsymbol{R}_{yy}^{FB}$ is persymmetric; i.e. $\boldsymbol{J}\boldsymbol{R}_{yy}^{FB}\boldsymbol{J} = \boldsymbol{R}_{yy}^{FB^{*}}$ and its elements are conjugate symmetric about both diagonals. The same technique is widely used in spectral estimation with the name covariance method [77], and in linear least-square signal estimation, where it is called forward–backward linear predication [77].

3.7.2. Diversity Techniques

Frequency, space and time diversity techniques are used in wireless communication systems to improve performance. Diversity techniques make use of the random nature of the radio propagation channel by finding and combining uncorrelated signal paths to optimize performance criteria. All diversity techniques used for wireless communication systems can be used for TOA estimation systems as well, but due to the complex nature of the indoor channel these techniques offer no remedies for problems such as UDP conditions, which are frequent in indoor environments.

The TOA estimates obtained independently from each branch can be optimally combined using a standard combining algorithm such as the equal gain algorithm:

$$\hat{\tau}_0 = \frac{1}{P}\sum_{i=1}^{P}\hat{\tau}_0^{(i)} \tag{3.31}$$

This is the simplest approach. Weights can also be assigned to each branch to improve results. Rather than combining time delay estimates the data vectors can be combined

prior to the autocorrelation matrix formulation, to reduce the computational load of the previous method, where Eigen decomposition has to take place P times.

If we ignore the complexity of the hostile behavior of the indoor channel, and the fact that the models developed for indoor channel characteristics for communication applications are not useful for indoor geolocation, use of diversity techniques may appear promising. In fact, the lack of understanding in the complexities prevalent in indoor environments for localization, as opposed to communication applications has been the main source of failure for precise indoor localization systems over the past decade or so. In principle, when the direct path is shadowed, none of the traditional diversity techniques are effective for precise indoor geolocation. For instance, consider the traditional frequency diversity technique used in frequency selective multipath fading on indoor channels for wireless communications. In telecommunications the basic principle is to send several streams of lower-rate data over multiple narrowband subchannels rather than transmitting all the information using one wideband channel. If one of the subchannels is hit by frequency selective fading, we can still use other subchannels to achieve reliable communications. If the same principle is applied to an indoor positioning system hit by UDP conditions, assuming the possibility to use multiple TOA estimates obtained from several subchannels to reduce the range error due to NLoS conditions, rather than using the single TOA estimate of a wideband channel. However, in the absence of a direct path, when the TOA estimate in one channel is not reliable, it is also unreliable for other subchannels too. Therefore, frequency diversity techniques are not capable of providing significant improvements to the performance in UDP conditions. Similarly time diversity cannot achieve the desired performance improvement either, due to the fact that UDP conditions last for comparably large durations of time, thus it

is unlikely that any of the multiple time diversity branches will find themselves outside the UDP time span. Finally spatial diversity, which makes use of multiple antennas for a single node is hardly a feasible solution for a commercial indoor positioning system, with its added cost and hardware complexity [78]. Therefore utilizing the information obtained from the pseudo-spectrum output of our super resolution techniques to construct a location based fingerprint is a much more reliable and simpler method to work around the UDP problem. Even much simpler basic fingerprinting approaches have proven to perform well under NLoS conditions.

Chapter 4

Behavioural Analysis of the Super Resolution Algorithms

The behavioural analysis of the TD-MUSIC, FD-MUSIC and FD-EV algorithms were compared and studied under various conditions, in our research work as the first step. In order to evade ambiguity in TOA estimation, the maximum delay was initially assumed to be less than the overall time period of the signal. The standard Gaussian signal template and a channel model of several multi-paths, in additions to the direct path, were used to study the performance under severe multi-path conditions prevailing in most practical indoor environments. The path separation as well as relative gain levels of these multi-paths was varied according to the attributes that were tested. In this analysis, key parameters such as the number of the signal subspace dimension, bandwidth, SNR, steering vector pulse spread etc. were varied from hostile to friendly conditions for proper analysis. The behavioural analysis was conducted using matlab simulations. The critical parameter values used are specified along with the results in the relevant sections. In most cases, to isolate the effect of one key parameter on the algorithm performance, the other parameters were kept at favourable conditions. Thereafter, to examine the overall versatility of each algorithm, the environment was made extremely hostile by varying multiple parameters towards adverse conditions. Therefore the analysis simulates extremely hostile conditions at times to properly identify the versatile nature of the super resolution algorithms in concern.

4.1 Normalized Pseudo-Spectrum

The analysis relies on the use of *'Pseudo-Spectrums'* as the final output; the placement of the local peaks as well as the *'actual shape'* of the pseudo-spectrum is put under scrutiny. This enables even minute changes in shape of the pseudo-spectrum to be captured under changes in certain variables. In practical applications, even when the theoretical peaks are placed correctly, due to the pseudo-spectrum shape not being '*pronounced enough at the local peaks'*, obtaining the local maxima in a peak detection process maybe tedious and error prone. In addition, the resultant pseudo-spectrums generated, are to be explored as possible location based fingerprints for radio map construction. This places even more importance on the 'shape' of the pseudo-spectrum, than if we were to utilize it as a mere time delay estimation tool. Normalization was done as defined below in equation (4.1), for comparative analysis among the algorithms. By defining the normalization as given below, it is ensured that no shape deformation takes place due to normalization.

$$F_{NORM}(\tau) = \frac{\mathrm{F}(\tau)}{\max_{\forall\, \tau} F(\tau)}\,. \tag{4.1}$$

4.2 Behavior of TD-MUSIC algorithm under steering vector variations

It was noticed in our behavioural analysis for the TD-MUSIC algorithm, when the steering vector pulse width (or in our case pulse spread) was varied, that some of the pseudo-spectrums generated, actually outperformed the original TD-MUSIC algorithm under certain conditions. The steering vector for the original TD-MUSIC algorithm was defined as:

$$\underline{s}(n-\tau_i)_{N\times 1} = [s(1-\tau_i) \quad \dots \quad s(N-\tau_i)]^T$$

in (3.4) and that was used to generate the pseudo-spectrum for the objective function defined in (3.11). It should be noted that the *steering vector is simply a delayed version of the original transmitted signal in the time domain*. Therefore theoretically the TD-MUSIC algorithm assumes that the data vector extracted from the received signal contains an undistorted linear combination of the original transmitted signal coupled with noise. Thus the unmodified steering vector does not account for signal distortions that may have occurred to the transmitted signal during propagation, due to the band limited nature of a practical indoor channel. In addition, it also assumes that, at the subspace separation stage in the TD-MUSIC algorithm, there is no leakages to and from the signal to noise subspaces. However, in practise the *'spectral leakage'* exists, coupled with the signal distortions due to band limited channels. This in turn causes the modified versions of the TD-MUSIC algorithm to perform better than the original TD-MUSIC algorithm at certain conditions.

For this analysis, we generated pseudo-spectrums for modified versions of the TD-MUSIC algorithm by varying the pulse spread of an idealized Gaussian steering vector as:

$$y\,(n) = A.e^{\left[n/(k\pm x)\right]^2} \tag{4.2}$$

where A and k are constants used to set amplitude and magnitude spread of the transmitted signal, and x is the variable used to modify the steering vector pulse spread. From hereafter in this report, if the denominator constant of the Gaussian function is modified by a value of $'(\pm x)'$, the resultant TD-MUSIC algorithm will be called the $'(\pm x) Deviant\ of\ the\ TD-MUSIC\ algorithm'$. A set of such modified steering vectors are depicted in Figure 4.1.

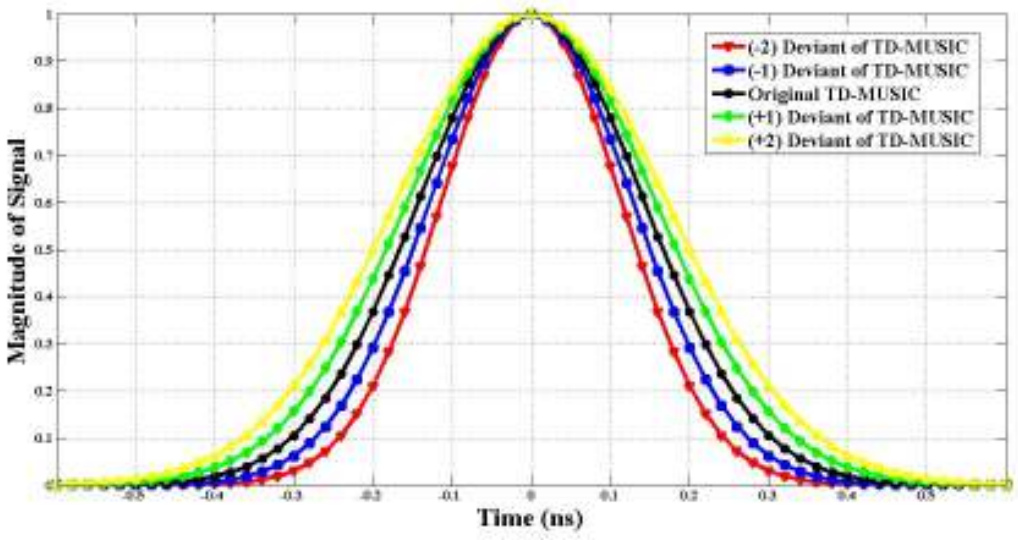

Figure 4.1 Set of Gaussian steering vectors with pulse spread varied

It was observed, that under certain conditions the deviants of the TD-MUSIC algorithm actually outperformed the original TD-MUSIC algorithm. Further analysis made aware that for a given bandwidth, there existed, only one *optimum deviant, which generated the best pseudo-spectrum.* Other parameters such as SNR, or the signal subspace dimensions, only increased or decreased the relative shape deformations among the deviants, while the optimum deviant remained unchanged as long as the bandwidth remained constant. The optimum deviant is the version of the TD-MUSIC algorithm which best replicates the impulsive multi-path profile of the indoor channel most effectively. We have to account for both accurate resolution of multi-paths as well as the pronounced and peaky nature of the pseudo-spectrum peaks at the local peaks.

The effective channels bandwidth above the noise floor was varied from 10 GHz to 2.25 GHz to determine the optimum deviant, for the TD-MUSIC algorithm for each bandwidth condition. As the transmitted signal is received undistorted at 10 GHz, this determined the upper bound; and below 2.25 GHz due to rather severe

shape deformations it was difficult to identify the optimum deviant, therefore it served as the lower bound. It should be highlighted that the actual ultimate performer for each bandwidth is of trivial importance, as this fact would vary according to the signal template, the channel bandwidth or various other environmental conditions. What we hope to highlight is not the identification of *the optimum deviant,* but, the existence of *optimum deviants* other than the original TD-MUSIC algorithm, which we believe is of practical significance for indoor positioning systems.

In this analysis, it was observed that for higher bandwidth, the negative deviants emerged as the ultimate performer. As for lower bandwidths the optimum performer gradually tended to zero and for very low bandwidths the positive deviants emerged as the ultimate performer. In addition, there was always a symmetric distribution of pseudo-spectrums centred on the ultimate performer for relatively higher bandwidths. Figure 4.2 and 4.3 shows the pseudo-spectrum spread for the *TD-MUSIC deviants* ranging from $(-4 \rightarrow 0)$, for a channel bandwidth of 7.5 GHz, where the SNR was maintained at a sound level of around 10 dB and the signal subspace dimensions were correctly estimated. It should be further stated that the SNR value as well as signal subspace dimensions did not have an effect on the *optimum deviant* which produces the best pseudo-spectrum output, in terms of both peak placement as well as pronounced and peaky nature of the local peaks, remained the (-3) *deviant* of the TD-MUSIC algorithm from bandwidth of 10 GHz to 5 GHz. Figure 4.2 shows the actual pseudo-spectrums prior to normalization presented here to highlight the rather drastic shape deformation in terms of the sheer magnitude fluctuations at the peak, which is attenuated when the pseudo-spectrums are normalized. Figure 4.3, post-normalization serves as a better means for relative comparisons among the deviants. It draws our attention to the fact that the

neighbouring deviants symmetrically deteriorate in shape around the ultimate performer, the (-3) *deviant* of the TD-MUSIC algorithm. For example the next best *deviants* are clearly the (-4) and (-1), which are the closest neighbours to the *optimum deviant.* In addition Figure 4.3 zooms in on the first two dominant signal paths for better clarity in the comparative analysis.

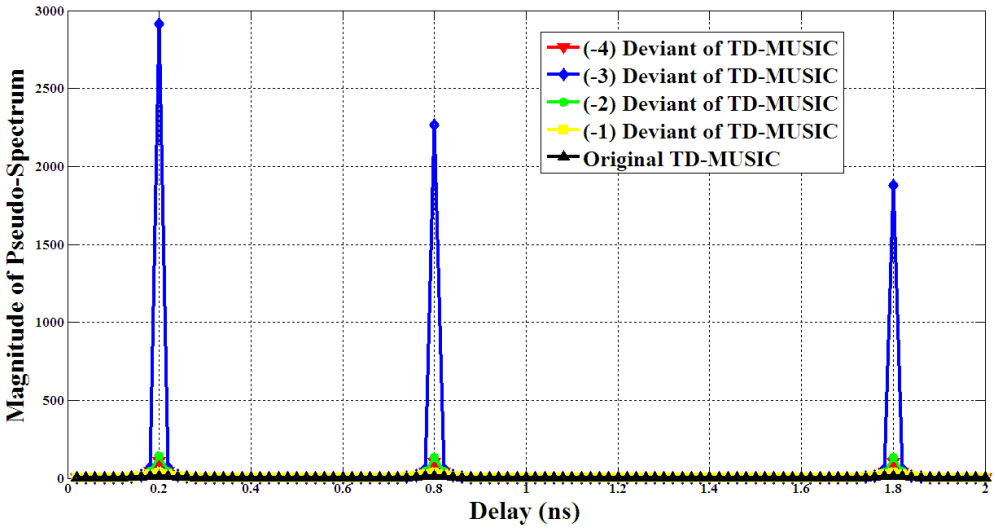

Figure 4.2 The Pseudo-spectrum spread for TD-MUSIC algorithm with the steering vector pulse spread varied at 7.5 GHz bandwidth and SNR = 10 dB

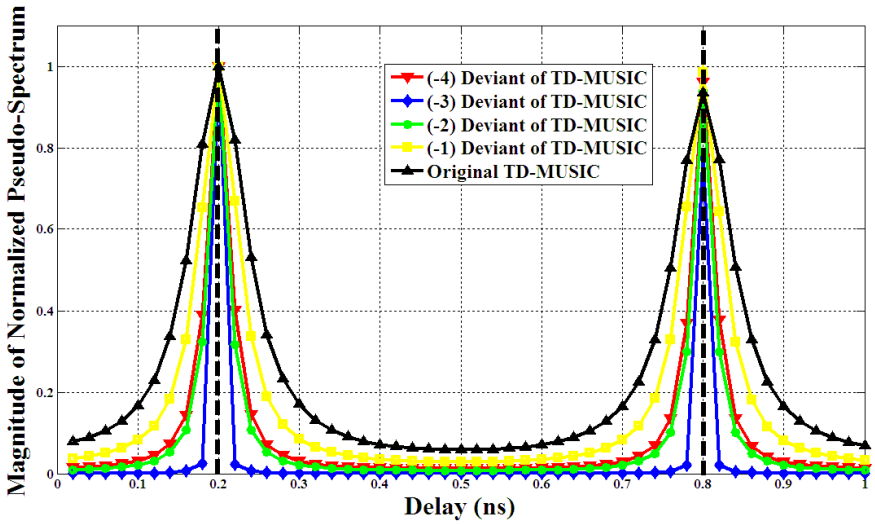

Figure 4.3 The normalized pseudo-spectrum spread for TD-MUSIC algorithm with the steering vector pulse spread varied at 7.5 GHz bandwidth and SNR = 10 dB

Figure 4.4 demonstrates a transition of the *optimum deviant* from the (-3) *deviant* to the (-2) *deviant*, at an effective channel bandwidth of 5 GHz. At 3 GHz, it is seen that the *optimum deviant* is in fact the original TD-MUSIC algorithm (see Figure 4.5). Further decrease of bandwidth results in the *optimum deviant* zero crossing, towards the positive side. As depicted in Figure 4.6, at 2.5 GHz bandwidth, the *optimum deviant* is the $(+1)$ *deviant* of the TD-MUSIC algorithm. For lower bandwidths, although the *optimum deviant* is a *positive deviant*, the actual ultimate performer becomes harder to determine, as almost all pseudo-spectrum have a certain degree of distortion making it harder to clearly identify an undisputable ultimate performer. It should be further stressed that at lower bandwidths, as illustrated in Figure 4.6, the *negative deviants* and the original TD-MUSIC algorithms in addition to having inferior performance to the *positive deviants*, also generate a non-existent signal peak at 0.5 ns, when the actual dominant signal peaks are placed at 0.2 and 0.8 ns. Though the placement of such unwanted peaks may differ from channel to channel, it should be noted that such erroneous pseudo-spectrums with false

information cause large range errors in location based fingerprinting schemes, as they create the false impression of a non-existent reflector in the environment.

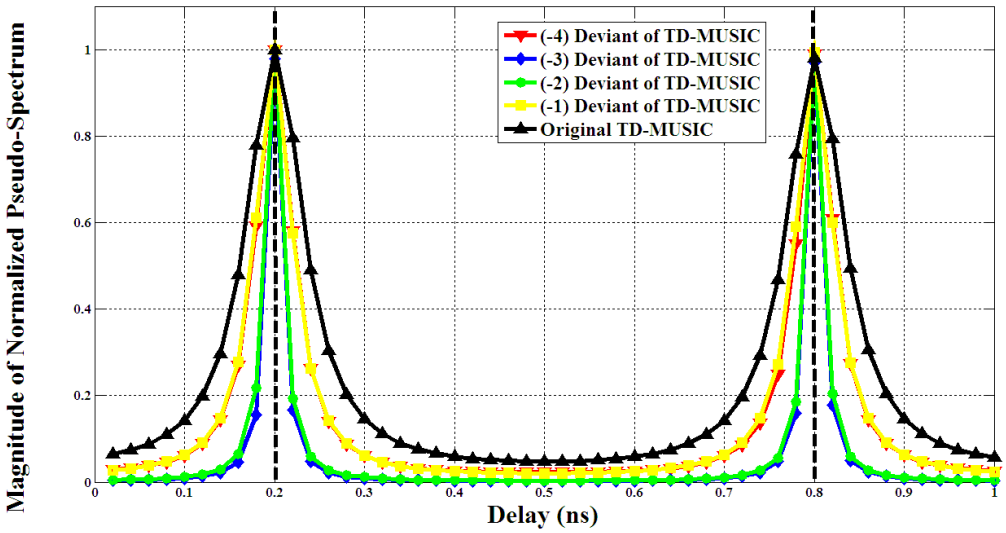

Figure 4.4 The normalized pseudo-spectrum spread for TD-MUSIC algorithm with the steering vector pulse spread varied at 5 GHz bandwidth and SNR = 10 dB

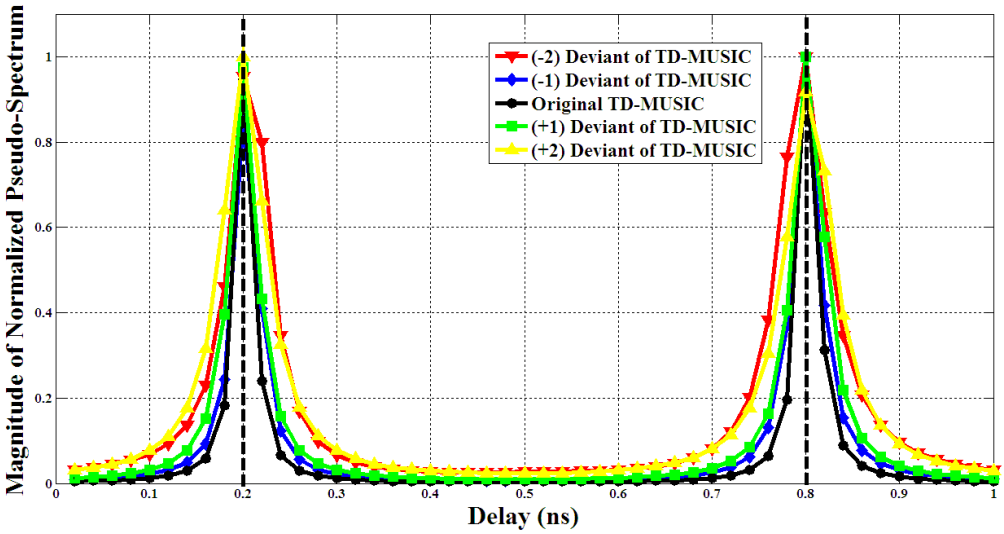

Figure 4.5 The normalized pseudo-spectrum spread for TD-MUSIC algorithm with the steering vector pulse spread varied at 3 GHz bandwidth and SNR = 10 dB

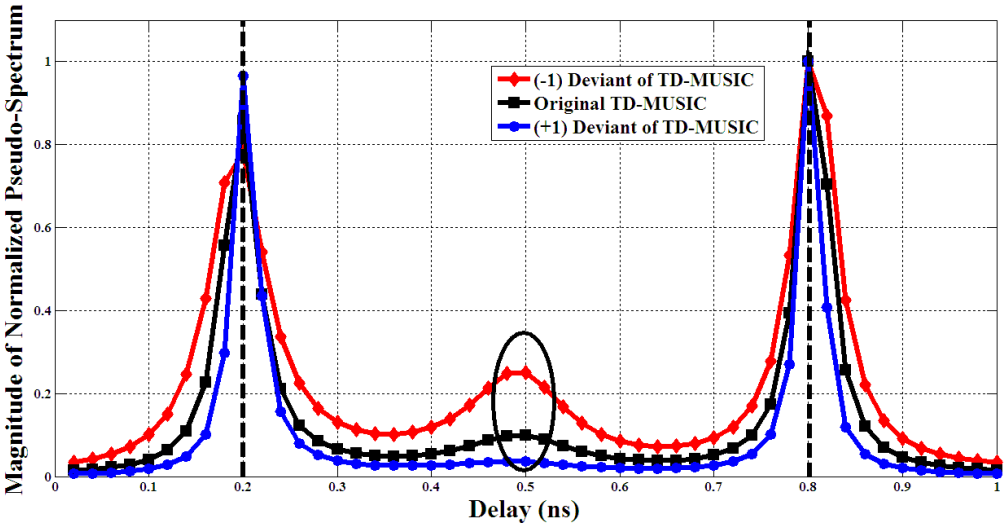

Figure 4.6 The normalized pseudo-spectrum spread for TD-MUSIC algorithm with the steering vector pulse spread varied at 2.5 GHz bandwidth and SNR = 10 dB

The variation of *optimum deviants* for certain bandwidths in terms of the algorithms ability to accurately resolve multi-paths effectively and generate pronounced and peaky local peaks is summarized in Table 4.1. The actual information as to which variant of the TD-MUSIC algorithm is the *optimum deviant* at a certain bandwidth is of little practical importance, as the *optimum deviant* varies according to different indoor channel conditions. What needs to be identified here is the existence of an *optimum deviant,* different to the original TD-MUSIC algorithm at certain channel bandwidths, as was observed through our analysis.

Table 4.1 TD-MUSIC Pseudo Spectrum Behaviour for varied steering vector pulse spread

Bandwidth /(GHz)	**Optimum Deviant**
7.5	(-3)
5	(-3) and (-2)
4	(-2)
3.5	(-1)
3	Original
2.5	(+1)
2.25	(+1) and (+2)

It can be interpreted that the *optimum deviant* is the performance maxima and other deviants deteriorate in performance symmetrically around it, for a given channel bandwidth. As the channel bandwidth decreases from 10 GHz to 2.25 GHz, the *optimum deviant* varies from (-3) to (+2). At lower bandwidths, when the *positive deviants* outperform the rest, it was also noticed that the original TD-MUSIC algorithm and other *deviants* may generate non-existant peaks at incorrect locations, leading to errornous conclusions. These observations are the result of what we termed the *"Spectral Leakage phenomena of the TD-MUSIC algorithm at the subspace separation stage"*.

The TD-MUSIC algorithm will account for the leaked noise in the sub-space seperation phase as a part of the signal. In addition, the signal suffers a certain level of distortion due to the bandlimited conditions of the channel. Therefore the 'signal vector' the algorithm assumes, was actually sent, becomes a more deviated version of the actual signal vector that was in fact sent. Therefore the best pseudo-spectrum is

generated for the steering vector, which best replicates the *assumed deviated version of the transmitted signal vector,* from the algorithm's point of view. We have termed this behaviour as the *"Spectral Leakage effect on the TD-MUSIC algorithm at the subspace seperation phase".* This causes the deviants of the TD-MUSIC algorithm to outperform the original TD-MUSIC algorithm at certain conditions.

When the FD-MUSIC algorithm was subjected to the same steering vector pulse width variations, it did not exhibit a spectral leakage phenomenon prominently, as it's time domain counterpart. Even though the relative shape deformation of the $(+/-)$ deviants may vary, but the *optimum deviant* the original FD-MUSIC algorithm remains unchanged.

The bandwidth versatility of the TD-MUSIC algorithm will be explained in more detail in the next chapter. In Figure 4.7 illustrates, how the bandwidth versatility, the spectrum leakage phenomenon and signal distortions can actually be used to our advantage. If properly identified, the *optimum deviant* relevant to the prevailing channel conditions, then as can be observed in Figure 4.7, at low bandwidth conditions, where both the frequency domain methods fail to provide reliable pseudo-spectrums, the *positive deviants* of the TD-MUSIC algorithm, not only outperform the FD-MUSIC and FD-EV methods, but also the original TD-MUSIC algorithm, to emerge as the ultimate performer. This in turn demonstrates how the spectral leakage effect, coupled with the versatility of the TD-MUSIC algorithm, can be used to our advantage under low bandwidth conditions for indoor positioning systems.

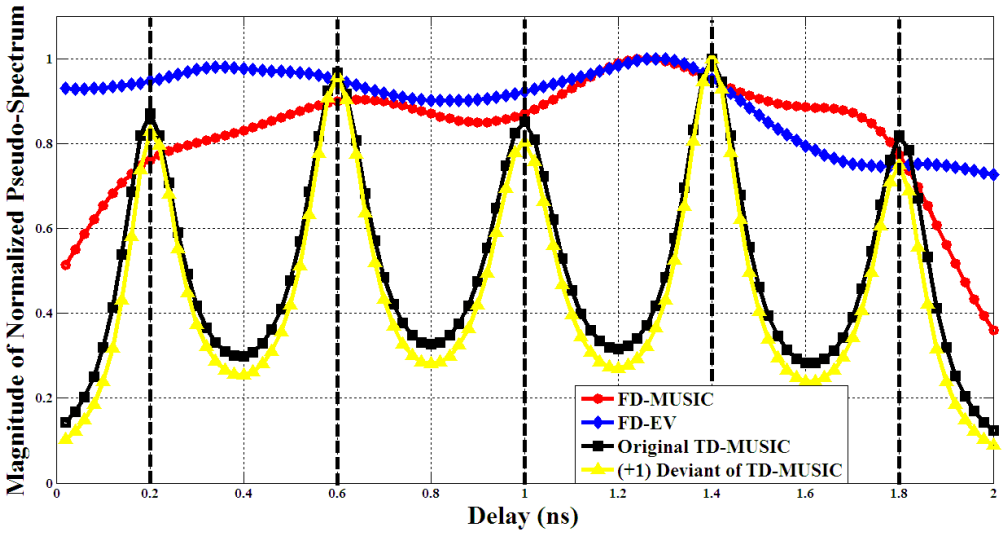

Figure 4.7 Comparison of super resolution techniques with the (+1) deviant of the TD-MUSIC algorithm for low bandwidth conditions (=2 GHz)

4.2.1 Performance of Finer Super Resolution Techniques

The finer super resolution techniques were devised by having the steering vector shifted at *fractions of the sample time,* when the objective functions were evaluated. For the *Finer TD-MUSIC algorithm* in Figure 4.8, the system sample time was set to 0.02 ns. This was done to verify whether any additional information can be obtained by decreasing the step size of the steering vector variations along the delay axis below the sample time of the received signal. Then the *Finer TD-MUSIC algorithm* was evaluated, by taking the product of the noise subspace with the delayed version of the transmitted signal in the denominator polynomial of the objective function at delay samples of 0.002 ns. In this example, for the *Finer FD-MUSIC algorithm,* we simply needed to vary the delay variable present in the steering vector, at sub-sample intervals of 0.01 ns. As can be noticed from Figure 4.8, the higher resolution of the delay parameter variation at the objective function evaluation, does not improve upon the performance of the original MUSIC algorithm. The pseudo-

spectrums generated are nearly identical in shape. From this outcome, it can be concluded that the highest possible resolution in the pseudo-spectrum with respect to the delay axis is already obtained by the original MUSIC algorithms, and cannot be improved further by *Finer MUSIC algorithms.*

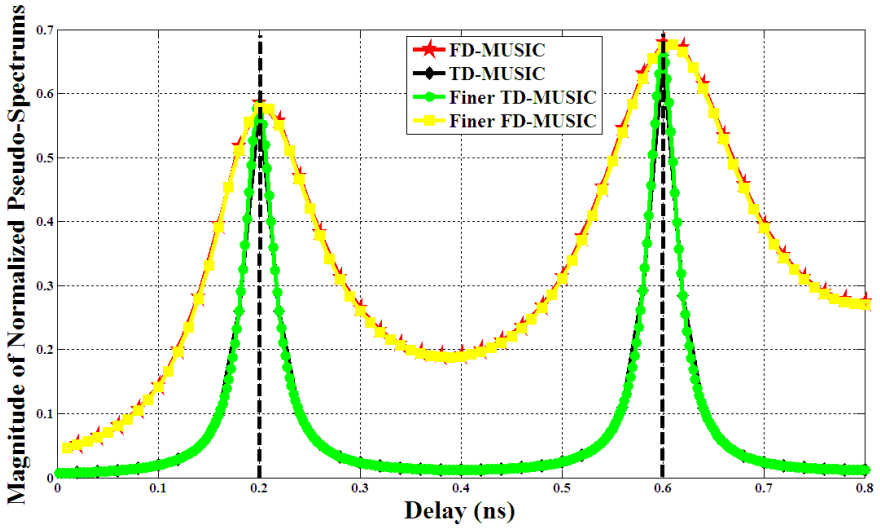

Figure 4.8 Comparison of standard FD-MUSIC and TD-MUSIC algorithms with Finer TD-MUSIC and FD-MUSIC algorithms with subsamples

4.3 Impact of erroneous estimation of the signal subspace dimension

The number of multi-path components $'M'$ is a critical parameter in TOA estimation using super resolution techniques. Theoretically $'M'$ is obtained via the ACM. The Eigen decomposition of $\boldsymbol{R}_{yy}$, defined in 3.5 in the time domain, or 3.15 in the frequency domain, yield a spread of $'N'$ Eigen values, where $'N'$ is the data vector length. From these, theoretically the smallest $'N-M'$ Eigen values are all equal to σ_w^2, the noise power spectral density. The larger $'M'$ Eigen values correspond

to the number of signal multipath components, thus enabling us to separate the signal Eigen vectors from the noise Eigen vectors, based on relative magnitudes of the corresponding Eigen values. In practice, when a limited number of data samples are available, and the noise has a certain degree of colour, the noise Eigen values tend to all be different, making it difficult to obtain $'M'$ easily using the prior approach. Especially in indoor environments, due to the existence of multiple reflectors of various materials, multi-paths will be found in large numbers, and they tend to have a widely distributed magnitude spread. Coupled together with the degree of colour in the noise, this makes the boundary between noise and signal Eigen values even more ambiguous. Figure 3.2 illustrates the smooth transition from the signal to noise Eigen values in terms of magnitude. These scenarios altogether increase the likelihood of an error occurring in the estimation of the subspace dimensions. In addition, over estimation of the signal subspace dimension causes unwanted non-existent signal peaks to occur in the pseudo-spectrum. This leads to erroneous conclusions in the positioning system. Further, the existence of relatively low amplitude multi-paths coupled with colour in the noise, all leads to the under estimation of the signal subspace dimension.

Therefore researchers have looked for alternative methods to determine $'M'$ with better accuracy. For example, the Rissanen minimum descriptive length criteria specified in [79] is one such a method. The minimum descriptive length criterion for estimation of $'M'$ is given by,

$$MDL(k) = -\log\left(\frac{\prod_{i=k}^{L-1}\lambda_i^{1/L-k}}{\frac{1}{L-k}\sum_{i=k}^{L-1}\lambda_i}\right)^{W(L-k)} + \frac{1}{2}k(2L-k)logM, \qquad (4.2)$$

where λ_i $(0 \leq i \leq L-1)$ are the Eigen vales of the auto correlation matrix in descending order. The value of $'M'$ is determined by the value $k \in [0, L-1]$, which

minimizes the minimum descriptive length. This can be computationally extensive and moreover does not guarantee 100% accuracy, mainly due to the unique conditions prevalent in indoor environments as described above.

The Eigen value de-weighting of the FD-EV method, as explained in the previous chapter, was introduced in [74] to reduce the spurious nature of the spectrum in spectral estimation applications. In this work, it was discovered for the first time that the Eigen value de-weighting enabled the FD-EV method to resolve all multi-paths properly, even if the signal subspace dimension was underestimated.

The Figures 4.9 to 4.11 illustrate the variations of the normalized pseudo-spectrums of the TD-MUSIC, FD-MUSIC and FD-EV methods when the signal subspace dimensions are varied from zero to five, when the actual number of dominant signal paths is five. Figures 4.9 and 4.10 demonstrate the inability of the MUSIC algorithms to properly identify and resolve the underestimated signal peaks. The bandwidth was kept above 5 GHz, and the SNR level was maintained above 5 dB to enable proper isolation of variations occurring merely due to the signal subspace dimension variations. It should be noted that the FD-EV method fails to produce a reliable pseudo-spectrum under low bandwidth and SNR conditions. A detailed analysis of versatility of these techniques under low bandwidth and SNR conditions will be conducted in the next chapter. As expected, only the FD-EV method's pseudo-spectrum was not affected considerably by the signal subspace dimension fluctuations. Another interesting feature to note was the capability of FD-EV to resolve multi-paths to a reasonable degree of accuracy, even without subspace separation. Multi-path resolution in pseudo-spectrum generation is a two-step process. First the algorithm needs to identify the existence of the correct number of signal

peaks, then, it needs to place the said peaks, at correct locations along the time delay axis.

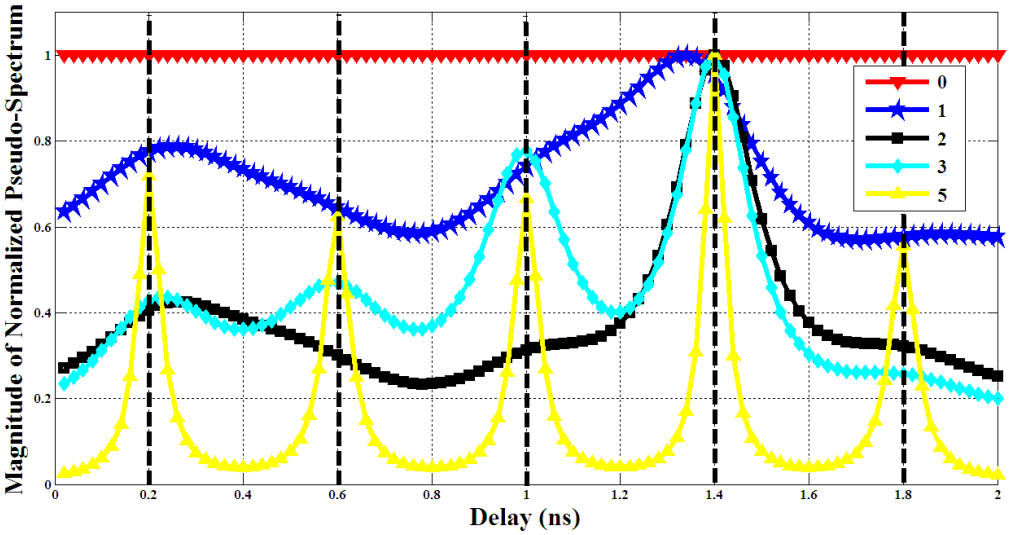

Figure 4.9 Variation of normalized pseudo-spectrums for TD-MUSIC algorithm when signal subspace dimensions are varied from 0 to 5 for sound bandwidth (above 5 GHz) and SNR (above 5 dB) conditions

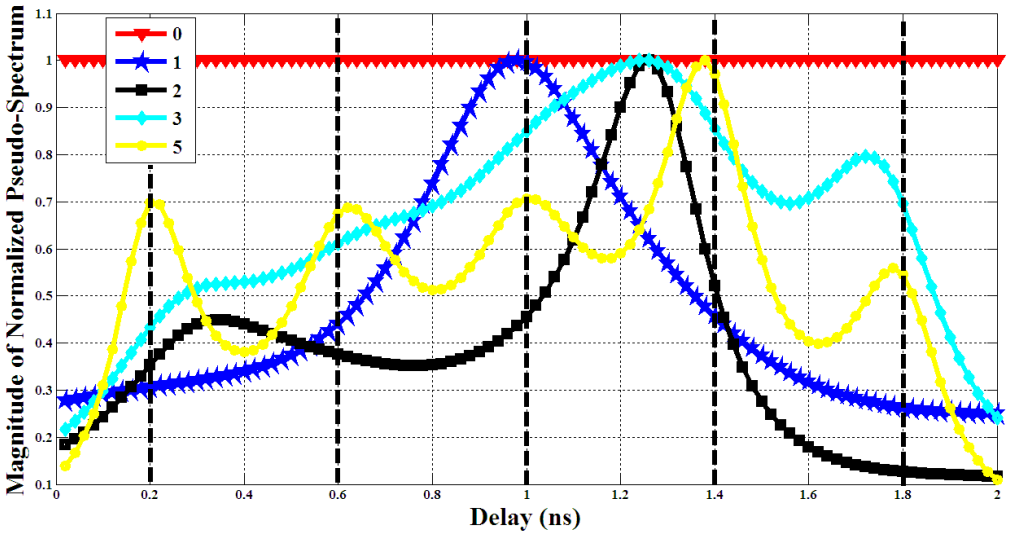

Figure 4.10 Variation of normalized pseudo-spectrums for FD-MUSIC algorithm when signal subspace dimensions are varied from 0 to 5 for sound bandwidth (above 5 GHz) and SNR (above 5 dB) conditions

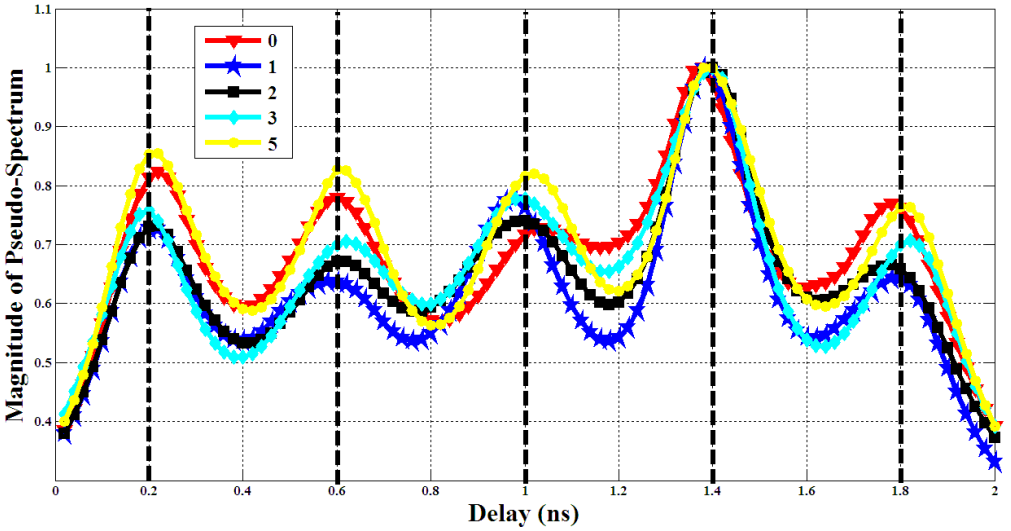

Figure 4.11 Variation of normalized pseudo-spectrums for FD-EV algorithm when signal subspace dimensions are varied from 0 to 5 for sound bandwidth (above 5 GHz) and SNR (above 5 dB) conditions

With the lowering of the SNR and bandwidth, the accuracy of the peak locations declined. As illustrated through Figures 4.12 to 4.14, when the bandwidth was lowered to around 2 GHz and SNR was set to 1 dB, due to the high versatility of

the TD-MUSIC algorithm, it was observed that TD-MUSIC was the only algorithm that did not forego a substantial shape deformation. The FD-EV algorithm fared the worst, as it has the lowest versatility under low bandwidth and SNR conditions. In spite of the FD-EV method's ability to resolve underestimated signal peaks, the relatively hostile environment simulated in Figure 4.13 rendered the FD-EV method unreliable for low SNR and bandwidth conditions. The MUSIC algorithms *despite holding its shape,* proved unreliable under these conditions due to their inability to resolve underestimated signal peaks. Thus, focus needed to be diverted to the development of an algorithm that can withstand both adverse bandwidth and SNR conditions, while still being able to resolve underestimated signal peaks. This led us to the development of the TD-EV method, which will be covered in more detail in the next chapter.

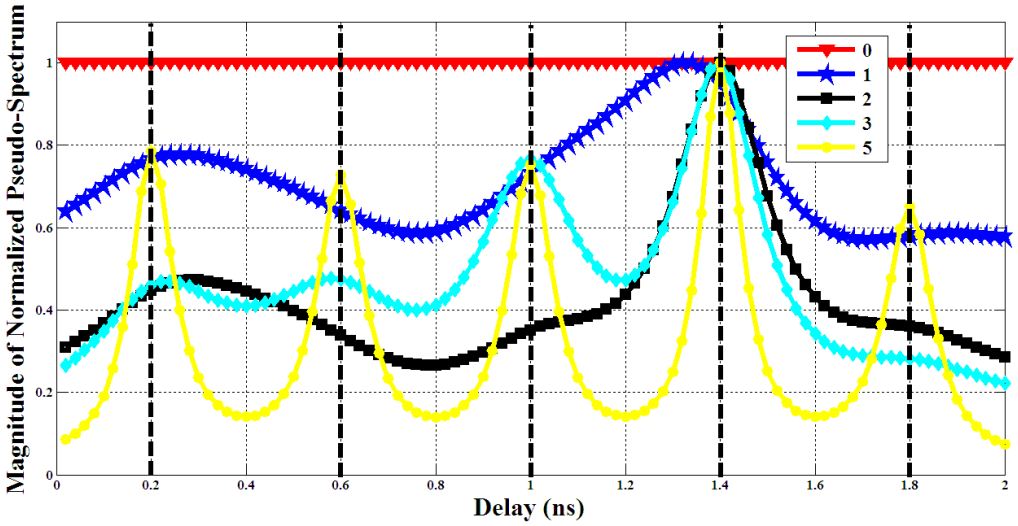

Figure 4.12 Variation of normalized pseudo-spectrums for TD-MUSIC algorithm when signal subspace dimensions are varied from 0 to 5 for low bandwidth (2 GHz) and SNR (1 dB) conditions

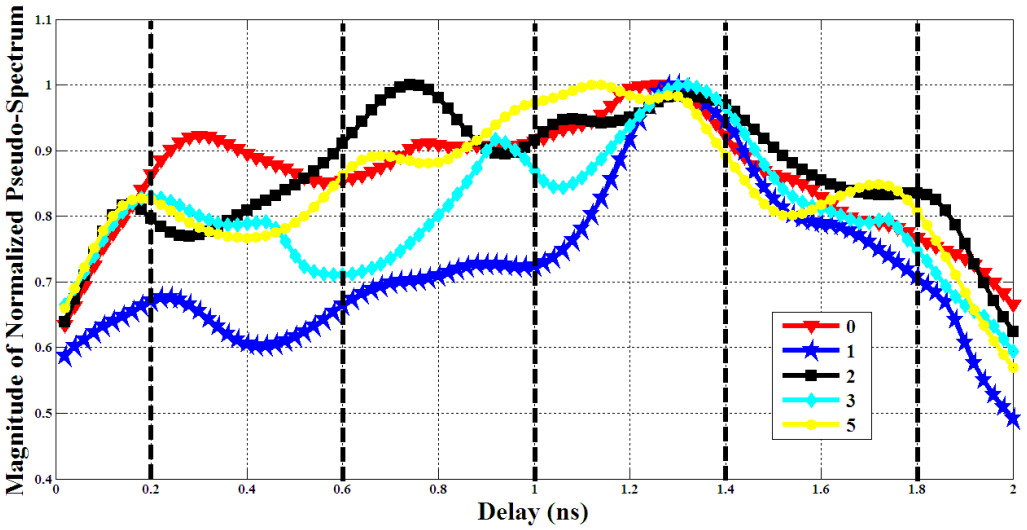

Figure 4.13 Variation of normalized pseudo-spectrums for FD-EV algorithm when signal subspace dimensions are varied from 0 to 5 for low bandwidth (2 GHz) and SNR (1 dB) conditions

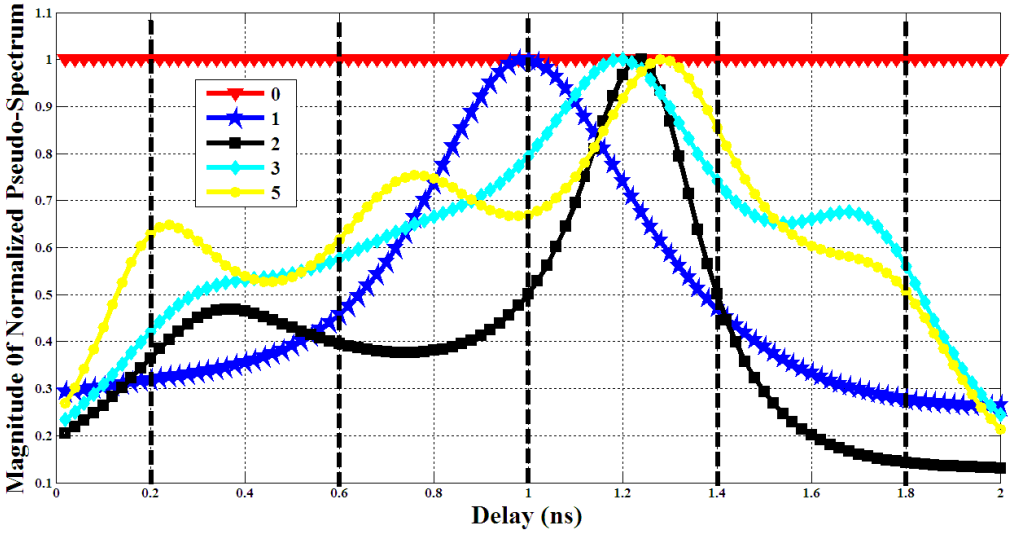

Figure 4.14 Variation of normalized pseudo-spectrums for FD-MUSIC algorithm when signal subspace dimensions are varied from 0 to 5 for low bandwidth (2 GHz) and SNR (1 dB) conditions

For scenarios where the signal subspace dimension was overestimated from 5 to 100 (for same channel conditions), the FD-EV method displayed a shape and peak magnitude fluctuation (see Figure 4.15). It can further be noticed that this fluctuation

is similar to the random variations displayed by the FD-EV method in Figure 4.11, where signal subspace dimension was underestimated. The claim that the Eigen value de-weighting renders the FD-EV method unable to coherently respond to signal subspace dimension variations is therefore further reinforced here.

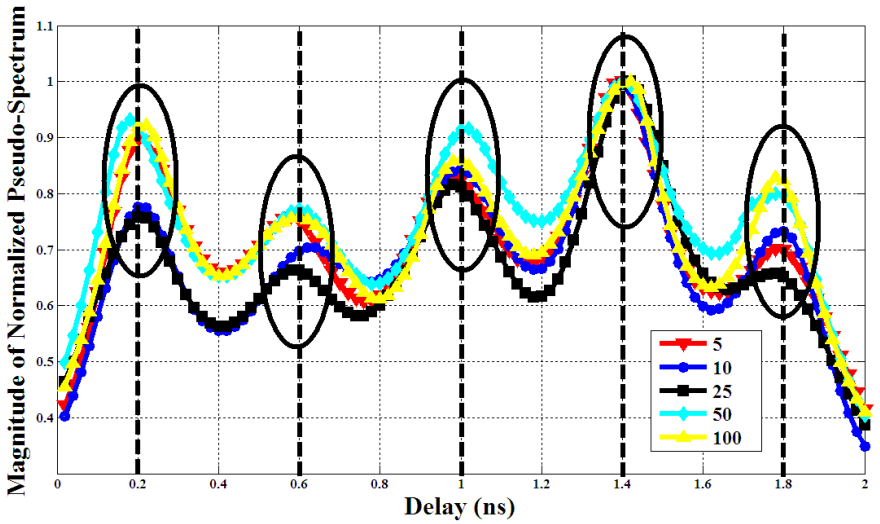

Figure 4.15 Variation of normalized pseudo-spectrums for FD-EV algorithm when signal subspace dimensions are varied from 5 to 100 for sound bandwidth (above 5GHz) and SNR (above 5dB) conditions

Figure 4.16 best summarizes the conclusions of this section, as it highlights the inability of both the MUSIC algorithms to resolve all five dominant multi-paths present, when the signal subspace dimension is underestimated to be two. As can be observed, a less pronounced signal peak emerges between 0.2 ns and 0.4 ns, in addition to the more pronounced peak around the 1.4 ns mark, with no semblance of the other three peaks which were underestimated. The same behavior can be observed for other cases of underestimated scenarios as verified earlier. The FD-EV method however, not only resolves the five signal paths, but also places them accurately at the correct locations. The resolution of all signal peaks is of utmost importance for both LoS as and NLoS conditions. The correct estimation of the DP-TOA parameter

suffers due to the existence of unresolved signal peaks for TOA based systems in LoS environments. As for location based fingerprinting techniques utilized for NLoS environments, every underestimated signal peak is simply *a missing piece of information about the details of the environment, as seen by the user at a calibration point, in a given localization system*. The lack of information in the pseudo-spectrum, translates to lack of reliability in its application, as a unique identifier in a location based fingerprinting system. Thus correct resolution of all signal paths is of paramount importance for proper localization irrespective of the underlying positioning system used in the final stage. All these points highlight the importance of this brand new property that we have identified in the FD-EV method through this research work.

In summary, we can conclude that due to the Eigen value de-weighting in the FD-EV method under sound bandwidth and SNR conditions, the '*submerged local peaks of the MUSIC pseudo-spectrum, corresponding to the underestimated signal paths resurfaced above the noise floor*'.

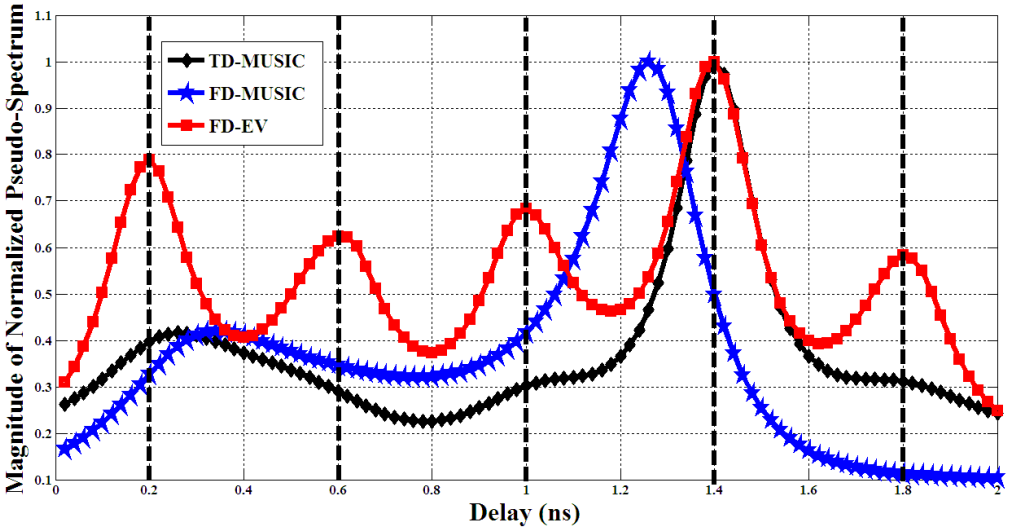

Figure 4.16 Comparison of normalized pseudo-spectrums when the number of signal subspace vectors is underestimated as 2 (For sound BW and SNR conditions)

Chapter 5

Versatility of Time Domain Techniques and the capability of the TD-EV Algorithm

The super resolution techniques introduced in our research work have shown tremendous versatility under a variety of strenuous conditions with each emerging as the leader in different scenarios. The extensive behavioral analysis conducted, has offered valuable insights into the capabilities of the super resolution algorithms, to yield satisfactory results in the most hostile radio environments, as well as the limitations of each technique under varied circumstances. This chapter presents the results of the comparative analysis conducted on these techniques.

Our focus was on constructing versatile super resolution algorithms capable of handling the most adverse conditions prevailing in indoor environments (Low SNR; limited bandwidth; erroneous estimation of signal subspace dimensions). It was identified that the TD-MUSIC algorithm had superior bandwidth versatility, resolution capability and noise immunity when compared to its frequency domain counterparts. In the previous chapter we also presented the FD-EV method's ability to resurface underestimated signal peaks submerged beneath the noise floor. However, it was discovered that the FD-EV method, unlike the TD-MUSIC algorithm, did not have high noise immunity and bandwidth versatility.

The strengths of TD-MUSIC and FD-EV methods lead to the development of the TD-EV method, which inherited *the best of both worlds*. It has the bandwidth

versatility and the noise immunity of the TD-MUSIC algorithm, and the FD-EV method's ability to resurface the underestimated signal peaks submerged beneath the noise floor, even under the most hostile channel conditions. The TD-EV method only suffers a slight but affordable decrease in resolution, while inheriting all the positive attributes of the TD-MUSIC and FD-EV algorithms. It is shown later that the TD-EV method produces the only informative pseudo-spectrum output under certain hostile radio conditions. The TD-EV method being successful where all other methods fail is a testament to its versatility and extreme usefulness.

First, we analyzed the resolution capability of all four super resolution techniques through path separation and low magnitude paths. Then, the noise performance and bandwidth versatility were tested. Finally the TD-EV method's ability to combine the positive attributes of both TD-MUSIC and FD-EV methods' was verified.

5.1 Resolution capability analyzed through path separation

A key criterion to be considered when determining the performance of any multi-path resolution technique is its path resolvability. The severe multi-path conditions prevailing in indoor environments exemplify the significance of having superior path resolution capabilities. The presence of clutter at close proximity, indoors, results in extremely closely spaced adjacent multi-paths, that arrive in clusters. Proper separation of these closely spaced multi-paths is essential for accurate positioning.

There can be many approaches to determine which algorithm has the best resolution capability. Our approach is to identify which method continues to accurately resolve all multi-paths correctly, when the path separation between two multi-paths is gradually decreased. In this study, to ensure other variables do not come into play, the effective bandwidth above the noise floor, as well as the SNR itself, were kept at friendly levels. It was also assumed that the signal subspace dimensions were accurately estimated.

An effective multi-path resolution comprises of two key steps. First, the algorithm should be able to identify the existence of two separate signal paths. This is ensured when there is evidence of two separately identifiable peaks present in the resultant pseudo-spectrum. Second, for the process to be deemed complete, the peaks must be placed at the correct locations corresponding to the relevant time delays of the paths in concern. This is a fundamental criterion in resolution because, as stated earlier the *'peak shift'* that takes place due to adjacent paths causes an estimation error for low resolution algorithms, and is one of the underlying reasons for opting for a super resolution technique in the first place.

For our analysis, the path separation between peak two and three was varied from the usual 0.4 ns to 0.2 ns. Figure 5.1 gives the outcome of the control experiment in which the multi-path separation is maintained at the 0.4 ns interval. Here all four techniques are able to resolve all paths accurately. The SNR level was maintained at 10 dB, while the effective channel bandwidth above the noise floor was kept at a sound level and the signal subspace dimension were correctly estimated. As mentioned earlier it should be observed in Figure 5.1, how all four local peaks are resolved and placed at the correct locations on the delay axis by all the four methods.

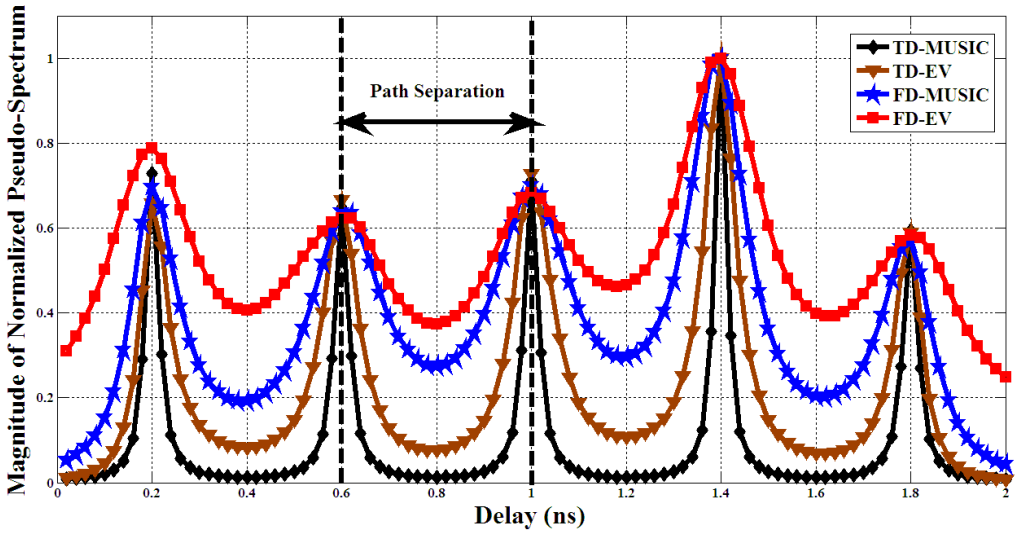

Figure 5.1 Comparison of normalized pseudo-spectrums for path separation of 0.4 ns at sound bandwidth conditions with SNR = 10 dB

As the path separation is lowered down to 0.3 ns it becomes apparent that the time domain techniques have an edge, when it comes to path resolvability. Figure 5.2 demonstrates how the FD-EV method is unable to resolve the two closely spaced multi-paths at even 0.3 ns separation. It is unable to properly identify the existence of two distinguished signal paths, and place one unresolved peak in between the two actual delay points at 0.6 and 0.9 ns. The FD-MUSIC algorithm, which fares slightly better, is able to identify the existence of two separate signal paths at a 0.3 ns interval and resolve them. Yet the FD-MUSIC method is unable to place the resolved local peaks at the correct locations on the resultant pseudo-spectrum. Thereby proving the superior resolution capability of the time domain methods to resolve, and accurately place, the local peaks at the correct locations. Figure 5.3 illustrates how the resolution capability of the FD-MUSIC and FD-EV methods further deteriorate at the same path separation when the SNR is lowered to 5 dB. Unable to resolve the 2nd and 3rd signal

paths, both methods lump the two signal paths together as one, to generate a non-existent local peak erroneously between 0.6 and 0.9ns.

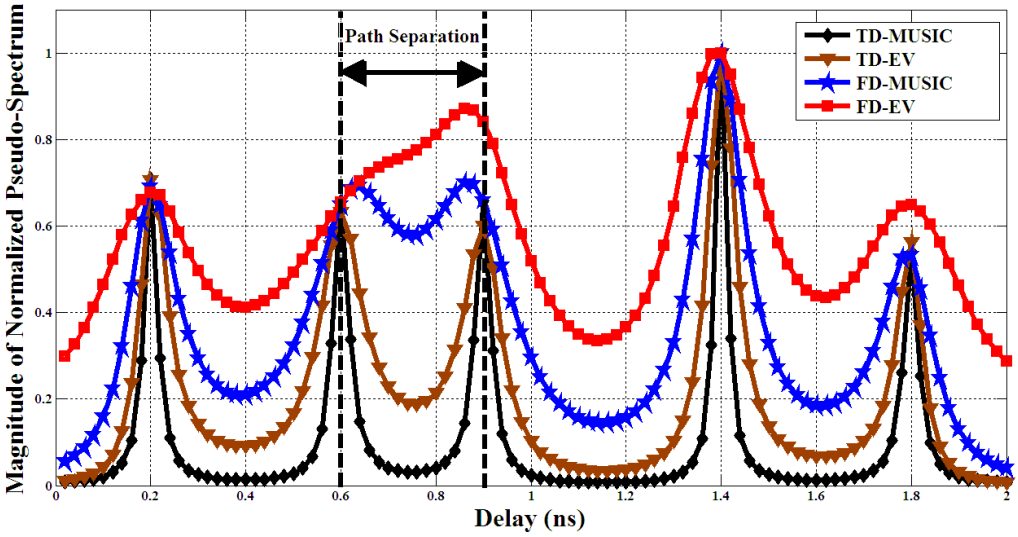

Figure 5.2 Comparison of normalized pseudo-spectrums for path separation of 0.3 ns at sound bandwidth conditions with SNR = 10 dB

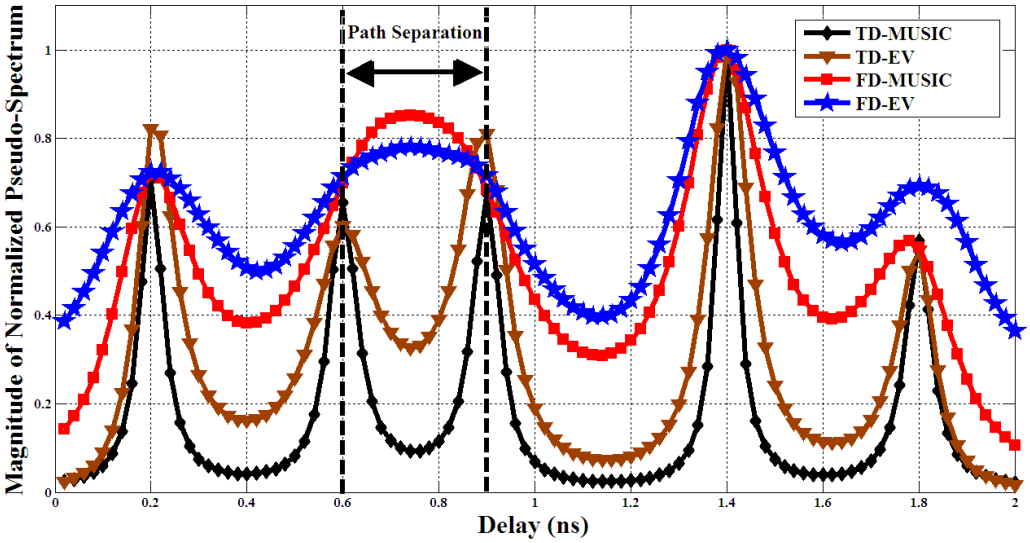

Figure 5.3 Comparison of normalized pseudo-spectrums for path separation of 0.3 ns at sound bandwidth conditions with SNR = 5 dB

Figure 5.4 however demonstrates that the TD-MUSIC algorithm is still the ultimate performer when it comes to resolution of closely spaced multi-paths as path separation is further decreased to 0.2 ns. The frequency domain methods are unable to resolve the two signal paths, while the TD-EV method though able to resolve the two paths, suffers a slight peak placement error. Hence it can be assumed that the path resolution capability of the TD-MUSIC algorithm is inherited by the TD-EV method with a slight but affordable decrease in resolution. The fact that even at this point, the TD-MUSIC method is not only able to identify, but also place the peaks at the correct locations, while the frequency domain methods cannot even detect two paths, speaks volumes about its resolution capability. The ability of the TD-EV and TD-MUSIC algorithms to resolve closely placed multi-paths makes them the prime candidates for generation of *'location information rich fingerprints'* when used in Non-LOS conditions. As more closely spaced multi-paths are resolved, the pseudo spectrum is enabled to provide more information about the surrounding environment to the location based fingerprinting system.

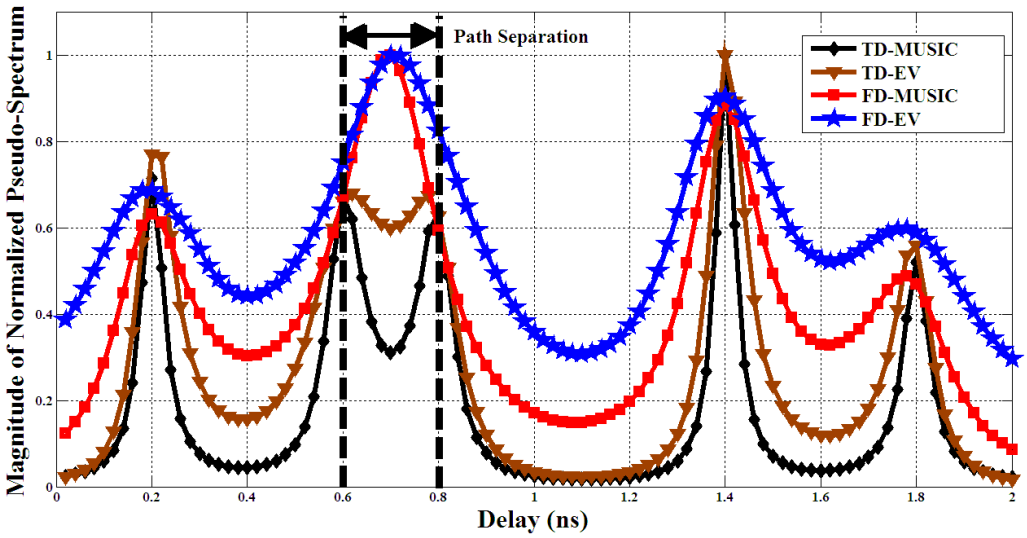

Figure 5.4 Comparison of normalized pseudo-spectrums for path separation of 0.2 ns at sound bandwidth conditions with SNR = 5 dB

5.2 Resolution capability for low gain paths

The ability of any super resolution technique to resolve low magnitude multi-paths is of the same importance as its ability to resolve closely spaced multi-paths. The inability to detect even a relatively low amplitude multi-path is essentially loss of information, when it comes to location based fingerprinting in NLoS environments. In addition, the ability to detect low amplitude signal paths increases the chance for better positioning accuracy in time delay estimation techniques as well.

In this study the relative magnitude of the 3rd dominant signal path was lowered compared to the other multi-paths, to test each methods capability to detect and accurately resolve the attenuated multi-path. Other conditions such as SNR, and effective channel bandwidth were kept at a friendly level to properly isolate this behavior. Figure 5.5 depicts each algorithm's low gain path resolution capability, when the 3rd dominant signal path has an average relative gain lower than 2 dB,

compared to the other dominant multi-paths. The circled region illustrates how the FD-MUSIC and FD-EV methods are barely able to detect the existence of the attenuated multi-path, while the TD-MUSIC and TD-EV methods have no problems detecting and resolving the attenuated signal path in question. As the relative magnitude is lowered by another 1 dB, as depicted in Figure 5.6, the frequency domain methods are completely oblivious to the existence of the low gain path (the pseudo-spectrum of the frequency domain methods are visibly flat in the encircled region), while the time domain methods continue to display their superior resolution capability. The analysis yet again demonstrates how the greater resolution capability of the TD-MUSIC algorithm is inherited by the TD-EV method.

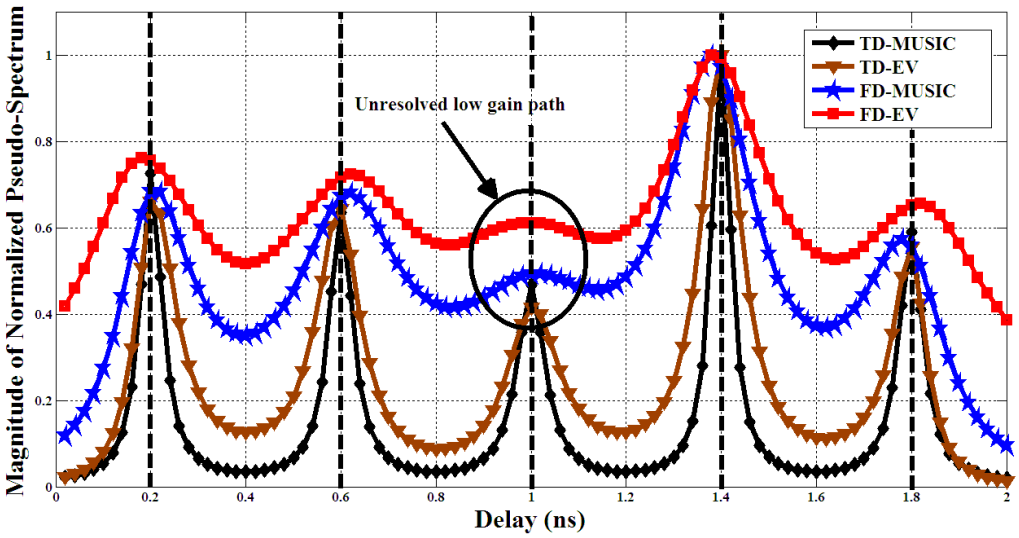

Figure 5.5 Comparison of normalized pseudo-spectrums for case where 3rd path is lower than 2 dB in relative gain compared to other dominant multi-paths

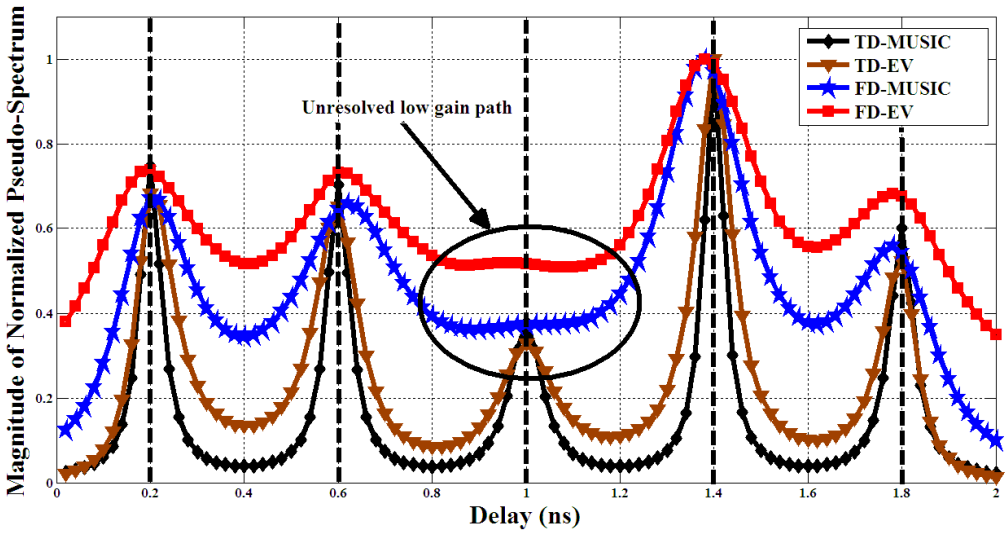

Figure 5.6 Comparison of normalized pseudo-spectrums for case where 3rd path is lower than 3 dB in relative gain compared to other dominant multi-paths

5.3 Relative noise immunity of the super resolution techniques

The noise immunity of a super resolution technique is measured by the impact that low SNR conditions have on the 'shape' of the pseudo-spectrum, and by the algorithm's ability to resolve all multi-paths, under such conditions. Noise immunity becomes the underlying criterion for selection, if we were to use less expensive signaling techniques, such as ultra sound or audible sound for positioning applications. For example as stated in [30], broadband, as well as narrowband, ultrasound positioning systems, display poor performance under ultrasonic noise, which occur due to people's everyday actions, as they employ simple correlator based techniques for time of flight estimation for LoS conditions.

On the other hand, even for UWB based systems, the signal processing tool's noise separation capability is essential for generating an accurate multi path profile of the transmitter to receiver channel. The noise maybe the result of interfering dynamic

scatterers present at the real-time application stage that were absent during the calibration stage of a location based fingerprinting positioning system. The accurate multi-path profile in turn can be used as the most accurate means of obtaining a *'location information rich fingerprint'* for localization on a radio map for NLoS scenarios. Figure 5.7 serves as the control experiment where the SNR level is maintained at 10 dB. Throughout the analysis the signal subspace dimensions are accurately estimated, and effective bandwidth is kept at a sound level for proper isolation of behavior under SNR fluctuations.

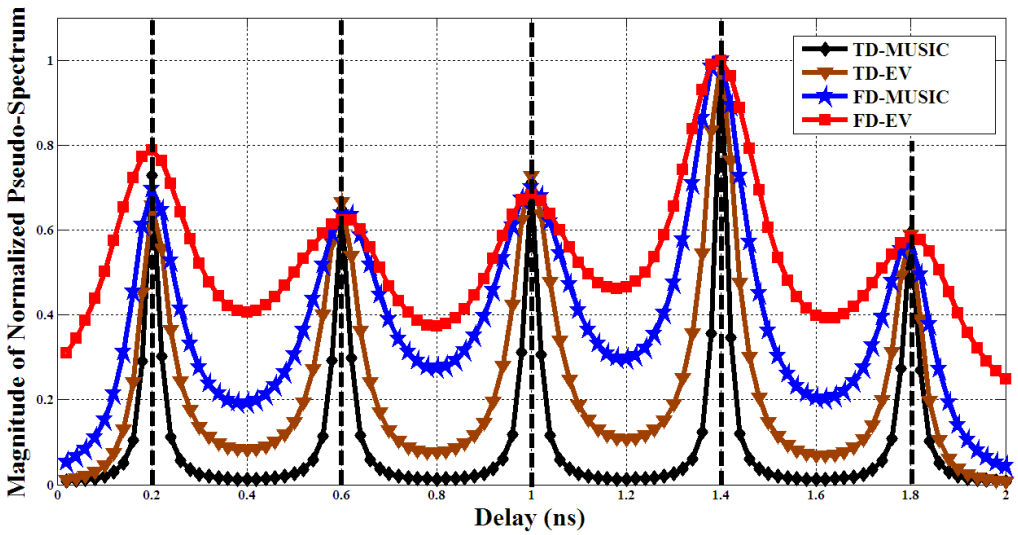

Figure 5.7 Comparison of normalized pseudo-spectrums for SNR = 10 dB

By comparison of Figure 5.7 with 5.8, the relatively higher rise of the noise floor in the FD-MUSIC and FD-EV methods compared to their time domain counterparts becomes clearly apparent for a SNR drop from 10 dB to 0 dB. Careful inspection of Figure 5.8 reveals that the barely resolved local peaks of the frequency domain methods are placed at incorrect locations due to the accentuated rise of the

noise floor. The relative rise in the noise floor shifts the local peaks to incorrect locations, while making the local peaks less pronounced. Alternatively, due to the relatively low rise of the noise floor in the time domain methods, the pseudo-spectrum shape around local peaks remain *pronounced and peaky* around the local maxima, enabling convenient and accurate peak detection for time delay estimation systems.

Now the SNR is lowered further to -5 dB in Figure 5.9. The extreme rise in the noise floor now engulfs most of the local peaks of the FD-MUSIC and FD-EV methods, leaving only two resolved peaks in the generated pseudo-spectrum. This clearly proves the superior noise immunity of the TD-MUSIC and TD-EV methods, which are still able to resolve all five multi-paths accurately, while maintaining almost negligible shape deformation in the resultant pseudo-spectrums. Both methods provide a *location information rich multi path profile* under low SNR conditions. Thus it may be inferred from these observations that the noise immunity of the TD-MUSIC algorithm is also present in the TD-EV method. These factors combined make the TD-MUSIC and TD-EV methods, prime candidates for high noise – low cost systems and NLoS location based finger printing applications.

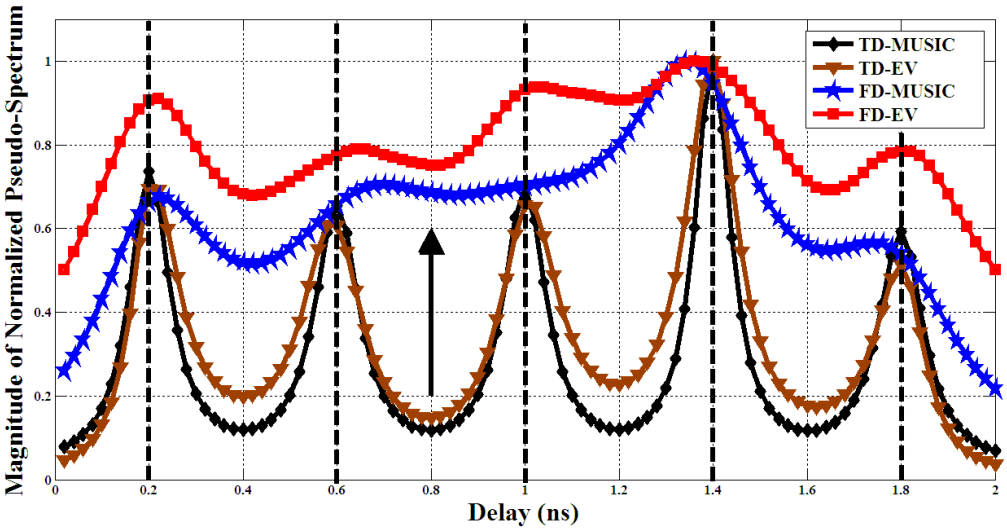

Figure 5.8 Comparison of normalized pseudo-spectrums for SNR = 0 dB

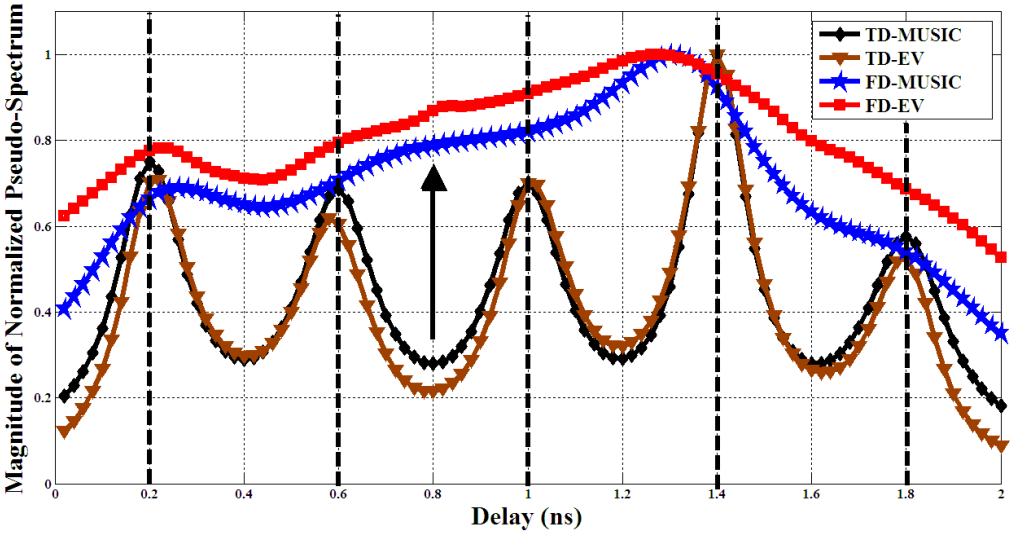

Figure 5.9 Comparison of normalized pseudo-spectrums for SNR = -5 dB

5.4 Bandwidth versatility of super resolution techniques

The bandwidth versatility of each algorithm was tested by varying effective channel bandwidth above noise floor from 10 GHz to 1.5 GHz. It is important to understand the impact of signal distortion due to band limited channels. Figures 5.10 to 5.13 contain the results of this analysis; the shape deformation of the respective pseudo-spectrums when the bandwidth is varied.

The FD-MUSIC algorithm is only able to accurately resolve the multi-paths above an effective bandwidth of 3 GHz. Even then it places some of the local peaks incorrectly along the delay axis as shown in Figure 5.10. The FD-EV method fares the worst when bandwidth is lowered, as it is unable to resolve the multipaths correctly for bandwidths below 5 GHz, resulting in a greater degree of shape deformation at 3 GHz bandwidth when compared to the FD-MUSIC algorithm. This phenomenon is illustrated in Figure 5.11. Both these methods convey no useful information about the channel multi-path profile for bandwidths below 2.25 GHz.

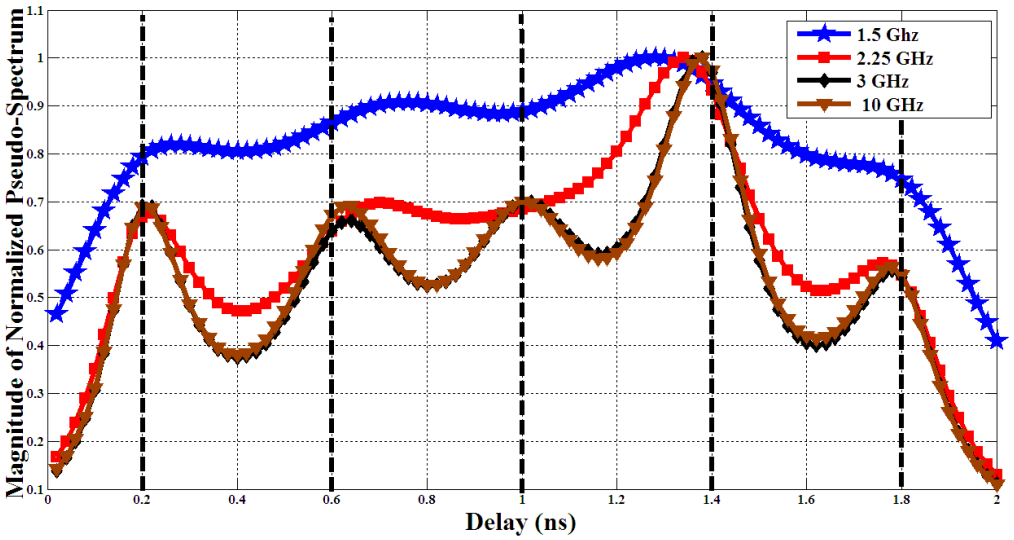

Figure 5.10 Variation of normalized pseudo-spectrums for FD-MUSIC algorithm under bandwidth change

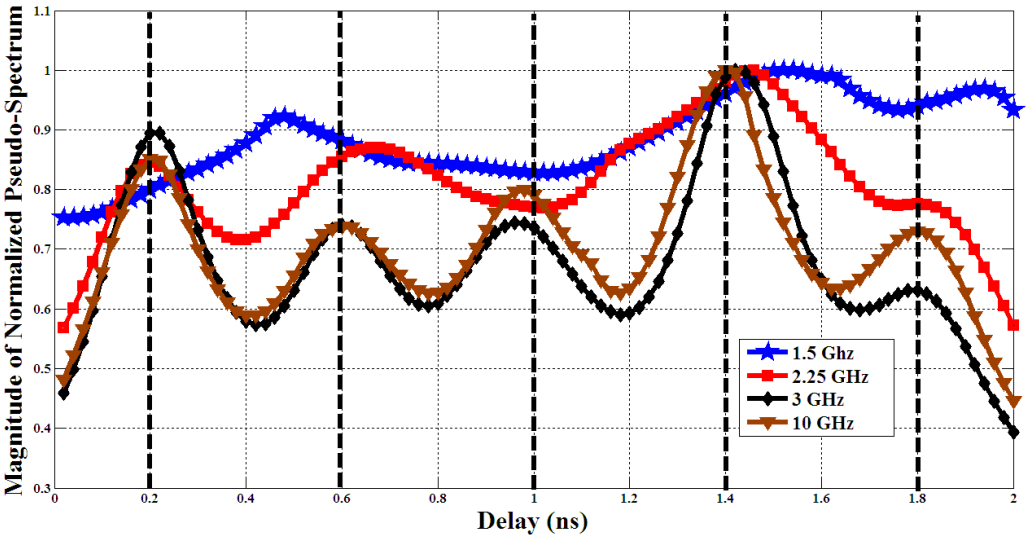

Figure 5.11 Variation of normalized pseudo-spectrums for FD-EV algorithm under bandwidth change

As visible from Figure 5.12, the TD-MUSIC algorithm under goes hardly any shape deformation above 2 GHz; and is able to resolve all five paths and estimate time delays accurately even under bandwidths below 2 GHz. This clearly illustrates the bandwidth versatility of the TD-MUSIC algorithm. Comparative examination of

Figures 5.12 and 5.13, verify that TD-EV and TD-MUSIC methods have nearly identical bandwidth versatility. Both of these algorithms show little if there is any shape deformation when the bandwidth is reduced. The pseudo-spectrum's shape remained nearly identical for bandwidth variations from 10 GHz to 2.25 GHz.

The local peaks become less and less pronounced for the frequency domain methods as bandwidth is lowered. The time domain methods tend to hold shape with as little deformation as possible. Thus it is evident that the TD-EV method has inherited the bandwidth versatility of the TD-MUSIC algorithm when the signal subspace dimension is correctly estimated.

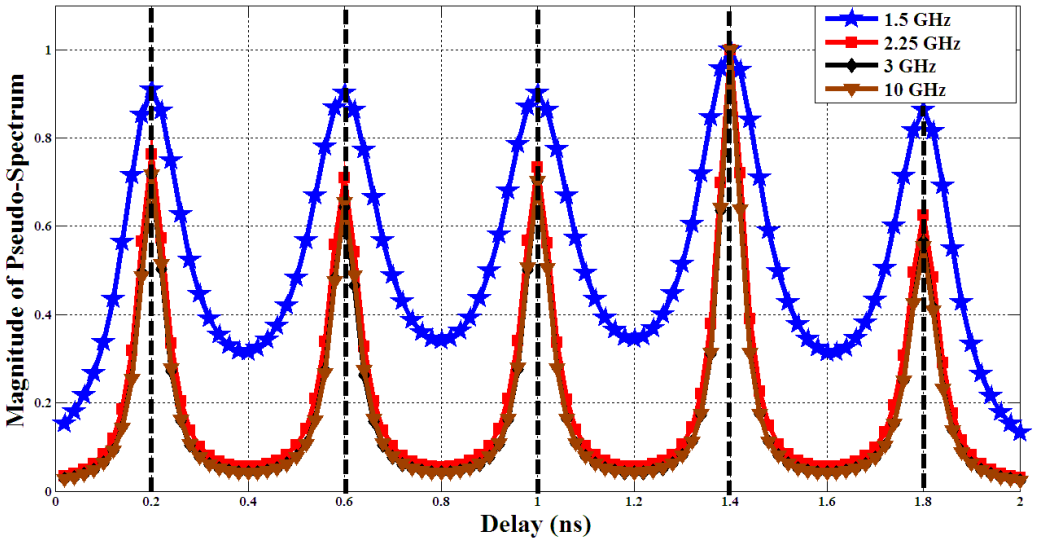

Figure 5.12 Variation of normalized pseudo-spectrums for TD-MUSIC algorithm under bandwidth change

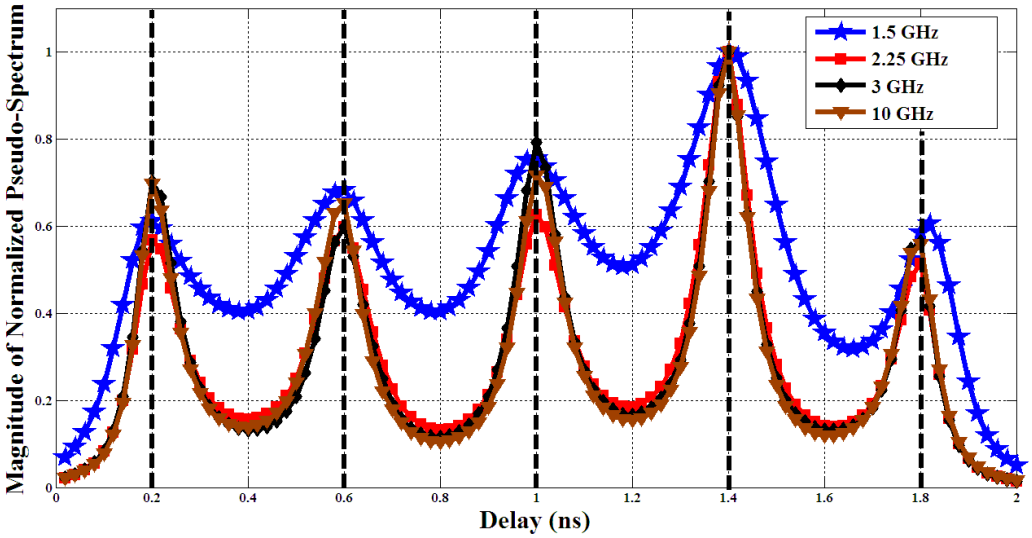

Figure 5.13 Variation of normalized pseudo-spectrums for TD-EV algorithm under bandwidth change

5.5 The best of both worlds from the TD-EV algorithm

The impact of erroneous estimation of signal subspace dimensions for the MUSIC algorithms and FD-EV method were analyzed in Section 4.3. The number of signal subspace vectors was varied from 0 to 5, for the case where the actual signal subspace dimension was 5, to study the effects for the underestimated scenario. Hence it was discovered that for sound bandwidth and SNR conditions, only the FD-EV method was able to resolve all 5 multi-paths. It was therefore concluded that the Eigen value de-weighting of the FD-EV method, enabled the underestimated signal peaks, submerged beneath the noise floor, for the MUSIC algorithm pseudo-spectrums' to resurface. Because the FD-EV method does not have the versatility of the TD-MUSIC algorithm, as verified in this chapter under hostile radio channel conditions, the FD-EV method fails to provide any useful information about the multi-path profile through its pseudo-spectrum. Therefore, we explored the possibility

of developing an algorithm that strives to combine the positive attributes of both these methods, resulting in the introduction of the TD-EV method.

In Figure 5.14, the TD-EV method undergoes the same analysis as its three counterparts. This was done to study its capabilities when the signal subspace dimension is underestimated. Here the bandwidth (around 10 GHz) and SNR (around 10 dB) are kept at a sound level. This enables us to verify whether the TD-EV method, through its de-weighting in the time domain, is able to replicate the resurfacing capability of the FD-EV method under similar conditions (see Figure 4.11). As can be observed from Figure 5.14, the TD-EV method hardly suffers any shape deformation when the signal subspace dimension is reduced. In fact the TD-EV algorithm does not even display the random fluctuations of the local peak magnitudes that were observed in the FD-EV method when the signal subspace dimension was varied (see Figure 4.15). This leads us to believe that the Eigen value de-weighting process of the TD-EV method *enables the underestimated local peaks, submerged beneath the noise floor, for the MUSIC algorithm pseudo-spectrums' to resurface,* similar to the FD-EV method, for good bandwidth and SNR conditions.

Now the bandwidth and SNR were lowered, as in our previous analysis in Section 4.3, to observe the versatility of the resurfacing capability. However, unlike the FD-EV method, the TD-EV method hardly underwent any shape deformation due to the higher bandwidth versatility and noise immunity. This behaviour is illustrated in Figure 5.15, when the effective channel bandwidth was lowered to 2 GHz and for an SNR of only 1 dB. The TD-EV method as demonstrated here was still able to accurately resolve all five multi-paths even for cases where the signal subspace dimension was underestimated.

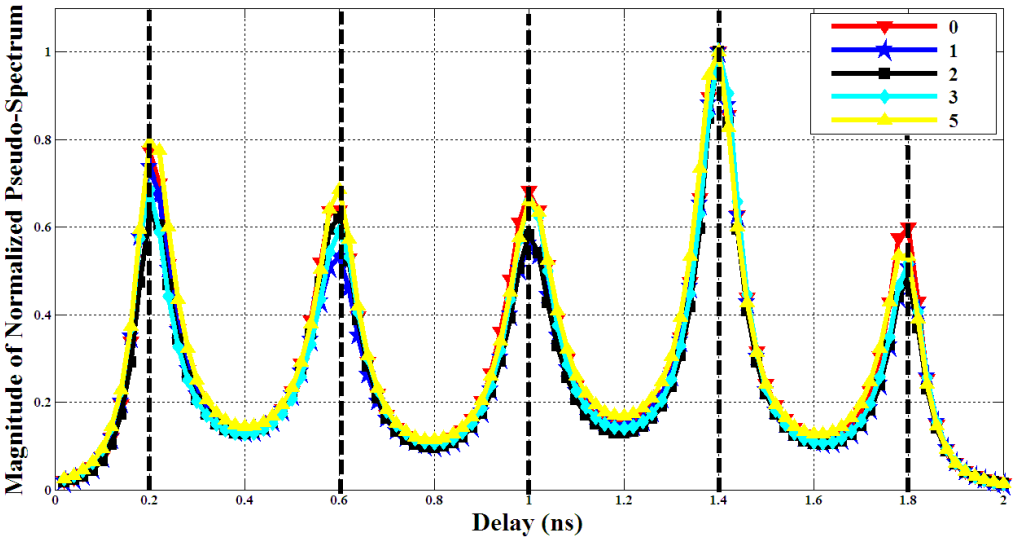

Figure 5.14 Variation of normalized pseudo-spectrums for TD-EV algorithm when signal subspace dimensions are varied from 0 to 5 for sound bandwidth (above 5 GHz) and SNR (above 5 dB) conditions

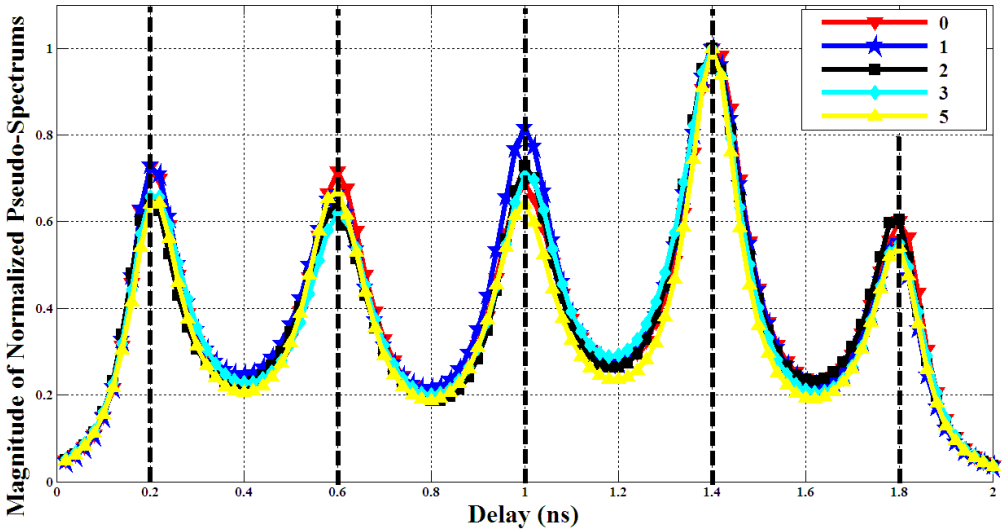

Figure 5.15 Variation of normalized pseudo-spectrums for TD-EV algorithm when signal subspace dimensions are varied from 0 to 5 for low bandwidth (2 GHz) and SNR (1 dB) conditions

As verified above and in previous sections of this chapter, the bandwidth versatility, higher resolution capability, and the noise immunity of the TD-MUSIC algorithm are inherited by the newly introduced TD-EV method. Furthermore, the FD-EV method's ability to resurface submerged local peaks when the signal subspace dimension is erroneously underestimated (under sound bandwidth and SNR conditions), can also be replicated by the TD-EV method. These observations are summarized in the Figure 5.16 for the case where the signal subspace dimensions are underestimated as two. The two EV methods are the only two methods having the ability to resolve all signal paths properly.

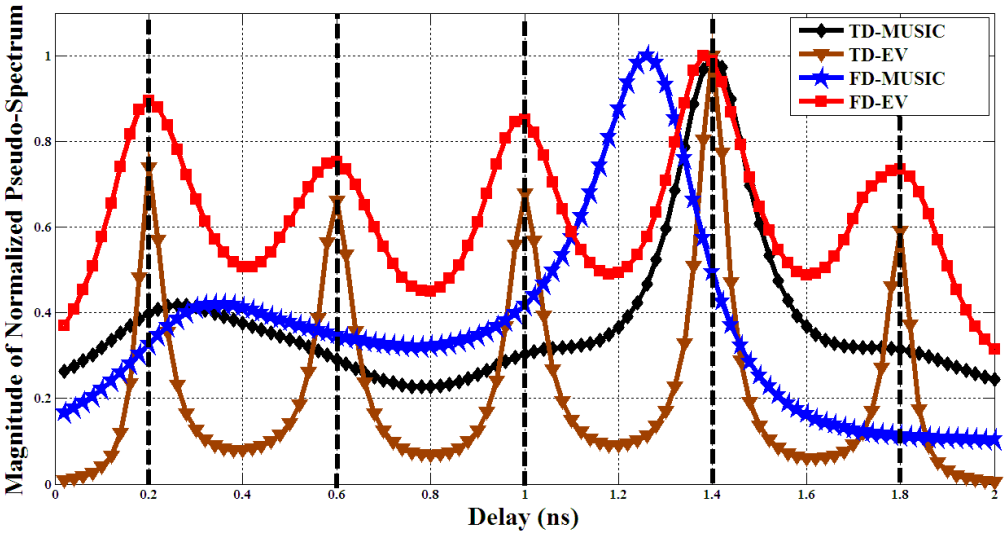

Figure 5.16 Comparison of normalized pseudo-spectrums when the number of signal subspace vectors is under estimated as 2. (For sound BW and SNR conditions)

For the case in Figure 5.17 the signal subspace dimensions are correctly estimated, but the effective channel bandwidth and SNR are lowered. This is the flipside of the previous case where the subspace dimensions were erroneously estimated, while the SNR and bandwidth remained at friendly levels. As expected, it

is clear that only the two time domain methods that are able to correctly resolve all five paths and place the local peaks at the correct locations.

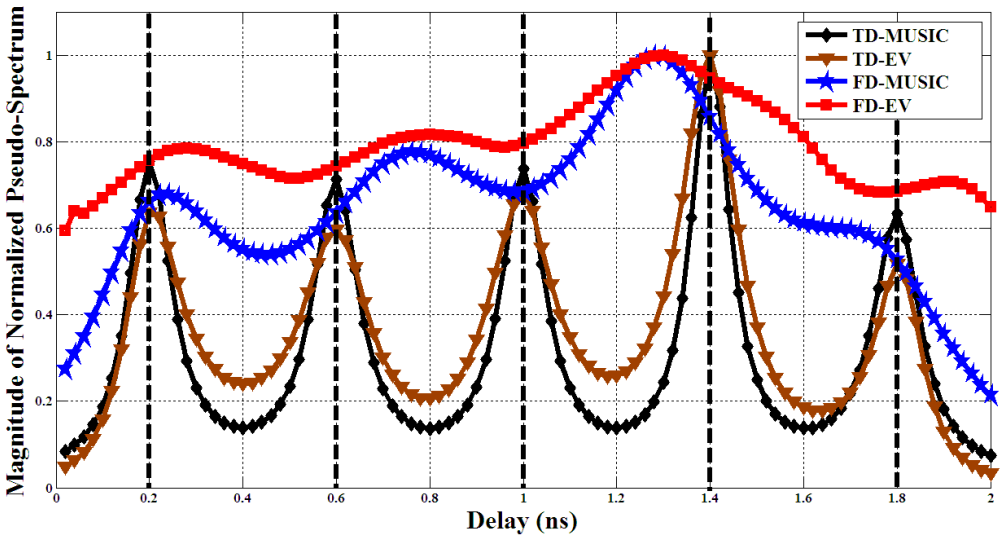

Figure 5.17 Comparison of normalized pseudo-spectrums when the number of signal subspace vectors is correctly estimated (For low BW and SNR conditions)

These results confirm that both the resurfacing capability of the FD-EV method, and the versatility and noise immunity of the TD-MUSIC method, is inherited by the TD-EV method. So far we have only seen the TD-EV method replicating these positive attributes under the same conditions the original algorithms displayed them. What remains to be examined is whether the TD-EV method can effectively *combine the best of both worlds.* In other words, "can it resolve all multi-paths properly when the signal subspace dimension is erroneously underestimated under hostile radio conditions where there is low SNR and low bandwidth?" As shown in Figure 5.18, the TD-EV method is able to resolve all five dominant multi-paths under low SNR and low bandwidth conditions when the signal subspace dimension is underestimated. As evident from Figure 5.18, the only method that produces a properly resolved pseudo-spectrum under these hostile channel conditions

is the TD-EV method. All other methods fail to provide any valuable information what-so-ever. The FD-EV and FD-MUSIC methods fail due to their comparably lower noise immunity and bandwidth versatility. The TD-MUSIC algorithm fails due to its inability to resurface underestimated signal peaks submerged beneath the noise floor. The TD-EV algorithm therefore not only has the versatility and noise immunity of the TD-MUSIC algorithm, but is also able to combine this attribute with the resurfacing capability it inherited from the FD-EV method, while facing low bandwidth and SNR conditions. The TD-EV method therefore is able to combine *the best of both worlds* effectively and accurately to improve performance of indoor positioning systems in hostile radio environments.

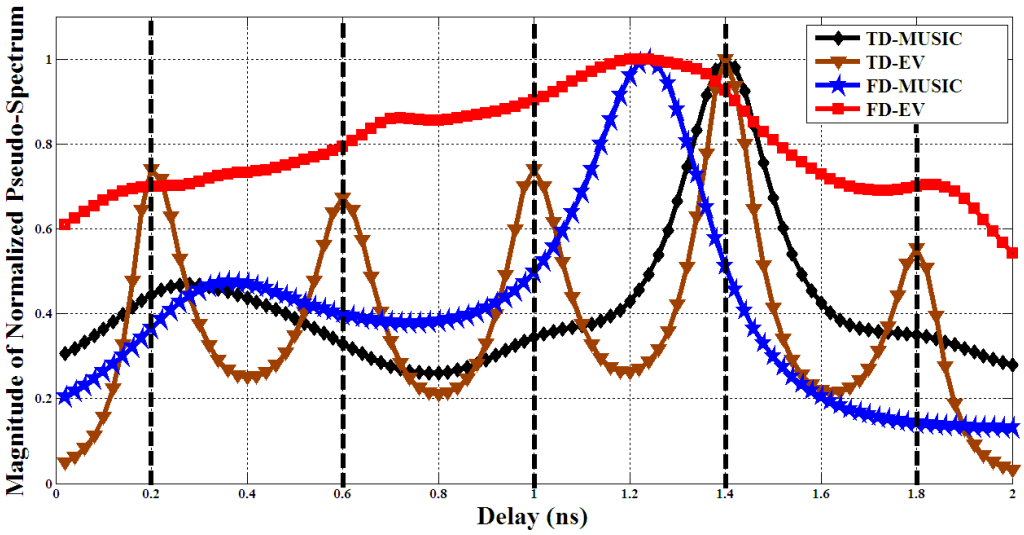

Figure 5.18 Comparison of normalized pseudo-spectrums when the number of signal subspace vectors is underestimated as 2 (For low BW and SNR conditions)

Chapter 6

Conclusions and Future Work

6.1 Conclusions

The hostile nature of indoor environments and the rapid growth of commercial indoor positioning systems have placed a significant emphasis on developing robust localization techniques. The presence of severe multi-path conditions and the frequent occurrence of NLoS conditions within indoor channels motivated us to develop signal processing algorithms, which can provide reliable information, for accurate localization in both LoS and NLoS conditions. Hence, our work focused on introducing super resolution techniques with a dual purpose:

I. Capability to accurately provide time delay estimates under LOS conditions with severe multi-path conditions and low SNR levels.

II. Ability to use the resultant pseudo-spectrums generated as location information rich fingerprints that can be utilized for localization under NLOS conditions by location fingerprinting based systems.

The subspace separation based MUSIC algorithms were identified as the prime candidate owing to their proven high resolution and noise immunity when compared to other standard time delay estimation techniques. Previous research works, only focused on mapping the MUSIC algorithm's fundamentals to a TOA estimation framework, while operating completely in the frequency domain. The applications tested were only limited for operation under LoS conditions. The analysis

focused on appreciating the resolution enhancement compared to the correlation based and inverse fast Fourier transform based methods.

Due to the limitations mentioned above, our research work focused on the development of new variants to the standard FD-MUSIC algorithm, such as the TD-MUSIC algorithm which can be utilized for positioning systems in both LoS and NLoS conditions. Then an in-depth behavioural analysis was conducted on both these methods as well as for the FD-EV method. This enabled proper identification of relative strengths and weaknesses of these super resolution techniques. The superior resolution capability of these techniques helped us to recognize them as ideal candidates for use in TOA based systems, under severe multipath conditions, as present in indoor environments with LoS conditions. These attributes, results in the presence of location rich information in the resultant pseudo-spectrum outputs generated from our algorithms. This in turn makes these pseudo-spectrums; ideal candidates to be used as fingerprints, for a location based fingerprinting system, in indoor environments with NLoS conditions. In addition, a time delay estimation model of the ESPRIT algorithm was introduced, for systems that wish to forego the computational burdens of peak detection or image matching at the expense of accuracy.

The *'spectral leakage phenomena'* of the TD-MUSIC algorithm was indentified and presented for the first time. Under steering vector pulse spread variations, an *'optimum deviant'* was identified for a given bandwidth, signal template and channel conditions. Under varying channel bandwidth conditions, the TD-MUSIC algorithm emerged as the most versatile technique. Further deviants of the TD-MUSIC algorithm were discovered to outperform the original TD-MUSIC algorithm under low bandwidth conditions. Thus, through proper identification of the

optimum deviant for a given channel condition, it was shown for band limited conditions, the spectral leakage phenomena can actually be used to our advantage.

Through an extensive behavioural analysis of the FD-EV method, we were able to identify for the first time that *Eigen value de-weighting process in the FD-EV method, resulted in the resurfacing of the under estimated signal peaks, which were otherwise submerged beneath the noise floor for MUSIC algorithms.* This behaviour only became apparent under friendly channel bandwidth and SNR conditions, as a result of the low versatility of the FD-EV method.

Resolution capability of the super resolution algorithms was tested for both closely spaced multi-paths and relatively low gain paths. In both cases TD-MUSIC algorithms emerged as the ultimate performer. It was demonstrated how the frequency domain methods failed under low SNR conditions, to resolve all paths properly, due to the relative rise in the noise floor. The TD-MUSIC algorithm however managed to resolve all paths accurately and efficiently, thereby verifying its superior noise immunity. Under variations of effective channel bandwidth, the TD-MUSIC algorithm yet again confirmed its versatility as it underwent the least amount of shape deformation under band limited conditions.

The observed behaviour provided the motivation to develop an algorithm that can combine the *best of both worlds*. The newly introduced TD-EV method therefore strived to combine the bandwidth versatility, noise immunity and superior resolution capability of the TD-MUSIC algorithm, with the resurfacing capability of the FD-EV method. The observations in Chapter 5 established that the newly introduced TD-EV method was able to emulate the path resolvability, bandwidth versatility, and noise immunity, present in the TD-MUSIC algorithm, when the signal subspace dimension was correctly estimated. The TD-EV method could also *resurface the local peaks*

submerged beneath the noise floor through its Eigen-value de-weighting process, in a manner similar to FD-EV method, under high SNR and bandwidth conditions.

Finally we examined whether the TD-EV method could effectively combine all the positive attributes it inherited from the TD-MUSIC and FD-EV methods to outshine as the ultimate performer under the most hostile channel conditions. It was observed that the TD-EV method is the only method to resolve all multi-paths accurately, and provide a location information rich pseudo-spectrum, under low SNR and bandwidth conditions, when the value of signal subspace dimension is erroneously underestimated. Under these conditions all other methods provide no useful information.

These versatile algorithms introduced in our research, provide the means for accurate geolocation in the most hostile indoor radio environment.

6.2 Future Work

The following are possible avenues that can be explored as future work with respect to the research work presented in this thesis.

The super resolution techniques introduced here can be used as the signal processing tools for indoor localization systems with context aware applications. The versatility of these tools can be utilized for accurate identification of the user's mobility limitations. This enables the system to determine the extent of context specific information that needs to be transmitted.

As the work here introduces versatile signal processing techniques that can provide accurate information independent of the signalling platform, the strengths and limitations can be tested for specific signalling applications. For example, the

performance enhancement in terms of positioning accuracy can be verified for an ultra sonic system, under severe multipath and noise conditions, when super resolution techniques are used as opposed to standard correlation based methods.

The possible implication of site-specific errors for location based fingerprinting systems can be analyzed. This entails matching our resultant pseudo-spectrums with the appropriate fingerprinting scheme, according to site-specific details such as density, and the nature of clutter.

The impact of multiple users, at close proximity, can be studied in terms of both signal interference as well as dynamic clutter. The possibility of considering dynamic clutter and multi-user signal interference as forms of coloured noise that can be separated at the subspace separation stage can be explored.

On work relating to implementation of the final stage of the positioning system that is the navigation solution, combining versus swapping techniques can be explored in the presence of both LoS and NLoS conditions. Combining techniques would strive to combine the information of both the parametric estimation system, as well as the location based fingerprinting system. Whereas swapping systems, will attempt to identify the current condition (whether LoS or NLoS), and select the system appropriately.

In addition, for indoor and underground environments, the possibility of utilizing repeater based systems with super resolution techniques can be studied. Especially due to the long, narrow and bendy nature of underground tunnels, repeaters would serve as an essential tool to maintain LoS conditions. The effects of repeaters as a performance enhancement tool on a location based fingerprinting system are also worth exploration, for comparative purposes.

The proper placement of the APs can be explored for further positioning accuracy enhancements in super resolution based systems. The AP placement can be adjusted according to the site, to provide better diversity in the location based fingerprint. The greater the diversity of the fingerprints, the more location rich information it contains. Further, the DOP parameters can also be improved by proper AP placement.

On work relating to non-localization applications, these techniques can be explored, for identification of the existence of a particular impulsive signal class in a noisy environment. Rather than attempting to find the delay of a known output, the steering vector can be altered to identify the existence of the signal class set in concern. The applications for this would be wide ranging.

References

[1] S. A. Golden, and S. S. Bateman, "Sensor measurements for Wi-Fi Location with emphasis on time-of-arrival ranging," *IEEE Trans. Mobile Computing,* Vol. 6, pp. 1185-1198, Oct. 2007.

[2] GPS / Dead Reckoning Application Note Trimble Placer GPS 455/DR, Trimble.

[3] I. F. Progri, W. Ortiz, W. R. Michalson, and J. Wang, "The performance and simulation of an OFDMA pseudolite indoor geolocation system," in *Proc.19th International Technical Meeting of the Satellite Division of the Institute of Navigation (ION GNSS 2006),* Fort Worth, TX, Sept. 2006, pp. 3149-3162.

[4] G. Lachapelle, "GNSS indoor location technologies," Journal of Global Positioning Systems, Vol. 3, No 1-2: 2-11, 2004.

[5] J. Hightower, and G. Borriello, "Location systems for ubiquitous computing" *Computer*, vol. 34, no. 8, Aug. 2001.

[6] K. Pahlavan, X. Li, and J. Makela, "Indoor geolocation science and technology," *IEEE Commun. Mag.*, vol. 40, no. 2, pp. 112–118, Feb. 2002.

[7] B. Alavi, and K. Pahlavan, "Analysis of undetected direct path in time of arrival based UWB indoor geolocation," in *Proc. IEEE 62nd Vehicular Technology Conference (VTC'05),* vol. 4, Dallas, TX, pp. 2627-2631, Sept. 2005.

[8] D. Cyganski, J.Orr, and W.R. Michalson, "A multi-carrier technique for precision geolocation for indoor/multipath environments," in *Proc. 16th Intl. Technical Meeting of the Satellite Division of the Institute of Navigation (ION GPS/GNSS)*, Portland, OR, pp. 1069-1073, Sept. 2003.

[9] T. Gigl, G.J.M. Janssen, V. Dizdarevic, K. Witrisal, and Z. Irahhauten, "Analysis of a UWB indoor positioning system based on received signal strength," in *Proc. 4th Workshop on Positioning, Navigation and Communication (WPNC'07)*, Hannover, Germany, pp. 97-101, Mar. 2007.

[10] I.A. Ibraheem, and J. Schoebel, "Time of arrival prediction for WLAN systems using Prony algorithm," in *Proc. 4th Workshop on Positioning, Navigation and Communication (WPNC'07)*, Hannover, Germany , pp. 29-32, Mar. 2007.

[11] M. Heidari, and K. Pahlavan, "A new statistical model for the behaviour of ranging errors in TOA-based indoor localization," in *Proc. Wireless Communications and Networking Conference (WCNC 2007),* Hong Kong, China, pp. 2564-2569, Mar. 2007.

[12] A.H. Quazi, "An overview on the time delay estimate in active and passive systems for target localization," *IEEE Trans. Acoust., Speech, Signal Processing*, Vol. ASSP-29, pp. 527-533, June 1981.

[13] C.D. Wann, and S.H. Hsu, "Estimation and analysis of signal arrival time for UWB systems," in *Proc. IEEE 60th Vehicular Technology Conference (VTC'04),* Los Angeles, CA, Vol. 5, pp. 26-29, Sept. 2004.

[14] S.L. Marple, *Digital Spectral Analysis with Applications,* Englewood Cliffs, NJ: Prentice-Hall, 1987.

[15] S.M. Kay, and S.L. Marple, "Spectrum analysis-a modern perspective," *Proceedings of the IEEE*, vol. 69, pp.1380-1419, 1981.

[16] B.D.Rao, and K.S. Arun, "Model based Processing of signals: A State Space Approach," *Proceedings of the IEEE,* vol. 80,no. 2, pp. 283 – 309, Feb. 1992.

[17] J.J. Fuchs, "Estimating the number of sinusoids in additive white noise," IEEE *Trans. Acoust., Speech, Signal Processing*, vol. ASSP-36, pp. 1846-1853, Dec. 1988.

[18] X. Li, and K. Pahlavan, "Super-resolution TOA estimation with diversity for indoor Geolocation," *IEEE Trans. on Wireless Comm.,* Vol. 3, No. 1, pp. 224-234, Jan. 2004.

[19] A. Aassie, and A. S. Omar, "Time of Arrival Estimation for WLAN Indoor Positioning Systems using Matrix Pencil Super Resolution Algorithm," *in Proc. 2nd workshop on positioning, navigation and communication (WPNC'05)*, Hannover, Germany, pp. 11-20, March 2005.

[20] D.H. Johson and S. R. De Graaf, "Improving the Resolution Bearing in Passive Sonar Arrays by Eigen Value Analysis," *IEEE Trans. Acoust., Speech, Signal Processing*, Vol. 30, No. 4, pp. 638-647, Aug. 1982.

[21] C. Drane, M. Macnaughtan, and C. Scott, "Positioning GSM telephones," *IEEE Commun. Mag.*, vol. 36, no. 4, pp. 46–54, 59, Apr. 1998.

[22] H. Mathis, D. Megnet, T. Kneubühler, A. Thiel, and E. Favey, "Indoor positioning using frequency translators," *in Proc. ION-GNSS 18th International Technical Meeting of the Satellite Division,* Long Beach CA, Sept. 2005, pp. 2789-2799.

[23] E. D. Kaplan and C. J. Hegarty, *Understanding GPS: Principles and Applications,* Boston: Artech House, 2006.

[24] B. Fang, "Simple solution for hyperbolic and related position fixes," *IEEE Trans. Aerosp. Electron. Syst.*, vol. 26, no. 5, pp. 748–753, Sep. 1990.

[25] B. B. Peterson, C. Kmiecik, R. Hartnett, P. M. Thompson, J. Mendoza, and H. Nguyen, "Spread spectrum indoor geolocation," *J. Inst. Navigat.*, vol. 45, no. 2, pp. 97–102, 1998.

[26] X. Li, K. Pahlavan, M. Latva-aho, and M. Ylianttila, "Comparison of indoor geolocation methods in DSSS and OFDM wireless LAN," in *Proc. IEEE Veh. Technol. Conf.*, Sep. 2000, vol. 6, pp. 3015–3020.

[27] A. Mandal, C.V. Lopes, T. Givargis, A. Haghighat, R. Jurdak, and P.Baldi, "Beep: 3D indoor positioning systems using audible sound," in *Proc. 2nd IEEE Consumer Communication and Networking Conference (CCNC'05),* Las Vegas, NV, Jan. 2005, pp. 348-353.

[28] Y. Fukuju, M. Minami, H. Morikawa, and T. Aoyama, "DOLPHIN: an autonomous indoor positioning system in ubiquitous computing environment," in *Proc. IEEE Workshop on Software Technologies for Future Embedded Systems* (WSTFES 2003)*,* Hakodate, Hokkaido, Japan, May 2003, pp. 53-56.

[29] M. McCarthy, P. Duff, H.L. Muller, and C. Randell, "Accessible Ultrasonic Positioning," *IEEE Pervasive Computing Mag.,* Vol. 5, pp. 86-93, Oct. – Dec. 2006.

[30] M. Hazas and A.Hopper, "Broadband ultrasonic location systems for improved indoor positioning," *IEEE Trans. Mobile Computing,* Vol. 5, pp. 536-547, May 2006.

[31] Y. T. Chan and K. C. Ho, "A simple and efficient estimator for hyperbolic location," *IEEE Transactions on Signal Processing*, vol. 42, no. 8, August 1994, pp. 1905–1915.

[32] W. H. Foy, "Position-location solutions by Taylor series estimation," *IEEE Transactions on Aerospace and Electronic Systems*, March 1976, pp. 187–194.

[33] D. J. Torrieri, “Statistical theory of passive location systems, *IEEE Transactions on Aerospace and Electronic Systems*, March 1984, pp. 183–198.

[34] A. Gunther and C. Hoene, “Measuring round trip times to determine the distance between WLAN nodes,” in *Proc. Netw. 2005.*, Waterloo, ON, Canada, May 2005, pp. 768–779

[35] M. Kossel, H. R. Benedickter, R. Peter, and W. Bachtold, “Microwave backscatter modulation systems,” *IEEE MTT-S Dig.*, vol. 3, pp. 1427–1430, Jun. 2000.

[36] J.Zhou, K. M.-K.Chu, and J. K.-Y. Ng, “Providing location services within a radio cellular network using ellipse propagation model,” in *Proc. 19th Int. Conf. Adv. Inf. Netw. Appl.*, Taipei, Taiwan, Mar. 2005, pp. 559–564.

[37] G. Bellusci, G.J.M. Janssen, J. Yan, and C.C.J.M. Tiberius, “Low Complexity Ultra-Wideband Ranging in Indoor Multipath Environments,” in *Proc. Position, Location and Navigation Symposium, 2008 IEEE/ION,* Monterey, CA, May 2008, pp. 394-401.

[38] A. Hatami and K. Pahlavan, “Performance Comparison of RSS and TOA Indoor Geolocation Based on UWB Measurement of Channel Characteristics,” in *Proc. 17th International Symposium on Personal, Indoor and Mobile Radio Communication (PIMRC’06),* Helsinki, Finland, Sept. 2006, pp. 1-6.

[39] A. Teuber, B. Eissfeller, and T. Pany, “A two-stage fuzzy logic approach for wireless LAN indoor positioning,” in Proc. *IEEE/ION Position, Location and Navigation Symposium (PLANS 2006),* San Diego, CA, April 2006, pp. 730-738.

[40] B. D. Van Veen and K. M. Buckley, “Beamforming: A versatile approach to spatial filtering,” *IEEE ASSP Mag.*, vol. 5, no. 2, pp. 4–24, Apr. 1988.

[41] P. Stoica and R. L. Moses, *Introduction to Spectral Analysis*. Englewood Cliffs, NJ: Prentice-Hall, 1997.

[42] M. Heidari and K. Pahlavan, "A Model for Dynamic Behavior of Ranging Error in TOA-based Indoor Geolocation Systems" in *Proc. Vehicular Technology Conference fall (VTC'06),* Montreal, Canada, Sept. 2006, pp. 1-5.

[43] K. Pahlavan, P. Krishnamurthy, and J. Beneat, "Wideband Radio Channel Modeling for Indoor Geolocation Applications," *IEEE Communication Magazine*, Apr. 1998.

[44] P. Bahl and V. N. Padmanabhan, "RADAR: An In-Building RF-based User Location and Tracking System", in *Proc. 19th Annual Joint Conference of the IEEE Computer and Communications Societies (INFOCOM 2000),* Tel Aviv, Israel, March, 2000, Vol. 2, pp.775 – 784.

[45] M. Kanaan and K. Pahlavan, "CN-TOAG a New Algorithm for Indoor Geolocation," in *Proc. 15th IEEE International Symposium on Personal, Indoor and Mobile Radio Communication (PIMRC'04),* Barcelona, Spain, Sept. 2004, vol. 3, pp. 1906-1910.

[46] K. Sayrafion-Pour and D. Kasper, "Indoor Positioning using Spatial Power Spectrum," in *Proc.16th IEEE International Symposium on Personal, Indoor and Mobile Radio Communication (PIMRC'05),* Berlin, Germany, Sept. 2005, Vol.4, pp. 2722-2726.

[47] Y. Rubner, C. Tomasi and L. J. Guibas, "A metric for distributions with applications to image databases", in *Proc. 6th International Conference on Computer Vision,* Bombay, India, Jan. 1998, pp. 59 – 66.

[48] R. Battiti, A. Villani, and T. Le Nhat, "Neural network models for intelligent networks: deriving the location from signal patterns," in *Proc. Autonomous Intelligent Networks and Systems Symposium (AINS2002)*, Los Angeles, CA, May 2002.

[49] H. Niwa, T. Ogata, K. Komatani, H. Okuno, "Multiple acoustic holography method for localization of objects in broad Range using audible sound," in *Proc. International Conference on Intelligent Robots and Systems (IROS'06),* Beijing, China, Oct. 2006, pp. 1146-1151.

[50] P. Kontkanen, P. Myllym¨aki, T. Roos, H. Tirri, K. Valtonen, and H.Wettig, "Topics in probabilistic location estimation in wireless networks," in *Proc. 15th IEEE International Symposium on Personal, Indoor and Mobile Radio Communication (PIMRC'04),* Barcelona, Spain, Sept. 2004, vol. 2, pp. 1052–1056.

[51] N. Cristianini and J. Shawe-Taylor, *An Introduction to Support Vector Machines,* Cambridge Univ. Press, 2000. [Online]. Available: http://www.support-vector.net

[52] H. Liu, A. Kshirsagar, J. Ku, D. Lamb, and C. Niederberger, "Computational models of intracytoplasmic sperm injection prognosis," in *Proc. 13th Eur. Symp. Artif. Neural Netw.*, Bruges, Belgium, Apr. 2005, pp. 115–120.

[53] V. Kecman, *Learning and Soft Computing*. Cambridge, MA: MIT Press, 2001.

[54] V.Vapnik, *The Nature of Statistical Learning Theory*. New York: Springer, 1995.

[55] M. Brunato and R. Battiti, "Statistical learning theory for location fingerprinting in wireless LANs," *Comput. Netw.*, vol. 47, pp. 825–845, 2005.

[56] C. L. Wu, L. C. Fu, and F. L. Lian, "WLAN location determination in e-home via support vector classification," in *Proc. IEEE Int. Conf. Netw., Sens. Control*, 2004, vol. 2, pp. 1026–1031.

[57] P. Prasithsangaree, P. Krishnamurthi, and P. K. Chrysanthis, "On indoor position with wireless LANs," in *Proc. 13th IEEE International Symposium on Personal, Indoor and Mobile Radio Communication (PIMRC'02),* Lisbon, Portugal, Sept. 2002, vol. 2, pp. 720–724.

[58] P. K. Engee, "The global positioning system: Signals, measurements and performance," *Int. J. Wireless Inf. Netw.*, vol. 1, no. 2, pp. 83–105, 1994.

[59] M. Chansarkar, and L.J. Garin, "Acquisition of GPS signals and very low signal to noise ratio," in *Proc. Institute of Navigation National Technical Meeting,* Anaheim CA, Jan. 2000, pp. 731-737.

[60] J. Caratori, M. Francois, N. Samama, and A. Vervisch-Picois, "UPGRADE RnS indoor positioning system in an office building," in Proc. *ION-GNSS 17th International Technical Meeting of the Satellite Division,* Long Beach CA, Sept. 2004, pp. 1959-1969.

[61] G.I. Jee, J.H. Choi, and S.C. Bu, "Indoor positioning using TDOA measurements from switching GPS repeater," in Proc. *ION-GNSS 17th International Technical Meeting of the Satellite Division,* Long Beach CA, Sept. 2004, pp. 1970-1976.

[62] M. Chiesa, R. Genz, F. Heubler, K. Mingo, and C. Noessel, RFID, (2002, Mar.). [Online]. Available: http://people.interactionivrea.it/c.noessel/RFID/research.html

[63] J. Hightower, R. Want, and G. Borriello, "SpotON: An indoor 3D location sensing technology based on RF signal strength," Univ. Washington, Seattle, Tech. Rep. UW CSE 2000–02-02, Feb. 2000.

[64] L. M. Ni,Y. Liu,Y. C. Lau, and A. P. Patil, "LANDMARC: Indoor location sensing using active RFID," *Wireless Netw.*, vol. 10, no. 6, pp. 701–710, Nov. 2004.

[65] J. J. Caffery and G. L. Stuber, "Overview of radiolocation in CDMA cellular system," *IEEE Commun. Mag.*, vol. 36, no. 4, pp. 38–45, Apr. 1998.

[66] V. Otsason, A. Varshavsky, A. LaMarca, and E. de Lara, "Accurate GSM indoor localization," *UbiComp 2005,* Lecture Notes Computer Science, Springer-Varlag, vol. 3660, pp. 141–158, 2005.

[67] M. Youssef, A. Agrawala, and A. Udaya Shankar, "WLAN location determination via clustering and probability distributions," *IEEE Int. Conf. Pervasive Comput. Commun.*, Mar. 2003, pp. 143–151.

[68] M. Youssef and A. K. Agrawala, "Handling samples correlation in the Horus system," *IEEE INFOCOM 2004*, Hong Kong, vol. 2, pp. 1023– 1031, Mar. 2004.

[69] T. Roos, P.Myllymaki, H. Tirri, P.Misikangas, and J. Sievanan, "A probabilistic approach to WLAN user location estimation," *Int. J. Wireless Inf. Netw.*, vol. 9, no. 3, pp. 155–164, Jul. 2002.

[70] P. Castro, P. Chiu, T. Kremenek, and R. R. Muntz, "A probabilistic room location service for wireless networked environments," in *Proc. 3rd Int. Conf. Ubiquitous Comput.*, Atlanta, GA, Sep. 2001, pp. 18–34.

[71] R. Battiti, T. L. Nhat, andA.Villani, "Location-aware computing:Aneural network model for determining location in wireless LANs," Tech. Rep. DIT-02–0083, 2002.

[72] S. Saha, K. Chaudhuri, D. Sanghi, and P. Bhagwat, "Location determination of a mobile device using IEEE 802.11b access point signals," in *Proc. IEEE Wireless Commun. Netw. Conf.*, Mar. 2003, vol. 3, pp. 1987–1992.

[73] A. Chehri, P. Fortier and P.M. Tardif, "Geolocation for UWB Networks in underground mines," *IEEE Annual Wireless and Microwave Technology Conference (WAMICON'06),* Clearwater Beach, FL, Dec. 2006, pp. 1-4.

[74] D.H. Johnson and S.R. De Graaf, "Improving the resolution bearing in passive sonar arrays by eigen value analysis," *IEEE Trans. Acoust., Speech, Signal Processing,* Vol. 3, pp. 638-647, Aug. 1982.

[75] R. Roy and T. Kailath, "ESPRIT-estimation of signal parameters via rotational invariance techniques," *IEEE Trans. Acoust., Speech, Signal Processing*, Vol. 37, No. 7, pp. 984-995, July 1989.

[76] R. Roy and T. Kailath, "Direction-of-arrival estimation by subspace rotation methods – ESPRIT," *IEEE International Conference on Acoustics, Speech, and Signal Processing (ICASSP'86),* Vol. 11, Tokyo, Japan, pp. 2495-2498, Apr. 1986.

[77] D. Manolakis, V. Ingle, and S. Kogon, *"Statistical and Adaptive Signal Processing,"* New York: McGraw-Hill, 2000.

[78] K. Pahlavan, F. O. Akgul, M. Heidari, A. Hatami, J. M. Elwell, and R. D. Tingley, "Indoor geolocation in the absence of a direct path," *IEEE Wireless Communications Magazine,* Vol. 13, No. 6, pp. 50-58, Dec. 2006.

[79] M. Wax and T. Kailath, "Detection of signals by information theoretic criteria," *IEEE Trans. Acoust., Speech, Signal Processing*, vol. ASSP-33, pp. 387–392, Apr. 1985.

List of Publications

- G.M.R.I. Godaliyadda and H.K. Garg, *"*Robust Techniques for Accurate Indoor Localization in Hazardous Environments," *Wireless Sensor Networks Journal of Scientific Research Publishing,* Vol. 2, No.5, pp. 390-401, May 2010. (Published)

- G.M.R.I. Godaliyadda and H.K. Garg, "A Time Domain Eigen Value Method for Indoor Localization," *in Proc. 9th Annual Wireless Telecommunications Symposium (WTS'10),* Tampa, Florida, USA, April 2010. (Published)

- G.M.R.I. Godaliyadda and H. K. Garg, "Versatile Algorithms for Accurate Indoor Geolocation," *in Proc. 16th International Conf. Digital Signal Processing (DSP'09),* Santorini, Greece, July 2009. (Published)

- G.M.R.I. Godaliyadda and H.K. Garg, "Analysis of Super Resolution Spectral Estimation Techniques for Indoor Positioning Applications," *in Proc. 9th international Conference on Signal Processing (ICSP'08),* Beijing, China, October 2008. (Published)